UNIVERSITY OF CALIFORNIA, SAN DIEGO

Analysis of Impulse Radio Ultra-Wideband Systems

A dissertation submitted in partial satisfaction of the

requirements for the Degree of Doctor of Philosophy

in

Electrical Engineering (Communication Theory & Systems)

by

Matteo Sabattini

Commitee in charge:

    Professor Elias Masry, Co-Chair
    Professor Laurence B. Milstein, Co-Chair
    Professor William Hodgkiss
    Professor Joseph Pasquale
    Professor Bhaskar Rao

2006

The dissertation of Matteo Sabattini is approved, and it is acceptable in quality and form for publication on microfilm:

_____

_____

_____

_____
Co-Chair

_____
Co-Chair

University of California, San Diego

2006

"Experience is the name everyone gives to their mistakes"

Oscar Wilde

To Fanny and Chiara

CONTENTS

List of Tables

viii

AoA	Angle of Arrival
AWGN	Additive White Gaussian Noise
BER	Bit Error Rate
BPPM	Binary Pulse Position Modulation
BPSK	Binary Phase Shift Keying
B-TH	Bi-orthogonal Time Hopping
CDMA	Code Division Multiple Access
CEPT	European Conference of Postal and Telecommunication
CR	Correlator Receiver
DS	Direct Sequence
ETSI	European Telecommunications Standards Institute
FCC	Federal Communications Commission
IR	Impulse Radio
LOS	Line of Sight
MAI	Multiple Access Interference
MLE	Maximum-Likelihood Estimation
MMSE	Minimum Mean-Square-Error
MRC	Maximal Ratio Combining
MSE	Mean-Square-Error
NBI	Narrow-Band Interference
pdf	Probability Density Function
PPM	Pulse Position Modulation
PSD	Power Spectral Density
QuadR	Quadrature Receiver
RF	Radio Frequency
SIR	Signal-to-Interference Ratio
SNIR	Signal-to-Noise-and-Interference Ratio
SNR	Signal-to-Noise Ratio
TH	Time Hopping
TR	Transmitted Reference
UWB	Ultra-Wideband

"La vita umana non dura che un istante.
Bisognerebbe trascorrerla a fare ció che piace.
In un mondo fugace come un sogno
Viver nell'affanno é follia."

Giovanni Lindo Ferretti

After five years in San Diego, five years of research, fun, sun and surfing, it is impossible to put together all the names of the significant people who accompanied me throughout this journey. This dissertation is dedicated to all the wonderful friends and the people I have met, without distinctions, and what follows is only a tiny part of them.

I am truly in debt to my advisors, Larry Milstein and Elias Masry: their support and guidance throughout these years has been invaluable, and this achievement would not have been possible without their help. Their dedication to research and teaching, their tireless work ethic, together with their different and yet stunning personalities, have been for me a great motivation to improve and learn.

My sincere thanks go to my committee members, Bhaskar Rao, William Hodgkiss, and Joseph Pasquale, for their help and suggestions.

Thanks to Claudio da Silva, whose friendship and companionship accompanied me throughout most of my Ph.D., Marco Villanti, with whom I shared much more than professional advices, and Gian Mario Maggio, a great scientist, friend and roommate. It was a honor (and always great fun) to work with you all.

My sincere appreciation goes to all the professors here at UCSD, in particular to Paul Siegel, who introduced me to trellis-coded modulation and Dilbert cartoons, Jack Wolf for his cheerful attitude, and Kenneth Kreutz-Delgado for his unique personality.

Over these years, I had the chance to work with several fine students: Jacopo Marzetti, Flavio Zabini, Hermon Fray, Eric Torkildson, Puda Liu, and David Chi. It has been a pleasure to do research with you guys.

Special thanks to some of the colleagues with whom I shared so much time here at UCSD, studying, drinking coffees, smoking cigarettes, or just having good times: Mishal, Jallow, Patrick, Laddan, Thanos, Steve, Brandon, and Farzad. Thanks also to all the administration people in the department, in particular to Karol Previte (btw: I still owe you a dinner...).

How to forget the friends I shared my first experience here at UCSD as an exchange student. Samora: I always underestimated your craziness before moving to San Diego. Curru, Mamma Curru e Colle Curru: sweet are the memories of wine and barbecues. Silvia: you introduced me to surfing, and I will never forgive you for this! MollyAnna: my apartment would have looked soooo empty without you.

Also, I want to thank sincerely my home-town friends, for being such great companions regardless of distance, time zones and forgotten e-mails: Nicola (the only person other than my family members I have known for 26 out of 30 years) and his wife Elena, Rullo, Alessandro Marelli, Carlo Salizzoni, and Paolo Feraboli.

To all my friends here in San Diego, especially Goran from Parma Carmen my rummeit Conte Mascetti who invented PB Alieno the fake italian Julio and his compasso Ethan for showing me how to share an apartment without sharing anything else Marco Zilberstein and his cane giallo Marius a.k.a. Mariuzzo Roberto and his wife Sanaz Maurizio and Pablo (Gooby and Moody) PaolaVincenzoShadowCloe Laura and Markus Valentina and Davide quelcomunistadiPiero and Jitka. To the soccer crowd, to the gym crowd, to the basketball crowd. To the Roma crew: without you and your bitter-sour caffeine infusions, I would have lost my espresso+cigarettes addiction. To the Porter's Pub crew, because life is too short to drink Round Table's beer.

To Fanny, who supported me towards this achievement and had to endure stressful

phone calls, moody afternoons, sleepless nights, frustrating nonsense complaints.

Above everybody, this dissertation is dedicated to my family, who always supported my dream. Un abbraccio!

The text of Chapter 2 is a reprint of the material as it appears in:

M. Sabattini, E. Masry, and L. B. Milstein, "A Non-Gaussian Approach to the Performance Analysis of UWB TH-BPPM Systems" - 2003 IEEE Conference on UWB System and Technology (published)

The text of Chapter 3 is a reprint of the material as it appears in:

M. Sabattini, E. Masry, and L. B. Milstein, "Beamforming for Interference Mitigation in TH Impulse Radio UWB Systems" - Best Paper award - 2005 IEEE International Conference on Personal Indoor and Mobile Radio Communications (published)

M. Sabattini, E. Masry, and L. B. Milstein, "Interference Mitigation via Beamforming for Impulse Radio Time Hopping CDMA Systems" - IEEE Transaction on Communications (submitted)

The text of Chapter 4, is a reprint of the material as it appears in:

M. Sabattini, E. Masry, and L. B. Milstein, "Joint Code Acquisition and Channel Estimation for UWB Transmission" - Invited Paper - 2006 IEEE Sarnoff Symposium

M. Sabattini, E. Masry, and L. B. Milstein, "Joint Acquisition/Channel Estimation for UWB Communications in the Presence of Narrow-band Interference" - Invited Paper - 2006 IEEE Military Communications Conference (submitted)

M. Sabattini, E. Masry, and L. B. Milstein, "Acquisition and Channel Estimation for Overlay UWB Transmission" -IEEE Transaction on Communications (submitted)

The dissertation author was the primary researcher and author, and the co-authors

listed in these publications directed and supervised the research which forms the basis

for these chapters.

Vita and Publications

September 1999 - April 2000	Educational Abroad Program University of California, San Diego
October 2000	*Laurea Magna cum Laude* Universitá di Bologna
October 2000 - August 2001	*Deutsches Zentrum für Luft- und Raumfahrt* (German Aerospace Center)
December 2003	Master of Science University of California, San Diego
June 2006	Doctor of Philosophy, University of California, San Diego

"MAC Protocol for ATM transmissions over Satellite" - *Laurea* dissertation, University of Bologna and German Aerospace Center

"Performance of an MC-CDMA System based on Space-Time Spreading in the Presence of Spatially Correlated Fading" - IEEE Transaction on Communications (submitted)

"A Non-Gaussian Approach to the Performance Analysis of UWB TH-BPPM Systems" - 2003 IEEE Conference on UWB System and Technology (published)

"Non-Coherent Code Acquisition for UWB Systems in Dense Multipath Fading Channels" - 2005 IEEE International Conference on Vehicular Technologies (published)

"Code Acquisition for UWB Systems in Multipath Fading Channels" - IEEE Transaction on Communications (in preparation)

"Beamforming for Interference Mitigation in TH Impulse Radio UWB Systems" - Best Paper Award - 2005 IEEE International Conference on Personal Indoor and Mobile Radio Communications (published)

"Interference Mitigation via Beamforming for Impulse Radio Time Hopping CDMA Systems" - IEEE Transaction on Communications (submitted)

"Joint Code Acquisition and Channel Estimation for UWB Transmission" - Invited Paper - 2006 IEEE Sarnoff Symposium

"Joint Acquisition/Channel Estimation for UWB Communications in the Presence

of Narrow-band Interference" - Invited Paper - 2006 IEEE Military Communications Conference (submitted)

"Acquisition and Channel Estimation for Overlay UWB Transmission" -IEEE Transaction on Communications (submitted)

Abstract of the Dissertation

Analysis of Impulse Radio Ultra-Wideband Systems

by

Matteo Sabattini

Doctor of Philosophy in Electrical Engineering (Communication Theory & Systems)

University of California, San Diego, 2006

Professor Elias Masry, Co-Chair

Professor Laurence B. Milstein, Co-Chair

Ultra-wideband communications are gaining popularity for future indoor wireless high-speed/low-power transmissions, thanks to their versatility and technological features. At the same time, the unlicensed spectrum allocated for ultra-wideband transmissions impose stringent constraints on power emission, as well as coexistence capabilities with other commercial systems. Many technical issues are still open at the present time: the extremely wide bandwidth results in a large number of resolvable multipaths, and, consequently, a high receiver complexity. Furthermore, ultra-wideband systems have to coexist with other ultra-wideband devices, as well as other narrow-band commercial systems. This dissertation addresses some of these issues, and sketches some possible solutions. First, a novel analytical technique is introduced, in order to accurately model the interference at the receiver from other ultra-wideband devices. Second, beamforming techniques are analyzed, in order to mitigate the effect of the aforementioned MAI, as well as the interference from narrow-band commercial systems and jammers. Another open issue for ultra-wideband devices deals with synchronization and acquisition in harsh multipath environments, and in the presence

of narrow-band interference. A technique to jointly estimate the channel attenuation and acquire code synchronization, based on an approximation of the maximum likelihood criterion, is presented and analyzed.

1 Introduction

"Through me you pass into the city of woe:
Through me you pass into eternal pain:
Through me among the people lost for aye.
Justice the founder of my fabric moved:
To rear me was the task of power divine,
Supremest wisdom, and primeval love.
Before me things create were none, save things
Eternal, and eternal I shall endure.
All hope abandon, ye who enter here."

Dante Alighieri

IN recent years, ultra-wideband (UWB) has become a potential candidate for future high-speed indoor communications. Its wide bandwidth, on the order of few gigahertz, and its very low power spectral density (PSD), can achieve high data rates as well as good coexistence with other commercial systems. The large bandwidth results in very precise localization features, while the low PSD guarantees a low probability of intercept/detection. However, so many unique features come at a cost.

The wide bandwidth, far wider than the coherence bandwidth of most channels, results in a high frequency selectivity of the propagating channel, with the received energy spread over a large number of low energy multipath components. In order to recover an acceptable power level, the receiver needs to be carefully designed, and the trade-off between complexity and energy collection must be adapted to the specific application. Furthermore, receiver operations like acquisition, synchronization, and channel estimation present new unique challenges, and have to be performed in the presence of very low signal-to-noise ratio (SNR) per path.

The unlicensed spectrum allocated by the Federal Communications Commission (FCC) imposes stringent constraints on power emissions [20], while coexistence capabilities with other commercial narrow-band systems are required. Moreover, the FCC regulations and the industry trend foresee the use of UWB radio for indoor/short range transmissions. This implies that a fairly large number of UWB devices might have to share the same bandwidth in a small office room environment.

The challenges of coping with low-power signals, harsh propagation environments, multiple UWB devices in close proximity, and the presence of narrow-band jammers, have to be carefully addressed before UWB can successfully hit the market. We will highlight the contribution of this dissertation in Section 1.3. Prior to this, the state of the art of UWB in terms of industrial interest and regulatory considerations is described in the next two sections.

1.1   Industry's and Agencies' Interest in UWB

Considerable attention surrounds the emergence of UWB radio as a technology ready for commercialization. UWB techniques hold the promise of solving critical propagation related problems that have plagued conventional radio techniques. Also, UWB opens up a huge new "wireless channel" with gigahertz capacities as well as the highest spatial capacities measured in bits-per-Hertz-per-square meter (see Fig. 1.1).

The US military developed UWB in the 1970s for various uses, including low-power communications capable of evading mainstream eavesdropping techniques. Fundamental UWB patents are based on the military research. Today, many vendors are developing UWB products. Xtreme Spectrum™ has shipped UWB chips to manufacturers, while consumer electronics makers have announced UWB-capable home entertainment products.

UWB has four widely recognized application areas which exploit the unique prop-
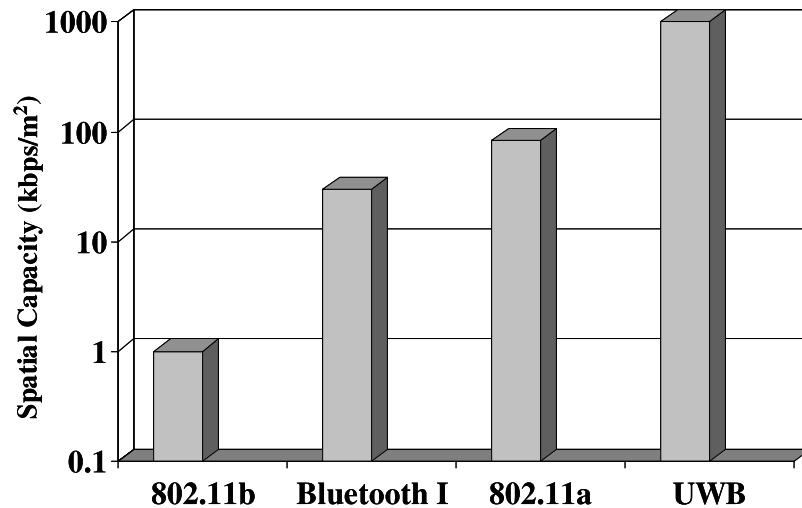
Figure 1.1: Because of their wide bandwidth, UWB systems provide the highest spatial capacities. Source: [53].

erties of short pulse transmission [45]:

- Multimedia communications;

- Wireless sensor networks;

- Bio-medical imaging and radar;

- Positioning.

UWB will primarily compete with Bluetooth technology for short-range device connectivity. The first big UWB market will be home networking, including the provision of links between computers and elements of home entertainment systems. UWB's fast transfer speeds could make the technology ideal for home theater systems because the high data rates would contribute to the smooth, uninterrupted viewing of data-intensive video programs. Many vendors are also excited about using UWB's connectivity capabilities to replace universal serial bus 2, the latter version of the USB plug-and-play interface between computers and add-on devices [38]. An exhaustive list of foreseen applications and technological challenges can be found, for example, in [3].

Given its promising benefits, it appears that UWB is less a question of "if" and more of "when and how". However, some scepticism about the effective deployment of UWB in the marketplace has been growing in the last couple of years, mostly driven by the deadlock in the IEEE standardization body, and the slow response of regulatory bodies outside the U.S.

1.2 Standardization Standpoint

In the U.S., Asia and Europe, there are ongoing UWB regulation activities. In the U.S., the open process was initiated by the FCC issuing a *Notice of Inquiry* in late 1998. After an intensive public discussion, the FCC then issued a *Notice of Proposed Rulemaking* in mid-2000 [20], [21]. The IEEE is the U.S. standardization body actively
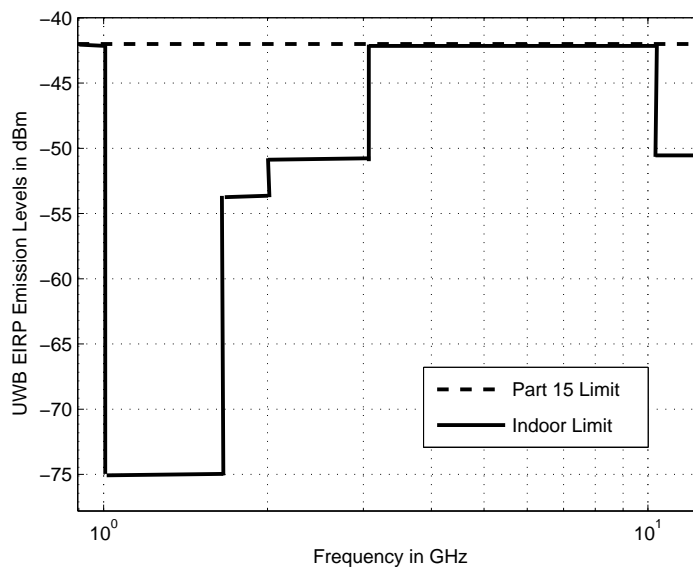
Figure 1.2: Regulatory spectral masks for the U.S. Source: [20].

working towards a common standard for UWB technology, and a first set of proposals was submitted in March 2003 [26].

The standards battle over UWB to agree on a unified physical layer interface specification for personal area networking has come to a very acrimonious stalemate. The

gap that has existed for over a year between two factions within the IEEE802.15.3 standardization working group has, over the past few months, turned into a deadlock. The impasse could lead to separate specifications emerging for this technology. Questions are now being asked over whether this would really dampen the prospects for UWB [62]. Furthermore, this process has been, so far, mostly a U.S.-led project. Regulatory groups, such as the European Conference of Postal and Telecommunication (CEPT), are generally negative on the whole issue because of potential spectrum interference and power level concerns. Drafts specifications are under development within European Telecommunications Standards Institute (ETSI), but, with the CEPT dominated by European operators rather than chip companies, delays can be expected. For a sour critic view of UWB, refer, for example, to [63].

1.3   Contribution of this work

As previously mentioned, one of the main issues for UWB communications is the need to operate in the presence of several interference sources: the indoor transmission environments (such as office spaces or apartment buildings) as well as the large bandwidth impose stringent coexistence capabilities with multiple access interference (MAI) and narrow-band interference (NBI). In order to accurately model the interference from other UWB devices, the Gaussian approximation fails in accurately predicting the performance of the system. For this reason, Chapter 2 is devoted to a new approach, based on a characteristic function argument, that enables one to predict the performance with great accuracy.

In order to reduce the effects of both MAI and NBI, Chapter 3 presents a Minimum Mean-Square-Error (MMSE) beamforming approach to reject interference. The use of multiple antennas - providing only marginal improvements from a spatial diversity perspective, given the large frequency diversity normally available in typical UWB

environments - can be very effective from a beamforming perspective to boost the capacity of the system.

The presence of narrow-band jammers can hurt many receiving operations, such as channel estimation and spreading code acquisition. Chapter 4 presents a joint acquisition/estimation technique based on an approximation of the maximum likelihood scheme. Finally, conclusions are drawn in Chapter 5.

2 A New Analytical Approach to the Performance Evaluation of UWB Time-Hopping Binary Pulse Position Modulation Systems

Recently, UWB communications schemes have been proposed as an alternative to certain indoor wireless systems, such as 802.11, in order to boost the short range capacity and coexist with other wireless networks. One of the proposed modulation schemes is based around the impulse radio (IR) model ([65], [64]), with multiple access capabilities achieved through the introduction of time hopping (TH).

Since the statistics of the MAI are very intricate, it is not possible to find an exact closed-form expression for the characteristic function (and, correspondingly, the pdf); for this reason, throughout the literature the MAI has typically been approximated by a Gaussian random variable, based on a Central Limit Theorem argument. However, as has been shown in [18], [23], and [2], for a TH pulse position modulation (PPM) system, the common approximation of the MAI as a Gaussian random variable can

lead to extremely poor results. What appears to be lacking in the above papers is an analysis employing a mathematical model of the MAI that can lead to an accurate expression for the probability of error of the system being considered.

In this chapter, a TH binary pulse position modulation (TH-BPPM) system is considered, and the multiple access capabilities of TH are investigated. No channel attenuation is considered at this point, so that the analysis focuses on the multi-user interference alone. This is consistent with the models used in the references with which we want to compare our results. A good (non Gaussian) approximation of the characteristic function of the MAI is derived, which allows us to build an accurate framework for evaluating the performance of an IR system; the analytical results are shown to predict very closely the actual behavior of the system.

The rest of the chapter is organized as follows. Section 2.1 describes the binary time hopped system, and the correlation procedure implemented at the receiver in order to recover the transmitted information, as proposed in [65] and [64]. Section 2.2 is devoted to the mathematical expression of the single-interferer case, which is simplified and used in Section 2.3 to obtain a good approximation for the MAI characteristic function. An explicit, but approximate, expression for the probability of error is derived and presented in Section 2.4, along with a comparison of the analytical results to both simulations and the common Gaussian approximation. The results show a very accurate match of the analytical expression for the bit error rate (BER) with simulations, while the Gaussian approximation is shown to fail in predicting the performance of the system for a reasonable number of users. The main proofs and derivations are collected in Section 2.5; auxiliary computations are given in Appendices A.1-A.4. Concluding remarks are given in Section 2.6.

2.1   Description of the System

Consider a TH-BPPM system (as described in [65]) with N_u users. Let $x(t)$ be the transmitted pulse that, under ideal channel conditions, is equal to the received pulse. We assume that $x(t)$ is limited in time, so that its support is limited to the interval $[0, T]$.

The transmitted pulse is "time-hopped" over a frame of duration T_f by a pseudo-random-noise sequence $\{c_j\}_{j=-\infty}^{+\infty}$ with a time shift T_c which is much smaller than T_f. We assume $c_j \in \{0, 1, ..., M-1\}$, and $MT_c = T_f$ (this is equivalent to partitioning the frame into M slots). Furthermore, the transmitted pulse is shifted by an additional time shift δ when the transmitted data symbol is a one. Each data symbol, d_i, is spread over N_s frames, meaning a repetition code of rate $r = 1/N_s$ is used.

Every user transmits a signal of the following form:

$$s^{(k)}(t) = \sum_{j=-\infty}^{+\infty} x(t - jT_f - c_j^{(k)}T_c - \delta d_{\lfloor \frac{j}{N_s} \rfloor}^{(k)} - \tau_k) \tag{2.1}$$

where the index k indicates the k-th user, and τ_k is a random delay which is assumed to be uniformly distributed over $[0, N_sT_f]$.

The parameters are defined as follows:

T_f: frame duration;

T_c: chip interval;

T: pulse duration;

c_j: pseudo-noise sequence's j-th symbol;

d_i: i-th data symbol;

δ: additional time shift;

τ_k: k-th user random delay.

Note that the system parameters ensure that each pulse is fully contained in a given frame; moreover, pulses shifted by different spreading symbols do not overlap,

i.e. $T_c \geq T + \delta$. Note also that throughout this chapter we assume an extra guard time of T seconds every chip, that is, we will set $T_c = 2T + \delta$ in order to simplify the analysis. Then, the limited support of $x(t)$ ensures furthermore that $x(t - c_j T_c - \delta) = 0$ for $t \notin [0, T_f]$, $\forall j$.

Usually, we want orthogonal (in time) binary transmission, i.e, the pulse transmitted when a one is to be sent does not overlap the pulse transmitted when a zero is to be transmitted. This is accomplished by setting $\delta \geq T$, so that $x(t)x(t - \delta) = 0$, $\forall t \in [0, T_f]$.

The transmitted signal for the k-th user can be re-written as

$$s^{(k)}(t) = \sum_{l=-\infty}^{+\infty} \sum_{j=lN_s}^{(l+1)N_s} x(t - jT_f - c_j^{(k)}T_c - \delta d_l^{(k)} - \tau_k) \text{ , for } 0 \leq k \leq N_u - 1. \quad (2.2)$$

Without loss of generality, we focus our attention on user zero. At the receiver, we assume perfect code synchronization, i.e., the code for the desired user is assumed to be deterministic and known. The spreading sequences for interfering users are modelled as equally likely random M-ary sequences.

Assuming N_u users, the received signal is the following:

$$
\begin{aligned}
r(t) &= \sum_{k=0}^{N_u-1} \sum_{l=-\infty}^{+\infty} \sum_{j=lN_s}^{(l+1)N_s-1} A_k x(t - jT_f - c_j^{(k)}T_c - \delta d_l^{(k)} - \tau_k) + n_w(t) \\
&= \sum_{l=-\infty}^{+\infty} \sum_{j=lN_s}^{(l+1)N_s-1} A_0 x(t - jT_f - c_j T_c - \delta d_l - \tau) \\
&\quad + \sum_{k=1}^{N_u-1} \sum_{l=-\infty}^{+\infty} \sum_{j=lN_s}^{(l+1)N_s-1} A_k x(t - jT_f - c_j^{(k)}T_c - \delta d_l^{(k)} - \tau_k) + n_w(t)
\end{aligned}
\quad (2.3)
$$

where the subscript for user zero has been dropped for simplicity of notation. Without loss of generality, the random delay τ for user zero can be considered perfectly tracked and set to zero, and $n_w(t)$ is additive white Gaussian noise (AWGN) with two sided PSD $\eta_0/2$. The A_k's are the channel attenuation coefficients. From here on, we will

assume perfect power control, i.e., $A_k = 1, \forall k = 0, 1, ..., N_u - 1$.

In order to recover the transmitted signal, the receiver accumulates the energy over N_s frames, and the received signal is then correlated with a copy of the transmitted pulse, as proposed in [65] and [64], in order to form the test statistic for the l-th data symbol:

$$
\begin{aligned}
\beta_l &= \sum_{j=l}^{(l+1)N_s-1} \int_{jT_f}^{(j+1)T_f} v(t - jT_f - c_jT_c)r(t)dt \\
&= \int_{lT_f}^{(l+1)N_sT_f} \sum_{j=l}^{(l+1)N_s-1} v(t - jT_f - c_jT_c)r(t)dt
\end{aligned}
$$

where $v(t) = x(t) - x(t - \delta)$. Here, we are focusing on the first data symbol (that is, on the first N_s frames, where $l = 0$). Once the test statistic has been formed, it is compared to a zero threshold and a decision on the symbol is made.

Noting that the interferers' delays are uniformly distributed over $[0, N_sT_f]$, the test statistic over the first N_s frames can be written as

$$
\begin{aligned}
\beta_0 &= \sum_{j=0}^{N_s-1} \int_{jT_f}^{(j+1)T_f} v(t - jT_f - c_jT_c)r(t)dt \\
&= \sum_{j=0}^{N_s-1} \int_{jT_f}^{(j+1)T_f} v(t - jT_f - c_jT_c)x(t - jT_f - c_jT_c - \delta d_0)dt \\
&\quad + \sum_{k=1}^{N_u-1} \sum_{j=0}^{N_s-1} \int_{jT_f}^{(j+1)T_f} v(t - jT_f - c_jT_c) \left\{ \sum_{i=0}^{N_s-1} x(t - iT_f - c_i^{(k)}T_c - \delta d_0^{(k)} - \tau_k) \right. \\
&\quad \left. + \sum_{i=-N_s}^{-1} x(t - iT_f - c_i^{(k)}T_c - \delta d_{-1}^{(k)} - \tau_k) \right\} dt \\
&\quad + \sum_{j=0}^{N_s-1} \int_{jT_f}^{(j+1)T_f} v(t - jT_f - c_jT_c)n_w(t)dt
\end{aligned}
$$

The first term represents the component of the test statistic due to the desired signal, and its value can be readily shown to be $\pm E_b = \pm N_s e_b$, with $e_b := \int_0^T x^2(t)dt$, where E_b represents the transmitted energy per bit. The second term of β_0 represents the

MAI, while the third term is filtered Gaussian noise, which is zero mean, and whose variance is readily shown to be $\sigma_n^2 = \eta_0 N_s e_b$. The final test statistic can be written as follows:

$$\beta_0 = E_b + m_I + n \tag{2.4}$$

2.2 Single-interferer component

We can write the MAI as follows:

$$
\begin{aligned}
m_I &= \sum_{k=1}^{N_u-1} \sum_{j=0}^{N_s-1} \int_{jT_f}^{(j+1)T_f} v(t - jT_f - c_j T_c) \times \left\{ \sum_{i=0}^{N_s-1} x(t - iT_f - c_i^{(k)} T_c - \delta d_0^{(k)} - \tau_k) \right. \\
&\left. + \sum_{i=-N_s}^{-1} x(t - iT_f - c_i^{(k)} T_c - \delta d_{-1}^{(k)} - \tau_k) \right\} dt =: \sum_{k=1}^{N_u-1} m_k
\end{aligned}
$$

Since users can be assumed to be independent from each other, the characteristic function of m_I can be written as

$$\varphi_{m_I}(\omega) = [\varphi_{m_1}(\omega)]^{N_u-1} \tag{2.5}$$

and we focus our attention on $\varphi_{m_1}(\omega)$. In order to simplify the expression for the single-interferer component m_1, we will use the following Lemma.

Lemma 2.1 *Let τ be a random variable which is uniformly distributed over $[0, NT]$ where N is a positive integer. Let $\eta = \lfloor \frac{\tau}{T} \rfloor$ and $\overline{\tau} = \tau - \eta T$. Then*

   i)   *$Pr[\eta = k] = \frac{1}{N}$, for $k = 0, 1, ..., N - 1$;*

   ii) *$\overline{\tau}$ is uniformly distributed over $[0, T]$;*

   iii) *$\overline{\tau}$ and η are independent.*

Using Lemma 2.1, we write the delay τ_1 as $\eta_1 T_f + \overline{\tau}_1$, where $\eta_1 = \lfloor \frac{\tau_1}{T_f} \rfloor$ and $\overline{\tau}_1 = \tau_1 - \lfloor \frac{\tau_1}{T_f} \rfloor T_f$. Thus, $\overline{\tau}_1$ is uniformly distributed over $[0, T_f]$, η_1 is a discrete equally likely random variable, taking values $0, 1, \ldots, Ns - 1$, and $\overline{\tau}_1$ and η_1 are

independent of each other. Therefore, we can rewrite the single-interferer component as follows:

$$
\begin{aligned}
m_1 = \; & \sum_{j=0}^{N_s-1} \int_{jT_f}^{(j+1)T_f} v(t - jT_f - c_j T_c) \left\{ \sum_{i=0}^{N_s-1} x(t - (i + \eta_1)T_f - c_i^{(1)} T_c - \delta d_0^{(1)} - \overline{\tau}_1) \right. \\
& \left. + \sum_{i=-N_s}^{-1} x(t - (i + \eta_1)T_f - c_i^{(1)} T_c - \delta d_{-1}^{(1)} - \overline{\tau}_1) \right\} dt.
\end{aligned}
\tag{2.6}
$$

As is shown in Section 2.5.1, the single-interferer component can be simplified as follows:

$$
\begin{aligned}
m_1 = \; & \sum_{j=0}^{\eta_1-1} [p(\overline{\tau}_1 + s_j^{(1)}(d_{-1}^{(1)}) - c_j T_c) + p(\overline{\tau}_1 - T_f + s_{j-1}^{(1)}(d_{-1}^{(1)}) - c_j T_c)] \\
& + [p(\overline{\tau}_1 + s_{\eta_1}^{(1)}(d_0^{(1)}) - c_{\eta_1} T_c) + p(\overline{\tau}_1 - T_f + s_{\eta_1-1}^{(1)}(d_{-1}^{(1)}) - c_{\eta_1} T_c)] \\
& + \sum_{j=\eta_1+1}^{N_s-1} [p(\overline{\tau}_1 + s_j^{(1)}(d_0^{(1)}) - c_j T_c) + p(\overline{\tau}_1 - T_f + s_{j-1}^{(1)}(d_0^{(1)}) - c_j T_c)]
\end{aligned}
\tag{2.7}
$$

where

$$
p(u) := \int_0^{T+\delta} v(t) x(t - u) dt \;, \quad s_j^{(1)}(d_i) := c_{j-\eta_1}^{(1)} T_c + \delta d_i^{(1)},
$$

and $\{c_j\}_{j=-\infty}^{+\infty}$ is the desired user's spreading sequence, assumed deterministic and known. The data symbols are equally likely, independent, identically distributed binary symbols. It is easy to see that the support of $p(u)$ is $[-T, T + \delta]$. Moreover, it is readily shown that $p(u)$ is odd around its midpoint $t = \delta/2$ when $x(t)$ is even around $t = T/2$. We furthermore notice that $s_j^{(1)}$ is the sum of two independent random variables, where the first one depends on η_1. Since the spreading sequences for interfering users are assumed to be random, taking values among $0, 1, \ldots, M - 1$, conditioning on $d_i^{(1)}$ and η_1, the $s_j^{(1)}$'s are conditionally independent, with conditional pdf given by

$$
f_{s_j^{(1)}}^*(s) = \frac{1}{M} \sum_{k=0}^{M-1} \delta(s - k T_c - \delta d_i^{(1)}).
$$

Note that the conditional pdf of $s_j^{(1)}$ does not depend on η_1; therefore, $s_j^{(1)}$ does not depend on η_1 as well.

We introduce the approximation $s_j^{(1)}(d_i^{(1)}) \approx s_j^{(1)}(0) =: s_j^{(1)}$, where $s_j^{(1)}$ is independent of the data, with pdf given by

$$f_{s_j^{(1)}}(s) = \frac{1}{M} \sum_{k=0}^{M-1} \delta(s - kT_c).$$

This approximation is justified in Appendix A.1, and is reasonable for M large. Therefore, we rewrite the single-interferer component as follows:

$$
\begin{aligned}
m_1 &\approx \sum_{j=0}^{\eta_1-1} [p(\bar{\tau}_1 + s_j^{(1)} - c_j T_c) + p(\bar{\tau}_1 - T_f + s_{j-1}^{(1)} - c_j T_c)] \\
&+ [p(\bar{\tau}_1 + s_{\eta_1}^{(1)} - c_{\eta_1} T_c) + p(\bar{\tau}_1 - T_f + s_{\eta_1-1}^{(1)} - c_{\eta_1} T_c)] \\
&+ \sum_{j=\eta_1+1}^{N_s-1} [p(\bar{\tau}_1 + s_j^{(1)} - c_j T_c) + p(\bar{\tau}_1 - T_f + s_{j-1}^{(1)} - c_j T_c)] \\
&= \sum_{j=0}^{N_s-1} [p(\bar{\tau}_1 - T_f + s_{j-1}^{(1)} - c_j T_c) + p(\bar{\tau}_1 + s_j^{(1)} - c_j T_c)]
\end{aligned}
$$

2.3 Closed Form Expression for the Characteristic Function of the MAI

The characteristic function for the single interferer is equal to

$$
\begin{aligned}
\varphi_{m_1}(\omega) &= E[e^{j\omega m_1}] = E_{\bar{\tau}}[E_{s_{-1},s_0,\ldots,s_{N_s-1}}[e^{j\omega m_1}]] = \frac{1}{T_f} \int_0^{T_f} E_{s_{-1},s_0,\ldots,s_{N_s-1}}[e^{j\omega m_1}] dt \\
&= \frac{1}{T_f} \sum_{k=0}^{M-1} \int_{kT_c}^{(k+1)T_c} E_{s_{-1},s_0,\ldots,s_{N_s-1}}[e^{j\omega m_1}] dt \qquad (2.8) \\
&= \frac{1}{T_f} \frac{1}{M^{N_s+1}} \sum_{k=0}^{M-1} \int_{kT_c}^{(k+1)T_c} \left(\sum_{l_{-1}=0}^{M-1} e^{j\omega p(t-(c_0+M-l_{-1})T_c)} \right)
\end{aligned}
$$

$$\times \prod_{i=0}^{N_s-2} \left(\sum_{l_i=0}^{M-1} e^{j\omega[p(t-(c_i-l_i)T_c)+p(t-(c_{i+1}+M-l_i)T_c)]} \right)$$

$$\times \left(\sum_{l_{N_s-1}=0}^{M-1} e^{j\omega p(t-(c_{N_s-1}-l_{N_s-1})T_c)} \right) \Bigg) dt$$

$$= \frac{1}{T_f} \frac{1}{M^{N_s+1}} \sum_{k=0}^{M-1} \int_0^{T_c} \left(\sum_{l_{-1}=0}^{M-1} e^{j\omega p(s-(c_0+M-l_{-1}-k)T_c)} \right)$$

$$\times \prod_{i=0}^{N_s-2} \left(\sum_{l_i=0}^{M-1} e^{j\omega[p(s-(c_i-l_i-k)T_c)+p(s-(c_{i+1}+M-l_i-k)T_c)]} \right) \tag{2.9}$$

$$\times \left(\sum_{l_{N_s-1}=0}^{M-1} e^{j\omega p(s-(c_{N_s-1}-l_{N_s-1}-k)T_c)} \right) \Bigg) ds$$

where we divided the interval $[0, T_f]$ into M intervals of length T_c, and we have let $t - kT_c = s$; moreover, we have used the fact that m_1 is the sum of conditionally independent random variables, conditioned on $\overline{\tau}$. Handling expression (2.9) without any simplification is a very difficult task; furthermore, our goal is to obtain a simple expression for the MAI characteristic function, which can be inverted and lead to an expression for the probability of error. With this goal in mind, we first introduce a simplified expression for (2.9), based on a "telescopic" relation between its terms, which is a key step in establishing a good approximation. The following Theorem 2.1 states the simplified exact characteristic function for the single-interferer component.

Theorem 2.1 *The expression for the characteristic function $\varphi_{m_1}(\omega)$ can be written as*

$$\varphi_{m_1}(\omega) = \frac{1}{T_f} \frac{1}{M^{N_s}} \sum_{k=0}^{M-1} \int_{-T}^{T+\delta} M^{z(k)} \left(2e^{j\omega p(s)} + M - 2 \right)^{z(k)} \left(e^{j\omega p(s)} + M - 1 \right)^{N_s-2z(k)} ds \tag{2.10}$$

where $z(0) = 0$, and for $k = 1, 2, \ldots, M-1$, $z(k) = \text{cardinality}(\mathcal{I}(k))$ with

$$\mathcal{I}(k) \quad := \quad \{i \in \{0, 1, \ldots, N_s - 2\} \text{ such that}$$

$$\sum_{l_i=0}^{M-1} e^{j\omega[p(s-(c_i-l_i-k)T_c)+p(s-(c_{i+1}+M-l_i-k)T_c)]} = 2e^{j\omega p(s)} + M - 2,$$

$$for \ s \in [-T, T+\delta]\}$$

As can be readily noticed, for $N_s > 1$ the characteristic function depends on the desired user's spreading sequence. In order to obtain a generic result, the dependance on the spreading sequence has to be eliminated. In the following, an approximate version of the single-interferer characteristic function is presented, based on a two-step approximation procedure (see Section 2.5.3 for details).

Theorem 2.2 *The characteristic function $\varphi_{m_1}(\omega)$ can be approximated by*

$$\hat{\varphi}(\omega) = \left(1 - \frac{N_s}{M}\right) + \frac{N_s}{M}\frac{1}{T_c}\int_{-T}^{T+\delta} e^{j\omega p(s)}ds, \tag{2.11}$$

where $\hat{\varphi}(\omega)$ is a characteristic function, and

$$\left|\frac{\varphi(\omega) - \hat{\varphi}(\omega)}{\hat{\varphi}(\omega)}\right| \leq \frac{\left[\left[1 + \left(\frac{2}{M-2}\right)^2\right]^{\lfloor\frac{N_s}{2}\rfloor} - 1\right] + \left[\left(1 + \frac{2}{M}\right)^{N_s} - 1 - \frac{2N_s}{M}\right]}{\left(1 - \frac{2N_s}{M}\right)} = O\left(M^{-2}\right)$$

The dependance on the spreading sequence has been avoided; furthermore, we have shown that the fractional error between the approximate and the exact characteristic functions decreases as the processing gain M increases. The proofs of both Theorem 2.1 and Theorem 2.2 are given in Section 2.5.2 and 2.5.4 respectively.

For M large, using Theorem 2.2, the single-interferer characteristic function is given by

$$\varphi_{m_1}(\omega) \cong \left(1 - \frac{N_s}{M}\right) + \frac{N_s}{M}\frac{1}{T_c}\int_{-T}^{T+\delta} e^{j\omega p(s)}ds = \left(1 - \frac{N_s}{M}\right) + \frac{N_s}{M}\frac{1}{T_c}c(\omega) \tag{2.12}$$

where

$$c(\omega) := \int_{-T}^{T+\delta} e^{j\omega p(s)}ds.$$

Thus, the MAI characteristic function is approximately given by

$$\varphi_{m_I}(\omega) \approx \hat{\varphi}_{m_I}(\omega) = [\varphi_{m_1}(\omega)]^{N_u-1} = \left[\left(1 - \frac{N_s}{M}\right) + \frac{N_s}{MT_c}c(\omega)\right]^{N_u-1},$$

which by the use of the binomial expansion is equal to

$$\hat{\varphi}_{m_I}(\omega) = \sum_{k=0}^{N_u-1} \binom{N_u-1}{k} \left(1 - \frac{N_s}{M}\right)^{N_u-k-1} \left(\frac{N_s}{M}\frac{1}{T_c}\right)^k c(\omega)^k. \qquad (2.13)$$

It is worth stressing that the above result is exact for $N_s = 1$, while it is an approximation for $N_s > 1$.

2.4 Probability of Error

Since the data symbols are equally likely, we can assume, without loss of generality, that $d_0 = 0$. Recall the expression for the test statistic of the system (2.4)

$$\beta_0 = E_b + m_I + n =: E_b + \chi$$

The probability of error is given by

$$
\begin{aligned}
P_e &= Pr[\beta_0 < 0] = Pr[\chi < -E_b] = \int_{-\infty}^{-E_b} f_\chi(x)dx \\
&= \int_{\infty}^{-E_b} \frac{1}{2\pi} \int_{-\infty}^{+\infty} \varphi_{m_I}(\omega)\varphi_n(\omega)e^{-j\omega x}d\omega dx \qquad (2.14)
\end{aligned}
$$

where $f_\chi(x)$ is the pdf of the random variable $\chi := m_I + n$, and $\varphi_n(\omega)$ is the noise characteristic function. We approximate the probability of error of the system by substituting in (2.14) the approximate expression for the MAI characteristic function

(2.11). Therefore we have

$$P_e \approx \hat{P}_e = \int_{\infty}^{-E_b} \frac{1}{2\pi} \int_{-\infty}^{+\infty} \hat{\varphi}_{m_I}(\omega)\varphi_n(\omega)e^{-j\omega x}d\omega dx$$

The following theorem gives a final result for $\hat{P}_e$.

Theorem 2.3 *The approximate probability of error $\hat{P}_e$ is given by*

$$\hat{P}_e = \left(1 - \frac{N_s}{M}\right)^{N_u-1} \Phi\left(-\frac{E_b}{\sigma_n}\right) + \sum_{k=1}^{N_u-1} \binom{N_u-1}{k} \left(1 - \frac{N_s}{M}\right)^{N_u-k-1} \left(\frac{N_s}{M}\frac{1}{T_c}\right)^k$$

$$\times \underbrace{\int_{-T}^{T+\delta} \int_{-T}^{T+\delta} \cdots \int_{-T}^{T+\delta}}_{k\ times} \Phi\left(-\frac{E_b + \sum_{l=1}^{k} p(s_l)}{\sigma_n}\right) ds_1 ds_2 \ldots ds_k \qquad (2.15)$$

where $\Phi(x)$ is the Gaussian distribution defined as

$$\Phi(x) := \frac{1}{\sqrt{2\pi}} \int_{-\infty}^{x} e^{-y^2/2}dy.$$

The proof of Theorem 2.3 is given in Section 2.5.5.

It is shown in Appendix A.2 that the approximate probability of error expression converges to the exact probability of error as $M \longrightarrow \infty$.

2.4.1   Rectangular pulses - Analysis

As a special case, we consider the following example of a rectangular pulse. We assume $T = \delta$, with $T_c = 2T + \delta = 3T$, and

$$x(t) = \begin{cases} \sqrt{\frac{e_b}{T}} & ; \text{ for } t \in [0, T] \\ 0 & ; \text{ elsewhere} \end{cases}$$

As shown in Appendix A.3, the approximate expression for the probability of error

is given by

$$\hat{P}_e = \left(1 - \frac{N_s}{M}\right)^{N_u - 1} \Phi\left(-\sqrt{\frac{N_s e_b}{\eta_0}}\right) \tag{2.16}$$

$$+ \frac{1}{2} \sum_{k=1}^{N_u - 1} \binom{N_u - 1}{k} \left(1 - \frac{N_s}{M}\right)^{N_u - 1 - k} \left(\frac{N_s}{M}\right)^k \left(-\sqrt{\frac{N_s \eta_0}{2 e_b}}\right)^k$$

$$\times \sum_{m=0}^{k} \binom{k}{m} (-1)^m F_k\left[\sqrt{\frac{e_b}{2 N_s \eta_0}} (N_s + k - 2m)\right],$$

where $F_k(x)$ is defined as

$$F_k(x) := 2^{-k} e^{-x^2} \left[\frac{{}_1F_1\left(\frac{1+k}{2}; \frac{1}{2}; x^2\right)}{\Gamma\left(1 + \frac{k}{2}\right)} - 2x \frac{{}_1F_1\left(1 + \frac{k}{2}; \frac{3}{2}; x^2\right)}{\Gamma\left(\frac{1+k}{2}\right)}\right]$$

and where ${}_1F_1(a; b; x)$ is the confluent hypergeometric function of the first kind and $\Gamma(x)$ is the gamma function.

2.4.2 Numerical Results

In Figures 2.1, 2.2, and 2.3, the analytical results are plotted for different values of the parameters and compared with both simulations and the Gaussian approximation for the MAI. Since the variance of the MAI depends on the desired user's spreading sequence (as shown in Appendix A.4), the plots of the Gaussian approximation curves are obtained assuming the MAI to be a Gaussian random variable with zero mean and variance

$$\sigma_{max}^2 = \frac{N_s(N_u - 1)}{MT_c} \left(1 + \frac{N_s - 1}{M}\right) \int_{-T}^{T + \delta} p^2(s) ds. \tag{2.17}$$

Note that for $N_s = 1$, the expression in (2.17) is equal to the exact variance, while for $N_s > 1$ expression (2.17) is shown (again in Appendix A.4) to be an upper bound on the exact variance of the MAI. As a consequence, the curve of the Gaussian
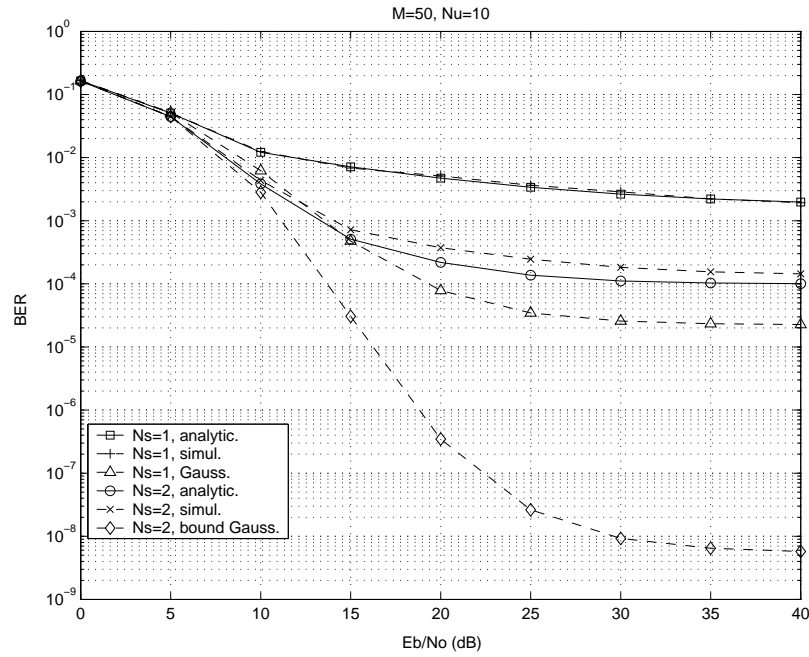
Figure 2.1: Performance analysis for 20 users, M=50
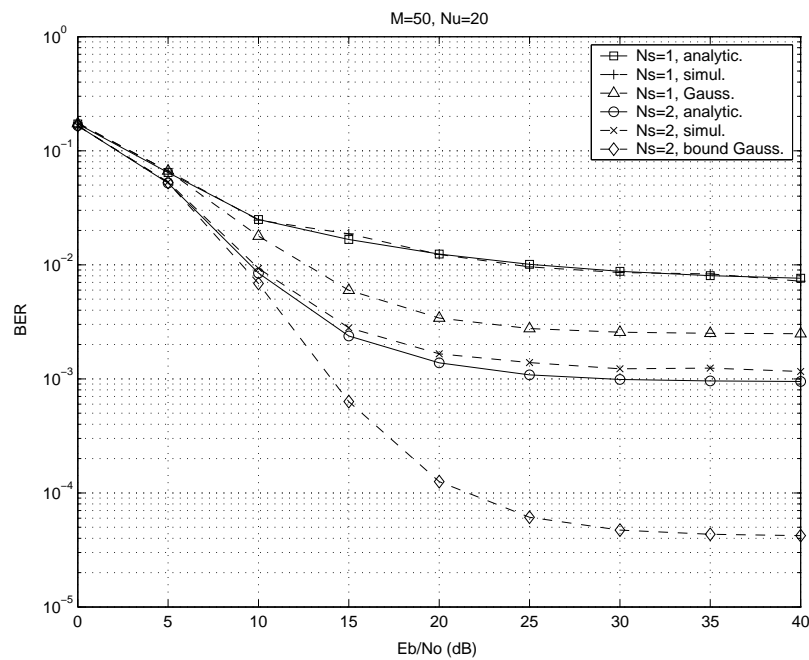
Figure 2.2: Performance analysis for 20 users, M=50

approximation using the actual variance of the MAI would lie somewhere below the

plotted one. As the reader can immediately notice, the accuracy of the analytical
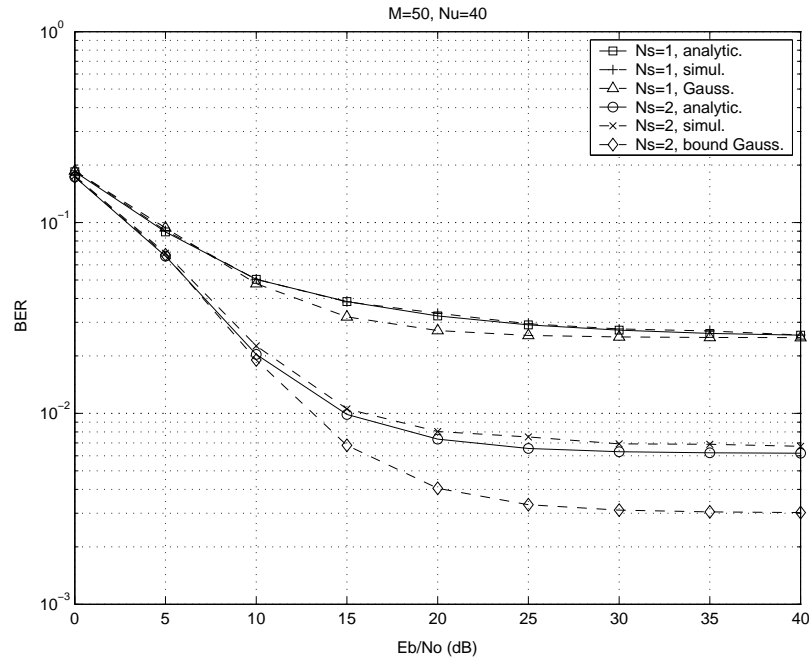
Figure 2.3: Performance analysis for 40 users, M=50

results presented is very high, while the Gaussian approximation (especially for a small number of users) gives very poor results for values of the E_b/N_0 grater than 10 - 15 dB, getting worse as the E_b/N_0 increases. It is worth stressing that the Gaussian approximation curve using the actual variance would lie below the plotted one, giving even more optimistic predictions.

Figure 2.4 shows the performance of the system for $N_s = 1$ and $N_s = 2$, keeping the bit rate fixed. Since the bit rate of the system is dictated by the symbol duration, it equals $1/N_s T_f$; to keep the bit rate fixed by increasing N_s, the frame has to be "chopped" in half, and the processing gain M would be halved as well. While reducing the processing gain enhances the probability of a collision between the desired user's signal and an interfering pulse, the coding gain achieved by a repetition code yields a net moderate improvement in the performance. One further advantage of using a repetition code is to reduce the peak transmitted power.

Finally, Figure 2.5 shows the dependance of the variance fractional error on the
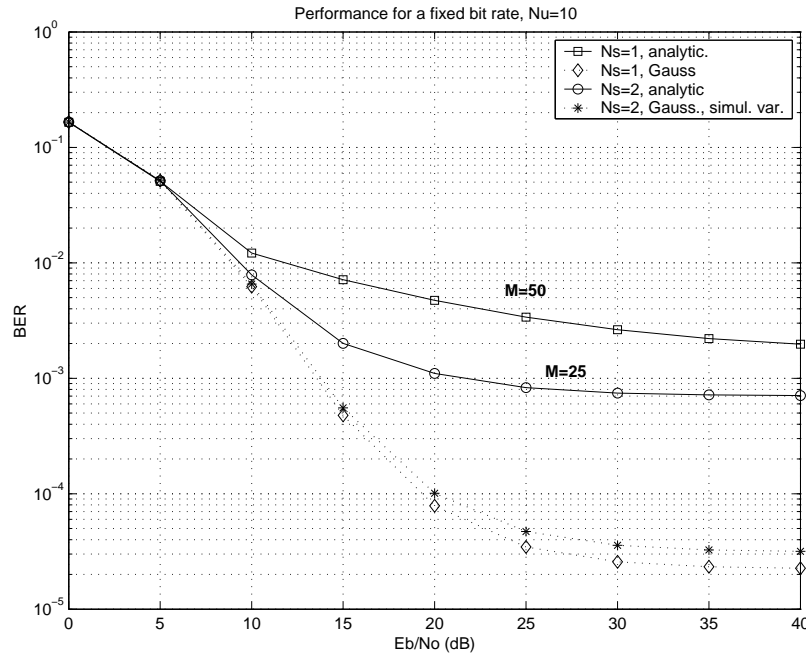
Figure 2.4: Performance analysis for 10 users, fixed bit rate

processing gain M and the repetition number N_s. As can be seen, the upper bound becomes tighter as M increases, while the approximate variance evaluated through the approximate characteristic function is always very close to the actual variance of the system.

2.5 Derivations

2.5.1 Proof of Equation (2.7)

We show how the characteristic function (2.6) can be written in the form of (2.7). Recall the expression of the MAI (2.6):

$$m_1 = \sum_{j=0}^{N_s-1} \int_{jT_f}^{(j+1)T_f} \overbrace{v(t - jT_f - c_jT_c)}^{(a)} \left\{ \sum_{i=0}^{N_s-1} \overbrace{x(t - (i + \eta_1)T_f - c_i^{(1)}T_c - \delta d_0^{(1)} - \overline{\tau}_1)}^{(b)} \right.$$
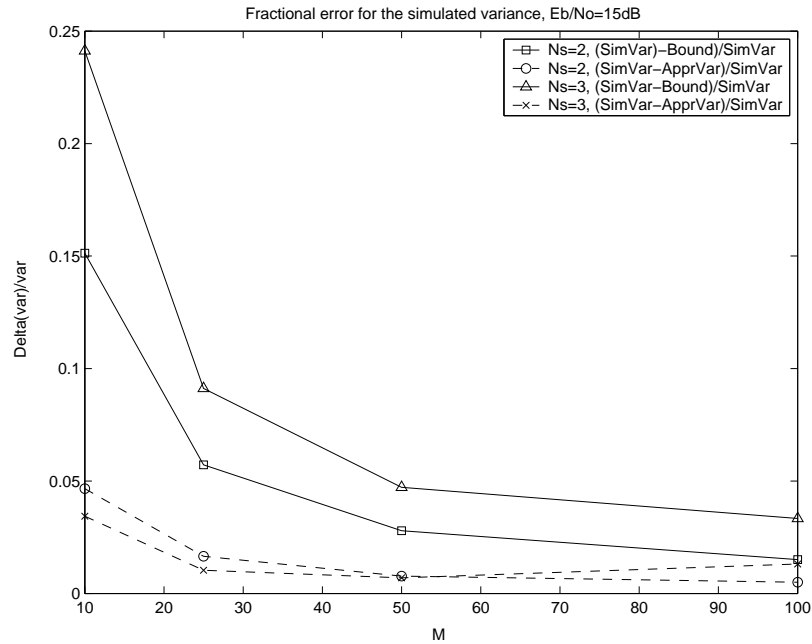
Figure 2.5: Error between the simulated variance, the upper bound and the approximate variance

$$+ \sum_{i=-N_s}^{-1} \overbrace{x(t - (i + \eta_1)T_f - c_i^{(1)}T_c - \delta d_{-1}^{(1)} - \overline{\tau}_1)}^{(c)} \Bigg\} \, dt.$$

In order to have overlapping regions, we need the supports of the different components of the integrand to overlap; that is, for $i = 0, 1, \ldots, N_s - 1$,

$$\overbrace{[jT_f + c_jT_c, jT_f + c_jT_c + T + \delta]}^{(i)} \cap$$

$$\overbrace{[(i + \eta_1)T_f + c_i^{(1)}T_c + \delta d_0^{(1)} + \overline{\tau}_1, (i + \eta_1)T_f + c_i^{(1)}T_c + \delta d_0^{(1)} + \overline{\tau}_1 + T]}^{(ii)} \neq \emptyset$$

or, for $i = -N_s, -N_s + 1, \ldots, -1$

$$\overbrace{[jT_f + c_jT_c, jT_f + c_jT_c + T + \delta]}^{(i)} \cap$$

$$\overbrace{[(i + \eta_1)T_f + c_i^{(1)}T_c + \delta d_{-1}^{(1)} + \overline{\tau}_1, (i + \eta_1)T_f + c_i^{(1)}T_c + \delta d_{-1}^{(1)} + \overline{\tau}_1 + T]}^{(iii)} \neq \emptyset$$

where *(i)*, *(ii)*, *(iii)* are the supports of *(a)*, *(b)* and *(c)*, respectively. Since $\bar{\tau}_1$ is uniformly distributed over $[0, T_f]$, $c_j T_c$ and $c_i^{(1)} T_c$ are always less than T_f for every i and j, and δ is a delay smaller than T_c and much smaller than T_f. A necessary condition for the above supports to overlap is the following:

$$
\begin{cases}
i + \eta_1 = j \\
or \\
i + \eta_1 = j - 1
\end{cases}
\Longrightarrow
\begin{cases}
i = j - \eta_1 \\
or \\
i = j - \eta_1 - 1
\end{cases}
$$

In order to prove the necessity of the above result, we need to prove that for $i \leq j - \eta_1 - 2$ or $i \geq j - \eta_1 + 1$, the previous intervals do not overlap.

Assume $i \geq j - \eta_1 + 1 \Rightarrow i + \eta_1 \geq j + 1$. Then

$$
\begin{aligned}
(i + \eta_1) T_f + c_i^{(1)} T_c + \delta d_m^{(1)} + \bar{\tau}_1 &\geq (i + \eta_1) T_f \geq (j + 1) T_f = j T_f + M T_c \\
&\geq j T_f + (c_j + 1) T_c > j T_f + c_j T_c + T + \delta
\end{aligned}
$$

since $T_c > T + \delta$. In the same way, for $i + \eta_1 \leq j - 2$

$$
(i + \eta_1) T_f + c_i^{(1)} T_c + \delta d_m^{(1)} + \bar{\tau}_1 \leq (i + \eta_1 + 2) T_f \leq j T_f \leq j T_f + c_j T_c
$$

For $j = 0, 1, \ldots, \eta_1 - 1$, the two solutions $i = j - \eta_1$ and $i = j - \eta_1 - 1$ are clearly negative; on the other hand, for $j = \eta_1 + 1, \eta_1 + 2, \ldots, N_s - 1$, the two solutions $i = j - \eta_1$ and $i = j - \eta_1 - 1$ are positive. For $j = \eta_1$, clearly $i = 0$ or $i = -1$.

In light of the above discussion, after defining the function

$$
p(u) := \int_0^{T+\delta} v(t) x(t - u) dt
$$

and the random variables $s_j^{(1)}(d_i) := c_{j-\eta_1}^{(1)} T_c + \delta d_i^{(1)}$, the single-interferer component can be simplified as follows:

$$\begin{aligned}
m_1 &= \sum_{j=0}^{\eta_1-1} \int_{jT_f}^{(j+1)T_f} v(t - jT_f - c_j T_c) \\
&\quad \times \Big[x(t - jT_f - c_{j-\eta_1}^{(1)} T_c - \delta d_{-1}^{(1)} - \overline{\tau}_1) \\
&\qquad + x(t - (j-1)T_f - c_{j-\eta_1-1}^{(1)} T_c - \delta d_{-1}^{(1)} - \overline{\tau}_1) \Big] dt \\
&\quad + \int_{\eta_1 T_f}^{(\eta_1+1)T_f} v(t - \eta_1 T_f - c_{\eta_1} T_c) \\
&\qquad \times \Big[x(t - \eta_1 T_f - c_0^{(1)} T_c - \delta d_0^{(1)} - \overline{\tau}_1) \\
&\qquad\quad + x(t - (\eta_1-1)T_f - c_{-1}^{(1)} T_c - \delta d_{-1}^{(1)} - \overline{\tau}_1) \Big] dt \\
&\quad + \sum_{j=\eta_1+1}^{N_s-1} \int_{jT_f}^{(j+1)T_f} v(t - jT_f - c_j T_c) \\
&\qquad \times \Big[x(t - jT_f - c_{j-\eta_1}^{(1)} T_c - \delta d_{-1}^{(1)} - \overline{\tau}_1) \\
&\qquad\quad + x(t - (j-1)T_f - c_{j-\eta_1-1}^{(1)} T_c - \delta d_{-1}^{(1)} - \overline{\tau}_1) \Big] dt \\
&= \sum_{j=0}^{\eta_1-1} [p(\overline{\tau}_1 + s_j^{(1)}(d_{-1}^{(1)}) - c_j T_c) + p(\overline{\tau}_1 - T_f + s_{j-1}^{(1)}(d_{-1}^{(1)}) - c_j T_c)] \\
&\quad + [p(\overline{\tau}_1 + s_{\eta_1}^{(1)}(d_0^{(1)}) - c_{\eta_1} T_c) + p(\overline{\tau}_1 - T_f + s_{\eta_1-1}^{(1)}(d_{-1}^{(1)}) - c_{\eta_1} T_c)] \\
&\quad + \sum_{j=\eta_1+1}^{N_s-1} [p(\overline{\tau}_1 + s_j^{(1)}(d_0^{(1)}) - c_j T_c) + p(\overline{\tau}_1 - T_f + s_{j-1}^{(1)}(d_0^{(1)}) - c_j T_c)]. \quad \square
\end{aligned}$$

2.5.2 Proof of Theorem 2.1

Set $a_i(k) := c_i - k$, for $i = 0, 1, \ldots, N_s - 1$ and $k = 0, 1, \ldots, M - 1$. Note that

$$a_i(k) \in \{-M+1, -M+2, \ldots, M-1\}.$$

Then, (2.9) can be written as

$$\varphi_{m_1}(\omega) = \frac{1}{T_f} \frac{1}{M^{N_s+1}} \sum_{k=0}^{M-1} \int_0^{T_c} \left(\sum_{l_{-1}=0}^{M-1} e^{j\omega p(s - (a_0(k) + M - l_{-1})T_c)} \right)$$

$$\times \quad \prod_{i=0}^{N_s-2} \left(\sum_{l_i=0}^{M-1} e^{j\omega[p(s-(a_i(k)-l_i)T_c)+p(s-(a_{i+1}(k)+M-l_i)T_c)]} \right)$$

$$\times \left(\sum_{l_{N_s-1}=0}^{M-1} e^{j\omega p(s-(a_{N_s-1}(k)-l_{N_s-1})T_c)} \right) ds.$$

Since $T_c = 2T + \delta$, we break the above integration in two non-overlapping regions:

$$
\begin{aligned}
\varphi_{m_1}(\omega) &= \frac{1}{T_f}\frac{1}{M^{N_s+1}}\sum_{k=0}^{M-1}\int_0^{T+\delta}\left(\sum_{l_{-1}=0}^{M-1}e^{j\omega p(s-(a_0(k)+M-l_{-1})T_c)}\right) \\
&\quad \times \prod_{i=0}^{N_s-2}\left(\sum_{l_i=0}^{M-1}e^{j\omega[p(s-(a_i(k)-l_i)T_c)+p(s-(a_{i+1}(k)+M-l_i)T_c)]}\right) \\
&\quad \times \left(\sum_{l_{N_s-1}=0}^{M-1}e^{j\omega p(s-(a_{N_s-1}(k)-l_{N_s-1})T_c)}\right)ds \\
&+ \frac{1}{T_f}\frac{1}{M^{N_s+1}}\sum_{k=0}^{M-1}\int_{T+\delta}^{T_c}\left(\sum_{l_{-1}=0}^{M-1}e^{j\omega p(s-(a_0(k)+M-l_{-1})T_c)}\right) \\
&\quad \times \prod_{i=0}^{N_s-2}\left(\sum_{l_i=0}^{M-1}e^{j\omega[p(s-(a_i(k)-l_i)T_c)+p(s-(a_{i+1}(k)+M-l_i)T_c)]}\right) \\
&\quad \times \left(\sum_{l_{N_s-1}=0}^{M-1}e^{j\omega p(s-(a_{N_s-1}(k)-l_{N_s-1})T_c)}\right)ds \\
&= \frac{1}{T_f}\frac{1}{M^{N_s+1}}\sum_{k=0}^{M-1}\int_0^{T+\delta}\left(\sum_{l_{-1}=0}^{M-1}e^{j\omega p(s-(a_0(k)+M-l_{-1})T_c)}\right) \quad (2.18) \\
&\quad \times \prod_{i=0}^{N_s-2}\left(\sum_{l_i=0}^{M-1}e^{j\omega[p(s-(a_i(k)-l_i)T_c)+p(s-(a_{i+1}(k)+M-l_i)T_c)]}\right) \\
&\quad \times \left(\sum_{l_{N_s-1}=0}^{M-1}e^{j\omega p(s-(a_{N_s-1}(k)-l_{N_s-1})T_c)}\right)ds \\
&+ \frac{1}{T_f}\frac{1}{M^{N_s+1}}\sum_{k=0}^{M-1}\int_{-T}^0\left(\sum_{l_{-1}=0}^{M-1}e^{j\omega p(s-(a_0(k)-1+M-l_{-1})T_c)}\right) \quad (2.19) \\
&\quad \times \prod_{i=0}^{N_s-2}\left(\sum_{l_i=0}^{M-1}e^{j\omega[p(s-(a_i(k)-1-l_i)T_c)+p(s-(a_{i+1}(k)-1+M-l_i)T_c)]}\right)
\end{aligned}
$$

$$\times \left(\sum_{l_{N_s-1}=0}^{M-1} e^{j\omega p(s-(a_{N_s-1}(k)-1-l_{N_s-1})T_c)} \right) ds$$

where the last step is obtained by shifting the second integral by T_c.

Note that $a_i(k) - 1 = c_i - k - 1 = a_i(k+1)$ for $k = 0, 1, \ldots, M-2$. Define $a_i(M) := c_i - M \in \{-M, -M+1, \ldots, -1\}$, and rewrite the above expression by isolating the term with $k = 0$ in (2.18) and the term with $k = M-1$ in (2.19).

Therefore,

$$
\begin{aligned}
\varphi_{m_1}(\omega) \;=\; & \frac{1}{T_f}\frac{1}{M^{N_s+1}} \int_0^{T+\delta} \left(\sum_{l_{-1}=0}^{M-1} e^{j\omega p(s-(a_0(0)+M-l_{-1})T_c)} \right) && (2.20) \\
& \times \prod_{i=0}^{N_s-2} \left(\sum_{l_i=0}^{M-1} e^{j\omega[p(s-(a_i(0)-l_i)T_c)+p(s-(a_{i+1}(0)+M-l_i)T_c)]} \right) \\
& \times \left(\sum_{l_{N_s-1}=0}^{M-1} e^{j\omega p(s-(a_{N_s-1}(0)-l_{N_s-1})T_c)} \right) ds \\[4pt]
+ & \frac{1}{T_f}\frac{1}{M^{N_s+1}} \sum_{k=1}^{M-1} \int_0^{T+\delta} \left(\sum_{l_{-1}=0}^{M-1} e^{j\omega p(s-(a_0(k)+M-l_{-1})T_c)} \right) && (2.21) \\
& \times \prod_{i=0}^{N_s-2} \left(\sum_{l_i=0}^{M-1} e^{j\omega[p(s-(a_i(k)-l_i)T_c)+p(s-(a_{i+1}(k)+M-l_i)T_c)]} \right) \\
& \times \left(\sum_{l_{N_s-1}=0}^{M-1} e^{j\omega p(s-(a_{N_s-1}(k)-l_{N_s-1})T_c)} \right) ds \\[4pt]
+ & \frac{1}{T_f}\frac{1}{M^{N_s+1}} \sum_{k=0}^{M-2} \int_{-T}^{0} \left(\sum_{l_{-1}=0}^{M-1} e^{j\omega p(s-(a_0(k+1)+M-l_{-1})T_c)} \right) && (2.22) \\
& \times \prod_{i=0}^{N_s-2} \left(\sum_{l_i=0}^{M-1} e^{j\omega[p(s-(a_i(k+1)-l_i)T_c)+p(s-(a_{i+1}(k+1)+M-l_i)T_c)]} \right) \\
& \times \left(\sum_{l_{N_s-1}=0}^{M-1} e^{j\omega p(s-(a_{N_s-1}(k+1)-l_{N_s-1})T_c)} \right) ds \\[4pt]
+ & \frac{1}{T_f}\frac{1}{M^{N_s+1}} \int_{-T}^{0} \left(\sum_{l_{-1}=0}^{M-1} e^{j\omega p(s-(a_0(M)+M-l_{-1})T_c)} \right) && (2.23)
\end{aligned}
$$

$$\times \prod_{i=0}^{N_s-2} \left(\sum_{l_i=0}^{M-1} e^{j\omega[p(s-(a_i(M)-l_i)T_c)+p(s-(a_{i+1}(M)+M-l_i)T_c)]} \right)$$

$$\times \left(\sum_{l_{N_s-1}=0}^{M-1} e^{j\omega p(s-(a_{N_s-1}(M)-l_{N_s-1})T_c)} \right) ds$$

With the simple change of variables $r = k+1$ in (2.22), combining (2.21) and (2.22) and rearranging the expression, we have

$$\varphi_{m_1}(\omega) = \frac{1}{T_f} \frac{1}{M^{N_s+1}} \sum_{k=1}^{M-1} \int_{-T}^{T+\delta} \left(\sum_{l_{-1}=0}^{M-1} e^{j\omega p(s-(a_0(k)+M-l_{-1})T_c)} \right)$$

$$\times \prod_{i=0}^{N_s-2} \left(\sum_{l_i=0}^{M-1} e^{j\omega[p(s-(a_i(k)-l_i)T_c)+p(s-(a_{i+1}(k)+M-l_i)T_c)]} \right)$$

$$\times \left(\sum_{l_{N_s-1}=0}^{M-1} e^{j\omega p(s-(a_{N_s-1}(k)-l_{N_s-1})T_c)} \right) ds$$

$$+ \frac{1}{T_f} \frac{1}{M^{N_s+1}} \int_0^{T+\delta} \left(\sum_{l_{-1}=0}^{M-1} e^{j\omega p(s-(a_0(0)+M-l_{-1})T_c)} \right)$$

$$\times \prod_{i=0}^{N_s-2} \left(\sum_{l_i=0}^{M-1} e^{j\omega[p(s-(a_i(0)-l_i)T_c)+p(s-(a_{i+1}(0)+M-l_i)T_c)]} \right)$$

$$\times \left(\sum_{l_{N_s-1}=0}^{M-1} e^{j\omega p(s-(a_{N_s-1}(0)-l_{N_s-1})T_c)} \right) ds$$

$$+ \frac{1}{T_f} \frac{1}{M^{N_s+1}} \int_{-T}^0 \left(\sum_{l_{-1}=0}^{M-1} e^{j\omega p(s-(a_0(M)+M-l_{-1})T_c)} \right)$$

$$\times \prod_{i=0}^{N_s-2} \left(\sum_{l_i=0}^{M-1} e^{j\omega[p(s-(a_i(M)-l_i)T_c)+p(s-(a_{i+1}(M)+M-l_i)T_c)]} \right)$$

$$\times \left(\sum_{l_{N_s-1}=0}^{M-1} e^{j\omega p(s-(a_{N_s-1}(M)-l_{N_s-1})T_c)} \right) ds$$

$$= \frac{1}{T_f} \frac{1}{M^{N_s+1}} \sum_{k=1}^{M-1} \int_{-T}^{T+\delta} A_{-1}(k) \prod_{i=0}^{N_s-2} A_i(k) A_{N_s-1}(k) ds \qquad (2.24)$$

$$+ \frac{1}{T_f} \frac{1}{M^{N_s+1}} \int_0^{T+\delta} A_{-1}(0) \prod_{i=0}^{N_s-2} A_i(0) A_{N_s-1}(0) ds \qquad (2.25)$$

$$+ \quad \frac{1}{T_f} \frac{1}{M^{N_s+1}} \int_{-T}^{0} A_{-1}(M) \prod_{i=0}^{N_s-2} A_i(M) A_{N_s-1}(M) ds \qquad (2.26)$$

where, for $k = 0, 1, \ldots, M$, we have defined

$$A_{-1}(k) \quad := \quad \sum_{l_{-1}=0}^{M-1} e^{j\omega p(s-(a_0(k)+M-l_{-1})T_c)} \qquad (2.27)$$

$$A_i(k) \quad := \quad \sum_{l_i=0}^{M-1} e^{j\omega[p(s-(a_i(k)-l_i)T_c)+p(s-(a_{i+1}(k)+M-l_i)T_c)]} \qquad (2.28)$$

$$A_{N_s-1}(k) \quad := \quad \sum_{l_{N_s-1}=0}^{M-1} e^{j\omega p(s-(a_{N_s-1}(k)-l_{N_s-1})T_c)} \qquad (2.29)$$

and we have used the following notation:

$$\prod_{i=\alpha}^{\beta} \gamma_i := \begin{cases} \gamma_\alpha \, \gamma_{\alpha+1} \ldots \gamma_\beta & ; \text{ for } \alpha \leq \beta \\ 1 & ; \text{ for } \alpha > \beta \end{cases}$$

Note that the support of $p(s - mT_c)$ is $[mT_c - T, mT_c + T + \delta]$, which overlaps $[-T, T + \delta]$ only for $m = 0$. As a consequence, the exponents in the above expression of the form $p(s - (a_i(k) - l_i)T_c)$ are always zero in the region $[-T, T + \delta]$, except when $l_i = a_i(k)$ and $a_i(k) \in \{0, 1, \ldots, M-1\}$. On the other hand, the exponents of the form $p(s - (a_{i+1}(k) + M - l_i)T_c)$ are non-zero only for $l_i = a_{i+1}(k) + M$. Now $0 \leq l_i \leq M - 1 \implies 0 \leq a_{i+1}(k) + M \leq M - 1 \implies -M \leq a_{i+1}(k) \leq -1$. Since $-(M-1) \leq a_{i+1}(k) \leq M - 1$, this implies $a_{i+1}(k) \notin \{0, 1, \ldots, M-1\}$. Set

$$V_0 \quad := \quad M$$

$$V_1 \quad := \quad e^{j\omega p(s)} + M - 1$$

$$V_2 \quad := \quad 2e^{j\omega p(s)} + M - 2$$

Since every summation in (2.27)-(2.29) has at most two l_i's which make the exponent

non-zero within the interval $[-T, T + \delta]$ (i.e., $M - 2$ terms in every summation are identically one), for the k-th integrand in (2.24) the following holds:

$$A_{-1}(k) = \begin{cases} V_0 & ; \text{ when } a_0(k) \in \{0, 1, \ldots, M - 1\} \\ V_1 & ; \text{ when } a_0(k) \notin \{0, 1, \ldots, M - 1\} \end{cases} \tag{2.30}$$

and

$$A_{N_s-1}(k) = \begin{cases} V_0 & ; \text{ when } a_{N_s-1}(k) \notin \{0, 1, \ldots, M - 1\} \\ V_1 & ; \text{ when } a_{N_s-1}(k) \in \{0, 1, \ldots, M - 1\} \end{cases} \tag{2.31}$$

while the inner term can only be equal to

$$A_i(k) = \begin{cases} V_0 & ; \text{ when } \begin{cases} a_i(k) \notin \{0, 1, \ldots, M - 1\} \\ \& \\ a_{i+1}(k) \in \{0, 1, \ldots, M - 1\} \end{cases} \\ \\ V_1 & ; \text{ when } \left\{ \begin{cases} a_i(k) \in \{0, 1, \ldots, M - 1\} \\ \& \\ a_{i+1}(k) \in \{0, 1, \ldots, M - 1\} \end{cases} \\ \text{ or } \\ \begin{cases} a_i(k) \notin \{0, 1, \ldots, M - 1\} \\ \& \\ a_{i+1}(k) \notin \{0, 1, \ldots, M - 1\} \end{cases} \right\} \\ \\ V_2 & ; \text{ when } \begin{cases} a_i(k) \in \{0, 1, \ldots, M - 1\} \\ \& \\ a_{i+1}(k) \notin \{0, 1, \ldots, M - 1\} \end{cases} \end{cases} \tag{2.32}$$

Contribution of (2.24)

For a specific k, using (2.30)-(2.32), we have

$$\int_{-T}^{T+\delta} A_{-1}(k) \prod_{i=0}^{N_s-2} A_i(k) A_{N_s-1}(k) ds = \int_{-T}^{T+\delta} V_0^{y(k)} V_2^{z(k)} V_1^{N_s+1-y(k)-z(k)} ds \qquad (2.33)$$

where

$$y(k) \ := \ |\{i \in \{-1, 0, \ldots, N_s - 1\} \text{ such that } A_i = V_0\}|$$

$$z(k) \ := \ |\{i \in \{0, 1, \ldots, N_s - 2\} \text{ such that } A_i = V_2\}|$$

Define $S := \{0, 1, \ldots, M - 1\}$. We now prove the following:

Proposition 2.1 $y(k) = z(k) + 1$ *for every* $k \in S$

Proof. We prove this result by induction on N_s. For $N_s = 1$, (2.33) equals $\int_{-T}^{T+\delta}$ $A_{-1}(k) \ A_0(k) ds$. Since $A_{-1}(k)$ and $A_0(k)$ can only equal V_0 or V_1 according to the value of $a_0(k)$ as shown in Table 2.1, (2.33) equals $\int_{-T}^{T+\delta} V_0 V_1 ds$. This result means,

Table 2.1: Proof of Proposition 2.1 (I)

	$a_0(k) \in S$	$a_0(k) \notin S$
$A_{-1}(k)$	V_0	V_1
$A_0(k)$	V_1	V_0

in terms of $y(k)$ and $z(k)$, that $y(k) = 1$, and $z(k) = 0$.

For $N_s = 2$, (2.33) equals

$$\int_{-T}^{T+\delta} A_{-1}(k) A_0(k) A_1(k) ds \qquad (2.34)$$

and the values taken by each term in the integrand are shown, according to the possible values taken by $a_0(k)$ and $a_1(k)$, in Table 2.2. Therefore, (2.34) equals

Table 2.2: Proof of Proposition 2.1 (II)

	$a_0(k) \in S$		$a_0(k) \notin S$	
$A_{-1}(k)$	V_0		V_1	
	$a_1(k) \in S$	$a_1(k) \notin S$	$a_1(k) \in S$	$a_1(k) \notin S$
$A_0(k)$	V_1	V_2	V_0	V_1
$A_1(k)$	V_1	V_0	V_1	V_0

$\int_{-T}^{T+\delta} V_0 V_1^2 ds$ or $\int_{-T}^{T+\delta} V_0^2 V_1 ds$, and the relation $y(k) = z(k) + 1$ still holds in each of the four columns corresponding to all possible values of $a_0(k)$ and $a_1(k)$.

Suppose now the hypothesis is true for $N_s = 1, 2, \ldots, m$. We show it is true for $N_s = m + 1$. Since $\{a_0(k), a_1(k), \ldots, a_{m-1}\}$ is specified when $N_s = m$, increasing N_s by one affects only terms $A_{m-1}(k)$ and $A_m(k)$. Specifically, there will be a new term $A_{m-1}(k)$, whose value depends on $(a_{m-1}(k), a_m(k))$, which also affects the value of the new end term $A_m(k)$. Note that the values of the exponents $y(k)$ and $z(k)$ change only when terms equal to V_0 or V_2 are added or subtracted. The additional middle term $A_{m-1}(k)$ and the new end term $A_m(k)$ take values as shown in Table 2.3. In

Table 2.3: Proof of Proposition 2.1 (III)

	(A) $a_{m-1}(k) \in S$ & $a_m(k) \in S$	(B) $a_{m-1}(k) \in S$ & $a_m(k) \notin S$	(C) $a_{m-1}(k) \notin S$ & $a_m(k) \in S$	(D) $a_{m-1}(k) \notin S$ & $a_m(k) \notin S$
$A_{m-1}(k)$ (new middle term)	V_1	V_2	V_0	V_1
$A_m(k)$ (new end term)	V_1	V_0	V_1	V_0
$A_{m-1}(k)$ (old end term)	V_1	V_1	V_0	V_0
comparison	no change	add V_2 add V_0	subtract V_0 add V_0	subtract V_0 add V_0

Column (A), term $A_{m-1}(k)$ stays the same, while $A_m(k)$ equals V_1, without affecting the values of $y(k)$ and $z(k)$. In Column (B), both V_0 and V_2 are added, incrementing both $y(k)$ and $z(k)$; therefore, the relation $y(k) = z(k) + 1$ still holds. Finally, both in Column (C) and (D), one term equal to V_0 is subtracted, while another term V_0 is added, without affecting $y(k)$ and $z(k)$.

Therefore, the relation $y(k) = z(k) + 1$ continues to hold for $N_s = m + 1$. $\square$

Using Proposition 2.1, (2.24) equals

$$\frac{1}{T_f} \frac{1}{M^{N_s+1}} \sum_{k=1}^{M-1} \int_{-T}^{T+\delta} \left(\sum_{l_{-1}=0}^{M-1} e^{j\omega p(s - (a_0(k) + M - l_{-1})T_c)} \right)$$

$$\times \prod_{i=0}^{N_s-2} \left(\sum_{l_i=0}^{M-1} e^{j\omega[p(s - (a_i(k) - l_i)T_c) + p(s - (a_{i+1}(k) + M - l_i)T_c)]} \right)$$

$$\times \left(\sum_{l_{N_s-1}=0}^{M-1} e^{j\omega p(s - (a_{N_s-1}(k) - l_{N_s-1})T_c)} \right) ds$$

$$= \frac{1}{T_f} \frac{1}{M^{N_s}} \sum_{k=1}^{M-1} \int_{-T}^{T+\delta} M^{x(k)} \left(2e^{j\omega p(s)} + M - 2 \right)^{x(k)} \left(e^{j\omega p(s)} + M - 1 \right)^{N_s - 2x(k)} ds$$

Contribution of (2.25)

Note that $a_i(0) = c_i \in \{0, 1, \ldots, M - 1\}$ for all i. Therefore, for $i \geq 0$,

$$A_{-1}(0) = V_0$$

$$A_i(0) = V_1 \; ; \; i = 0, 1, \ldots, N_s - 2$$

$$A_{N_s-1}(0) = V_1$$

Thus (2.25) equals to

$$\frac{1}{T_f} \frac{1}{M^{N_s+1}} \int_0^{T+\delta} A_{-1}(0) \prod_{i=0}^{N_s-2} A_i(0) A_{N_s-1}(0) ds$$

$$= \frac{1}{T_f} \frac{1}{M^{N_s+1}} \int_0^{T+\delta} M \left(e^{j\omega p(s)} + M - 1 \right)^{N_s} ds$$

Contribution of (2.26)

Since $a_i(M) = c_i - M \notin \{0, 1, \ldots, M-1\}$ for all i, for (2.26) the following holds:

$$
\begin{aligned}
A_{-1}(M) &= V_1 \\
A_i(M) &= V_1 \ ; \ i = 0, 1, \ldots, N_s - 2 \\
A_{N_s - 1}(M) &= V_0.
\end{aligned}
$$

Then (2.26) equals

$$
\begin{aligned}
\frac{1}{T_f} \frac{1}{M^{N_s + 1}} \int_{-T}^{0} A_{-1}(M) \prod_{i=0}^{N_s - 2} A_i(M) A_{N_s - 1}(M) ds \\
= \frac{1}{T_f} \frac{1}{M^{N_s + 1}} \int_{-T}^{0} M \left(e^{j\omega p(s)} + M - 1 \right)^{N_s} ds.
\end{aligned}
$$

Combining (2.25) and (2.26), we have

$$
\frac{1}{T_f} \frac{1}{M^{N_s}} \int_{-T}^{T+\delta} \left(e^{j\omega p(s)} + M - 1 \right)^{N_s} ds.
$$

The characteristic function $\varphi_{m_1}(\omega)$ can now be written as

$$
\begin{aligned}
\varphi_{m_1}(\omega) = \ & \frac{1}{T_f} \frac{1}{M^{N_s}} \sum_{k=1}^{M-1} \int_{-T}^{T+\delta} M^{z(k)} \left(2e^{j\omega p(s)} + M - 2 \right)^{z(k)} \\
& \qquad \qquad \qquad \left(e^{j\omega p(s)} + M - 1 \right)^{N_s - 2z(k)} ds \\
& + \frac{1}{T_f} \frac{1}{M^{N_s}} \int_{-T}^{T+\delta} \left(e^{j\omega p(s)} + M - 1 \right)^{N_s} ds
\end{aligned}
$$

which, by setting $z(0) := 0$, can be rewritten as follows:

$$
\begin{aligned}
\varphi_{m_1}(\omega) = \ & \frac{1}{T_f} \frac{1}{M^{N_s}} \sum_{k=0}^{M-1} \int_{-T}^{T+\delta} M^{z(k)} \left(2e^{j\omega p(s)} + M - 2 \right)^{z(k)} \\
& \qquad \qquad \qquad \left(e^{j\omega p(s)} + M - 1 \right)^{N_s - 2z(k)} ds. \ \square
\end{aligned}
$$

2.5.3 Two-step approximation

Note that the following holds:

$$M^z \left(2e^{j\omega p(s)} + M - 2\right)^z = \left(e^{j\omega p(s)} + M - 1\right)^{2z} - \left(e^{j\omega p(s)} - 1\right)^{2z}$$

Since $\left|e^{j\omega p(s)} + M - 1\right| \gg \left|e^{j\omega p(s)} - 1\right|$, the above expression can be approximated only by the first term, and the integrand in (2.10) can be approximated as follows:

$$M^{z(k)} \left(2e^{j\omega p(s)} + M - 2\right)^{z(k)} \left(e^{j\omega p(s)} + M - 1\right)^{N_s - 2z(k)} \approx \left(e^{j\omega p(s)} + M - 1\right)^{N_s} \quad (2.35)$$

Recall the binomial expansion approximation $(a + b)^n \approx a^n + na^{n-1}b$, which is valid when $|b| \ll |a|$. Since $\left|e^{j\omega p(s)}\right| \ll |M - 1|$ for M large, (2.35) can be approximated by $(M - 1)^{N_s} + N_s e^{j\omega p(s)}$. Substituting this approximate result into (2.10) leads, after some manipulations, to (2.11), which is the approximate function used in Theorem 2.2.

$\square$

2.5.4 Proof of Theorem 2.2

$\hat{\varphi}(\omega)$ is a characteristic function

We first show that $\hat{\varphi}(\omega)$ of (2.11) is indeed a characteristic function, i.e., we prove that

i) $\hat{\varphi}(0) = 1$;

ii) $\hat{\varphi}(\omega)$ is non-negative definite.

Clearly,

$$\hat{\varphi}(0) = \left(1 - \frac{N_s}{M}\right) + \frac{N_s}{M} \frac{1}{T_c} \int_{-T}^{T+\delta} dt = 1$$

To prove *ii)*, we need to show that

- $\hat{\varphi}(\omega)$ is continuous;

- for any positive integer N, any real $\omega_1, \ldots, \omega_N$ and any complex $\xi_1, \ldots, \xi_N$, the sum

$$S = \sum_{i=1}^{N} \sum_{k=1}^{N} \hat{\varphi}(\omega_i - \omega_k) \xi_i \bar{\xi}_k$$

  is real and non-negative.

To show that $\hat{\varphi}(\omega)$ is continuous in ω, we want to show that

$$\lim_{\omega \to \omega_0} \hat{\varphi}(\omega) = \hat{\varphi}(\omega_0)$$

for every ω_0. Note that

$$\lim_{\omega \to \omega_0} \hat{\varphi}(\omega) = \lim_{\omega \to \omega_0} \left\{ \left(1 - \frac{N_s}{M} \right) + \frac{N_s}{M} \frac{1}{T_c} \int_{-T}^{T+\delta} e^{j\omega p(t)} dt \right\}$$

and we can take the limit inside the integral by using dominated convergence, since $\left| e^{j\omega p(t)} \right| \le 1$, $\int_{-T}^{T+\delta} dt = 2T + \delta < \infty$, and $e^{j\omega p(t)}$ is a continuous function in ω.

To prove that

$$S = \sum_{i=1}^{N} \sum_{k=1}^{N} \hat{\varphi}(\omega_i - \omega_k) \xi_i \bar{\xi}_k$$

is real and non-negative, we have

$$
\begin{aligned}
S &= \left(1 - \frac{N_s}{M} \right) \left| \sum_{k=1}^{N} \xi_k \right|^2 + \sum_{i=1}^{N} \sum_{k=1}^{N} \frac{N_s}{M} \frac{1}{T_c} \int_{-T}^{T+\delta} e^{j(\omega_i - \omega_k)p(t)} dt \ \xi_i \bar{\xi}_k \\
&= \left(1 - \frac{N_s}{M} \right) \left| \sum_{k=1}^{N} \xi_k \right|^2 + \frac{N_s}{M} \frac{1}{T_c} \int_{-T}^{T+\delta} \left(\sum_{i=1}^{N} \xi_i e^{j\omega_i p(t)} \right) \left(\sum_{k=1}^{N} \bar{\xi}_k e^{-j\omega_k p(t)} \right) dt \\
&= \left(1 - \frac{N_s}{M} \right) \left| \sum_{k=1}^{N} \xi_k \right|^2 + \frac{N_s}{M} \frac{1}{T_c} \int_{-T}^{T+\delta} \left| \sum_{k=1}^{N} \xi_k e^{j\omega_k p(t)} \right|^2 dt
\end{aligned}
$$

which is clearly real and non-negative for $M \ge N_s$. $\square$

Bound on $\Delta\varphi(\omega)$

Let $\Delta\varphi(\omega) := \varphi_{m_1}(\omega) - \hat{\varphi}(\omega)$, and we simplify the expression for the characteristic function (2.10) by introducing the following notation: $a := e^{j\omega p(s)} + M - 1$ and $b := e^{j\omega p(s)} - 1$. Therefore, we rewrite

$$
\begin{aligned}
\varphi_{m_1}(\omega) &= \frac{1}{T_f}\frac{1}{M^{N_s}}\sum_{k=0}^{M-1}\int_{-T}^{T+\delta}(a-b)^{z(k)}(a+b)^{z(k)}a^{N_s-2z(k)}ds \\
&= \frac{1}{T_f}\sum_{k=0}^{M-1}\int_{-T}^{T+\delta}\left(\frac{a}{M}\right)^{N_s}\left(1-\frac{b^2}{a^2}\right)^{z(k)}ds
\end{aligned}
$$

On the other hand, the approximate characteristic function can be rewritten as follows:

$$
\begin{aligned}
\hat{\varphi}(\omega) &= \left(1-\frac{N_s}{M}\right) + \frac{N_s}{M}\frac{1}{T_c}\int_{-T}^{T+\delta}e^{j\omega p(s)}ds = \left(1-\frac{N_s}{M}\right) + \frac{N_s}{M}\frac{1}{T_c}\int_{-T}^{T+\delta}(b+1)ds \\
&= 1 + \frac{N_s}{T_c}\int_{-T}^{T+\delta}\frac{b}{M}ds \\
&= \frac{1}{T_c}\int_{-T}^{T+\delta}\left(1+\frac{b}{M}\right)^{N_s}ds - \frac{1}{T_c}\sum_{l=2}^{N_s}\binom{N_s}{l}\int_{-T}^{T+\delta}\left(\frac{b}{M}\right)^l ds
\end{aligned}
$$

Since $1+\frac{b}{M}=\frac{a}{M}$, and recalling that $T_f = MT_c$, we have

$$
\hat{\varphi}(\omega) = \frac{1}{T_f}\sum_{k=0}^{M-1}\int_{-T}^{T+\delta}\left(\frac{a}{M}\right)^{N_s}ds - \frac{1}{T_c}\sum_{l=2}^{N_s}\binom{N_s}{l}\int_{-T}^{T+\delta}\left(\frac{b}{M}\right)^l ds
$$

Then

$$
\begin{aligned}
\Delta\varphi(\omega) &= \frac{1}{T_f}\sum_{k=0}^{M-1}\int_{-T}^{T+\delta}\left(\frac{a}{M}\right)^{N_s}\left[\left(1-\frac{b^2}{a^2}\right)^{z(k)}-1\right]ds \\
&+ +\frac{1}{T_c}\sum_{l=2}^{N_s}\binom{N_s}{l}\int_{-T}^{T+\delta}\left(\frac{b}{M}\right)^l ds.
\end{aligned}
$$

Since $M \geq 2$, $M - 2 \leq |a| \leq 2$ and $|b| \leq 2$, this implies $\left|\frac{b}{a}\right| \leq \frac{2}{M-2}$, $\left|\frac{a}{M}\right| \leq 1$, and $\left|\frac{b}{M}\right| \leq \frac{2}{M}$. Therefore,

$$
\begin{aligned}
|\Delta\varphi(\omega)| \quad \leq \quad & \frac{1}{T_f} \sum_{k=0}^{M-1} \int_{-T}^{T+\delta} \left|\frac{a}{M}\right|^{N_s} \left|\left(1 - \frac{b^2}{a^2}\right)^{z(k)} - 1\right| ds \\
+ \quad & \frac{1}{T_c} \sum_{l=2}^{N_s} \binom{N_s}{l} \int_{-T}^{T+\delta} \left|\frac{b}{M}\right|^l ds \\
\leq \quad & \frac{1}{T_f} \sum_{k=0}^{M-1} \int_{-T}^{T+\delta} \left|\frac{a}{M}\right|^{N_s} \sum_{l=1}^{z(k)} \binom{z(k)}{l} \left|\frac{b}{a}\right|^{2l} ds \\
+ \quad & \frac{1}{T_c} \sum_{l=2}^{N_s} \binom{N_s}{l} \left|\frac{b}{M}\right|^l \int_{-T}^{T+\delta} ds \\
\leq \quad & \frac{1}{T_f} \sum_{k=0}^{M-1} \left[\left[1 + \left(\frac{2}{M-2}\right)^2\right]^{z(k)} - 1\right] \int_{-T}^{T+\delta} ds \\
+ \quad & \sum_{l=2}^{N_s} \binom{N_s}{l} \left(\frac{2}{M}\right)^l .
\end{aligned}
$$

Since $T_f = MT_c$ and $2T + \delta = T_c$, and using the fact $z(k) \leq \lfloor \frac{N_s}{2} \rfloor$, we have

$$
\begin{aligned}
|\Delta\varphi(\omega)| \quad \leq \quad & \frac{1}{M} \sum_{k=0}^{M-1} \left[\left[1 + \left(\frac{2}{M-2}\right)^2\right]^{z(k)} - 1\right] + \sum_{l=2}^{N_s} \binom{N_s}{l} \left(\frac{2}{M}\right)^l \\
\leq \quad & \left[\left[1 + \left(\frac{2}{M-2}\right)^2\right]^{\lfloor \frac{N_s}{2} \rfloor} - 1\right] + \left[\left(1 + \frac{2}{M}\right)^{N_s} - 1 - \frac{2N_s}{M}\right] = O\left(M^{-2}\right)
\end{aligned}
$$

Consider now $|\hat{\varphi}(\omega)|$.

$$
|\hat{\varphi}(\omega)| \quad = \quad \left|\left(1 - \frac{N_s}{M}\right) + \frac{N_s}{M} \frac{1}{T_c} \int_{-T}^{T+\delta} e^{j\omega p(t)} dt\right| \geq \left(1 - \frac{N_s}{M}\right) - \frac{N_s}{M} \frac{1}{T_c} \left|\int_{-T}^{T+\delta} e^{j\omega p(t)} dt\right|
$$

$$\geq \left(1 - \frac{N_s}{M}\right) - \frac{N_s}{M}\frac{1}{T_c}\int_{-T}^{T+\delta}\left|e^{j\omega p(t)}\right|dt = \left(1 - \frac{2N_s}{M}\right)$$

which is a valid bound for $M \geq 2N_s$. Therefore,

$$\left|\frac{\Delta\varphi(\omega)}{\hat{\varphi}(\omega)}\right| \leq \frac{\left[\left[1+\left(\frac{2}{M-2}\right)^2\right]^{\lfloor\frac{N_s}{2}\rfloor} - 1\right] + \left[\left(1+\frac{2}{M}\right)^{N_s} - 1 - \frac{2N_s}{M}\right]}{\left(1 - \frac{2N_s}{M}\right)} = O\left(M^{-2}\right). \quad \square$$

2.5.5 Proof of Theorem 2.3

Recall the test statistic (2.4)

$$\beta_0 = E_b + m_I + n =: E_b + \chi.$$

Since χ is the sum of two independent random variables, its characteristic function is given by

$$\varphi_\chi(\omega) = \varphi_{m_I}(\omega)\varphi_N(\omega).$$

Since n is a Gaussian random variable with zero mean and variance $\sigma_n^2 = \eta_0 N_s\left(e_b - \Delta_e\right)$, its characteristic function is

$$\varphi_n(\omega) = e^{-\frac{\sigma_n^2\omega^2}{2}}.$$

The probability density of χ is given by

$$f_\chi(x) = \frac{1}{2\pi}\int_{-\infty}^{+\infty}\varphi_\chi(\omega)e^{-j\omega x}d\omega = \frac{1}{2\pi}\int_{-\infty}^{+\infty}\varphi_{m_I}(\omega)e^{-\frac{\sigma_n^2\omega^2}{2}}e^{-j\omega x}d\omega$$

By replacing the MAI characteristic function with the approximate characteristic function $\hat{\varphi}_{m_I}(\omega)$, we approximate the pdf of the random variable χ with

$$\hat{f}_\chi(x) = \frac{1}{2\pi}\int_{-\infty}^{+\infty}\hat{\varphi}_{m_I}(\omega)e^{-\frac{\sigma_n^2\omega^2}{2}}e^{-j\omega x}d\omega$$

$$= \frac{1}{2\pi} \sum_{k=0}^{N_u-1} \binom{N_u - 1}{k} \left(1 - \frac{N_s}{M}\right)^{N_u-k-1} \left(\frac{N_s}{M}\frac{1}{T_c}\right)^k$$

$$\times \int_{-\infty}^{+\infty} c(\omega)^k e^{-\frac{\sigma_n^2\omega^2}{2}} e^{-j\omega x} d\omega$$

$$= \left(1 - \frac{N_s}{M}\right)^{N_u-1} \frac{1}{2\pi} \int_{-\infty}^{+\infty} e^{-\frac{\sigma_n^2\omega^2}{2}} e^{-j\omega x} d\omega$$

$$+ \sum_{k=1}^{N_u-1} \binom{N_u - 1}{k} \left(1 - \frac{N_s}{M}\right)^{N_u-k-1}$$

$$\times \left(\frac{N_s}{M}\frac{1}{T_c}\right)^k \frac{1}{2\pi} \int_{-\infty}^{+\infty} e^{-\frac{\sigma_n^2\omega^2}{2}} e^{-j\omega x}$$

$$\times \underbrace{\int_{-T}^{T+\delta} \int_{-T}^{T+\delta} \cdots \int_{-T}^{T+\delta}}_{k\ times} \prod_{l=1}^{k} e^{j\omega p(s_l)} ds_1 ds_2 \ldots ds_k \ d\omega$$

$$= \frac{\left(1 - \frac{N_s}{M}\right)^{N_u-1}}{\sqrt{2\pi\sigma_n^2}} e^{-\frac{x^2}{2\sigma_n^2}} + \sum_{k=1}^{N_u-1} \binom{N_u - 1}{k} \left(1 - \frac{N_s}{M}\right)^{N_u-k-1} \left(\frac{N_s}{M}\frac{1}{T_c}\right)^k$$

$$\times \underbrace{\int_{-T}^{T+\delta} \int_{-T}^{T+\delta} \cdots \int_{-T}^{T+\delta}}_{k\ times} \frac{1}{2\pi} \int_{-\infty}^{+\infty} e^{-\frac{\sigma_n^2\omega^2}{2}} e^{-j\omega x} e^{j\omega \sum_{l=1}^{k} p(s_l)} d\omega \ ds_1 ds_2 \ldots ds_k.$$

Note that the swap in the order of integration is allowed by Fubini's theorem, since

$$\int_{-\infty}^{+\infty} \underbrace{\int_{-T}^{T+\delta} \int_{-T}^{T+\delta} \cdots \int_{-T}^{T+\delta}}_{k\ times} \left| e^{-\frac{\sigma_n^2\omega^2}{2}} e^{-j\omega\left(x-\sum_{l=1}^{k} p(s_l)\right)} \right| ds_1 ds_2 \ldots ds_k d\omega < \infty$$

Clearly

$$\int_{-\infty}^{+\infty} e^{-\frac{\sigma_n^2\omega^2}{2}} e^{-j\omega\left(x-\sum_{l=1}^{k} p(s_l)\right)} d\omega = \frac{1}{\sqrt{2\pi\sigma_n^2}} e^{-\frac{\left(x-\sum_{l=1}^{k} p(s_l)\right)^2}{2\sigma_n^2}}.$$

Therefore

$$\hat{f}_\chi(x) = \frac{\left(1 - \frac{N_s}{M}\right)^{N_u-1}}{\sqrt{2\pi\sigma_n^2}} e^{-\frac{x^2}{2\sigma_n^2}} + \sum_{k=1}^{N_u-1} \binom{N_u - 1}{k} \left(1 - \frac{N_s}{M}\right)^{N_u-k-1} \left(\frac{N_s}{M}\frac{1}{T_c}\right)^k$$

$$\times \frac{1}{\sqrt{2\pi\sigma_n^2}} \underbrace{\int_{-T}^{T+\delta} \int_{-T}^{T+\delta} \ldots \int_{-T}^{T+\delta}}_{k \ times} e^{-\frac{\left(x-\sum_{l=1}^{k} p(s_l)\right)^2}{2\sigma_n^2}} ds_1 ds_2 \ldots ds_k, \quad (2.36)$$

and the probability of error is

$$
\begin{aligned}
\hat{P}_e &= Pr[\chi < -E_b] = \int_{-\infty}^{-E_b} f_\chi(x) dx = \frac{\left(1 - \frac{N_s}{M}\right)^{N_u-1}}{\sqrt{2\pi\sigma_n^2}} \int_{-\infty}^{-E_b} e^{-\frac{x^2}{2\sigma_n^2}} dx \\
&+ \sum_{k=1}^{N_u-1} \binom{N_u-1}{k} \left(1 - \frac{N_s}{M}\right)^{N_u-k-1} \left(\frac{N_s}{M}\frac{1}{T_c}\right)^k \frac{1}{\sqrt{2\pi\sigma_n^2}} \\
&\qquad \times \int_{-\infty}^{-E_b} \underbrace{\int_{-T}^{T+\delta} \int_{-T}^{T+\delta} \ldots \int_{-T}^{T+\delta}}_{k \ times} e^{-\frac{\left(x-\sum_{l=1}^{k} p(s_l)\right)^2}{2\sigma_n^2}} ds_1 ds_2 \ldots ds_k dx \\
&= \left(1 - \frac{N_s}{M}\right)^{N_u-1} \Phi\left(-\frac{E_b}{\sigma_n}\right) + \sum_{k=1}^{N_u-1} \binom{N_u-1}{k} \left(1 - \frac{N_s}{M}\right)^{N_u-k-1} \left(\frac{N_s}{M}\frac{1}{T_c}\right)^k \\
&\qquad \times \underbrace{\int_{-T}^{T+\delta} \int_{-T}^{T+\delta} \ldots \int_{-T}^{T+\delta}}_{k \ times} \frac{1}{\sqrt{2\pi\sigma_n^2}} \int_{-\infty}^{-E_b} e^{-\frac{\left(x-\sum_{l=1}^{k} p(s_l)\right)^2}{2\sigma_n^2}} dx ds_1 ds_2 \ldots ds_k
\end{aligned}
$$

where the swap in the order of integration is allowed by Tonelli's theorem, since the integrand is positive. $\Phi(x)$ is the Gaussian distribution defined as

$$\Phi(x) := \frac{1}{\sqrt{2\pi}} \int_{-\infty}^{x} e^{-y^2/2} dy.$$

The probability of error is therefore

$$
\begin{aligned}
\hat{P}_e &= \left(1 - \frac{N_s}{M}\right)^{N_u-1} \Phi\left(-\frac{E_b}{\sigma_n}\right) + \sum_{k=1}^{N_u-1} \binom{N_u-1}{k} \left(1 - \frac{N_s}{M}\right)^{N_u-k-1} \left(\frac{N_s}{M}\frac{1}{T_c}\right)^k \\
&\qquad \times \underbrace{\int_{-T}^{T+\delta} \int_{-T}^{T+\delta} \ldots \int_{-T}^{T+\delta}}_{k \ times} \Phi\left(-\frac{E_b + \sum_{l=1}^{k} p(s_l)}{\sigma_n}\right) ds_1 ds_2 \ldots ds_k. \quad \square
\end{aligned}
$$

2.6   Conclusion

We have investigated the performance of a TH-BPPM system in the presence of multi-user interference. Since the exact characteristic function (and, consequently, the pdf) for the MAI is not known, and the Gaussian approximation has been shown to be very poor, a new non-Gaussian approach has been proposed.

Theorem 2.1 presents the exact characteristic function for multi-user interference, which depends on the desired user's spreading sequence. In order to obtain a generic result, the dependance on the spreading sequence has to be eliminated. In Theorem 2.2, an approximate version of the MAI characteristic function is presented, where the dependance on the spreading sequence has been avoided; furthermore, it was shown that the fractional error between the approximate and the exact characteristic functions decreases as the processing gain M increases, specifically, at rate $O(M^{-2})$.

The expression for the characteristic function presented in Theorem 2.2 leads to the principal result of this chapter, presented in Theorem 2.3: An approximate, but explicit expression for the probability of error of the system for an arbitrary pulse shape has been derived, which does not involve the pdf of the MAI. The result stated in Theorem 2.3 involves multiple finite-limits integrals, where the dimension is of the order of the number of users. For a typical UWB scenario wherein the number of users is small, this expression can be readily evaluated by numerical techniques. Note that it is the region of small number of users where the Gaussian approximation performs the worst. Note also that in the case of rectangular-shaped pulse, the multiple integration was carried out explicitly, leading to a closed-form expression for the probability of error given in (2.16).

Finally, it was verified via comparison with simulation that our analytical results for the probability of error are very accurate.

The text of Chapter 2 is a reprint of the material as it appears in:

M. Sabattini, E. Masry, and L. B. Milstein, "A Non-Gaussian Approach to the Performance Analysis of UWB TH-BPPM Systems" - 2003 IEEE Conference on UWB System and Technology (published)

The dissertation author was the primary researcher and author, and the co-authors listed in this publication directed and supervised the research which forms the basis for this chapter.

3 Interference Mitigation via Beamforming for Impulse Radio Time Hopping CDMA Systems

"No, she had had enough of interference."

Jane Austen

THE ability of IR to resolve a large number of multipaths in a dense frequency selective channel suggests only a marginal improvement in performance by the use of multiple antennas from a diversity perspective, since performance enhancements due to diversity very rapidly become a diminishing returns function of the diversity order [14]. Furthermore, the small size of UWB receivers for in-home or sensor networking would result in a very high correlation among antenna elements, reducing even more the exploitable diversity. To the best of the authors' knowledge, very few works dealing with multiple antennas for IR-TH systems exist in the literature. In [14], some preliminary results and measurements on spatial correlation for IR are presented. In [28], a strategy for determining the desired user's angle of arrival (AoA) is introduced, based on so-called space-time and space-frequency resolution functions. Reference [66] presents a technique to exploit frequency diversity when the channel is unknown at the receiver. In [55], the performance improvement of an IR system in the presence of uncorrelated antennas is presented: the authors study the system from a purely divesity point of view, considering a frequency selective channel, and

in the absence of interference.

What appears to be lacking in the literature is a strategy to suppress interference by exploiting multiple antennas and beamforming in a realistic frequency selective, spatially correlated, channel. One of the main issues still open in TH systems is the capability to protect the desired user's signal from both other users' interference (see [48]) and NBI. Interference mitigation through beamforming, by using antenna arrays at the receiver, is addressed in this chapter. Beamforming techniques for MAI mitigation and NBI suppression are presented and analyzed in the presence of a frequency selective channel with spatially correlated receiving antennas. In the literature, a baseband correlator receiver (CR) is commonly considered when dealing with IR systems [48], [65], [64]. Unfortunately, a baseband CR does not exploit the practical band-pass nature of an IR system. The presence of a quadrature branch at the receiver enhances the interference suppression capabilities by fully exploiting the correlation among in-phase and quadrature components of the received interference process. We propose a quadrature receiver (QuadR) for IR UWB systems, and we present some results in terms of interference suppression for both schemes, compared with maximal ratio combining (MRC), showing that the use of a QuadR greatly improves the performance, while a baseband CR performs just slightly better than a system exploiting diversity combining only.

The rest of the chapter is organized as follows: Section 3.1 presents the system model for an IR TH system, while Section 3.2 describes the QuadR structure, presents the complex-equivalent received signal, and introduces the MMSE combining scheme. In Section 3.3, the performance measure used throughout this chapter, namely, the BER, is introduced, and one of the main results of this chapter is presented in Theorem 3.1, where an analytical expression for the bit error probability of a system employing MMSE combining is obtained. Section 3.4 presents some numerical results in terms of performance of the system in the presence of MAI and NBI. Finally,

conclusions are drawn in Section 3.5.

3.1 System Model

Assume the desired user transmits the following signal:

$$s_{tr}(t) = \sqrt{E_b} \sum_{i=-\infty}^{+\infty} (1 - 2\beta b_i) w_{tr}(t - iT_f - c_i T_c - \delta b_i - \tau_0; T) \qquad (3.1)$$

where E_b is the energy-per-bit, b_i is a binary data symbol, taking values $1, 0$ with equal probability, T_f is the frame duration, T_c is the chip duration, $\{c_i\}_{i=-\infty}^{+\infty}$ is an M-ary pseudo-random sequence of period N_P, and τ_0 is an asynchronous delay. Also, $w_{tr}(t; T)$ is a Gaussian pulse of the form

$$w_{tr}(t; T) = \begin{cases} A_{tr} \exp\left[-\frac{t^2}{2\tau_P^2}\right] & ; \quad \text{for } |t| \leq \frac{T}{2} \\ 0 & ; \quad \text{for } |t| > \frac{T}{2} \end{cases} \qquad (3.2)$$

where A_{tr} is an appropriate normalization constant, and τ_P is a parameter related to the width of the pulse. Note that the parameters β and δ in (3.1) are introduced in order to include in the same framework both data modulation formats proposed for IR UWB, namely, binary phase shift keying (BPSK; $\beta = 1$, $\delta = 0$) and BPPM ($\beta = 0$, $\delta = 0.1556 \ nsec$)[1].

The transmitted signal goes through a frequency selective multipath channel modeled as a tapped-delay-line[2], and it is received in the presence of AWGN and interference. By considering an antenna array at the receiver with N_r omni-directional

---

[1]See [48], [65] for more details.

[2]Following the seminal work by Turin [56], the directions of arrival of different paths to an omni-directional antenna in a dense multipath environment result in the sum of attenuated and delayed copies of the transmitted signal, whose overall effect on the transmitted signal can be modelled as a weighted tapped-delay-line.

elements, each of them spaced Δ from neighboring elements, and modeling the effect of both transmitting and receiving dipole antennas as derivatives, the signal received at the l-th element of the array is given by

$$
\begin{aligned}
r_\ell(t) \;=\; & \sqrt{E_b} \sum_{i=-\infty}^{+\infty} \sum_{h=0}^{P_{tot}-1} x_{\ell h}(i)(1 - 2\beta b_i) \\
& \times w(t - iT_f - c_i T_c - \delta b_i - hT_p - \ell\frac{\Delta}{\mathbf{c}}\sin\theta_D - \tau_0; T) \\
+ & \sum_{n=1}^{N_i} y_\ell^{(n)}(t - \ell\frac{\Delta}{\mathbf{c}}\sin\theta_n) + n_w^{(\ell)}(t)
\end{aligned}
\tag{3.3}
$$

for $\quad \ell = 0, 1, \ldots, N_r - 1$, where P_{tot} is the total number of resolvable paths, $\{x_{\ell h}(i)\}_{h=0,\ldots,P_{tot}-1}^{\ell=0,\ldots,N_r-1}$ are channel attenuation coefficients independent in h (but not in ℓ), and, in general, non-identically distributed, and assumed to remain constant over the observation window. Also, T_p is the multipath resolution time, $\mathbf{c}$ is the speed of light, and θ_D is the desired user's AoA. We stress that different multipaths received at an omni-directional antenna from different directions of arrival result in delayed replicas of the transmitted signal, whose overall effect can be modelled as in [57]. The term $n_w^{(\ell)}(t)$ is AWGN at the ℓ-th sensor with two-sided PSD $N_0/2$, and $y_\ell^{(n)}(t)$ is the n-th ($n = 1, \ldots, N_i$) wide-sense-stationary (WSS) interfering process, whose direction of arrival is θ_n. We study the performance of the system in the presence of MAI and NBI, where $y_\ell^{(n)}(t)$ denotes either a UWB interfering user or a narrow-band interferer. Note that $w(t; T)$ takes into account the double derivative from the transmitting and receiving antennas, and is of the form

$$
w(t; T) = \begin{cases} A\left(1 - \frac{t^2}{\tau_P^2}\right)\exp\left[-\frac{t^2}{2\tau_P^2}\right] & ; \quad \text{for } |t| \le \frac{T}{2} \\ 0 & ; \quad \text{for } |t| > \frac{T}{2} \end{cases}
\tag{3.4}
$$

where A is an appropriate normalization constant such that $A^2 \int_{-\infty}^{+\infty} \left(1 - \frac{t^2}{\tau_P^2}\right)\exp\left[-\frac{t^2}{2\tau_P^2}\right]dt = 1$, so that $A = \sqrt{\frac{4}{3\sqrt{\pi}\tau_P}}$. The pulse width T is chosen such that

$A^2 \int_{-T/2}^{T/2} w^2(t;T)dt = 0.99$; specifically $T = 7.95\tau_P$.

We now show that the error made by considering a non-truncated monocycle is small for an appropriate choice of the parameter T. Consider

$$\varphi(t) = A \left(1 - \frac{t^2}{\tau_P^2} \right) \exp \left[-\frac{t^2}{2\tau_P^2} \right] \tag{3.5}$$

with A defined above such that $\varphi(t)$ has unit energy, and let $\varphi_n(t)$ and $\psi_n(t;T)$ represent the n-th fold convolution of $\varphi(t)$ with itself and $w(t;T)$ with itself, respectively. Define the $\mathcal{L}^2$-error as

$$\lambda_n(T) := \frac{\int_{-\infty}^{+\infty} \left[\varphi_n(t) - \psi_n(t;T) \right]^2 dt}{\int_{-\infty}^{+\infty} \varphi_n^2(t)dt}. \tag{3.6}$$

Proposition 3.1 *The $\mathcal{L}^2$-error is bounded by $\lambda_n(T) \leq \varepsilon_n \, \mathcal{P} \left(\frac{T}{\tau_P} \right)$, where*

$$\varepsilon_n = \frac{2^{2n-1} n^{2n+5/2} e^{-2(n-1)}}{\Gamma(2n+1/2)} \tag{3.7}$$

and

$$\mathcal{P}(u) = \frac{1}{2} \Gamma \left(\frac{1}{2}, \left(\frac{u}{2} \right)^2 \right) - \Gamma \left(\frac{3}{2}, \left(\frac{u}{2} \right)^2 \right) + \frac{1}{2} \Gamma \left(\frac{5}{2}, \left(\frac{u}{2} \right)^2 \right) \tag{3.8}$$

and the bound holds with equality for $n = 1$.

Proof: See Appendix B.1.

A plot of the above upper bound as a function of T is presented in Fig. 3.1 for different values of n, and shows that for $T = 8\tau_P$ the $\mathcal{L}^2$-error is negligible. Note that the performance of the system is primarily a function of the received energy, making the $\mathcal{L}^2$-metric appropriate to test the "goodness" of an approximation. We will show in Section 3.4, by means of simulations, that this approximation is accurate.

λ_n (T)
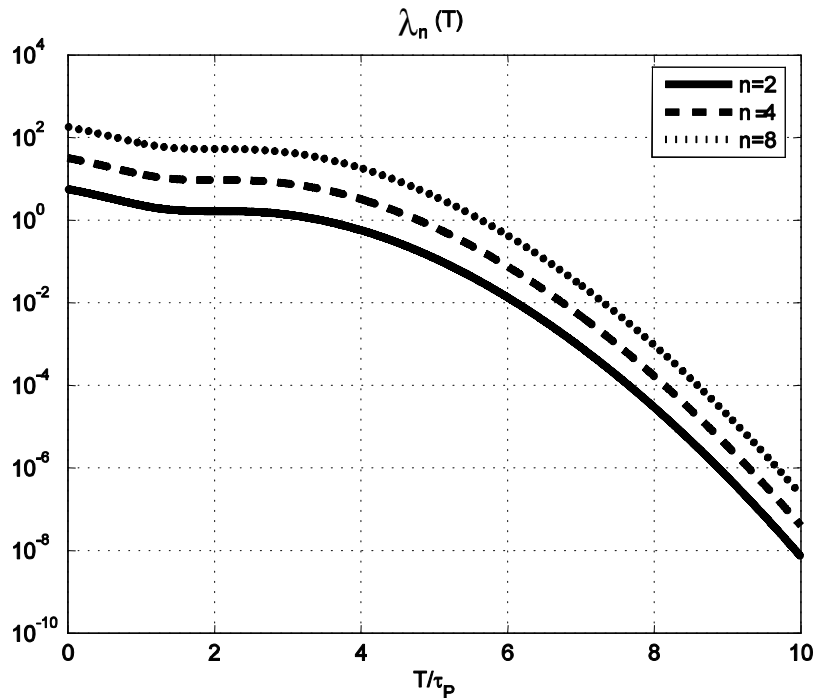
Figure 3.1: Upper Bound for $\lambda_n(T)$ for different values of n.

3.2 Receiver Structure

In the literature, a baseband CR is commonly considered when dealing with IR systems ([48], [65], [64]). Unfortunately, a baseband CR does not exploit the practical band-pass nature of an IR system (even if no carrier is present, the received spectrum of an IR system employing a Gaussian monocyle [65] has the vast majority of its energy at band-pass).We propose a QuadR as shown in Fig. 3.2.

We assume the delay τ_0, the AoA θ_D and the spreading sequence are known for the desired user. Thus, by focusing on data b_0, and considering a RAKE receiver with $P \leq P_{tot}$ fingers at each antenna, the output of the k-th finger at the ℓ-th antenna is the output of a filter matched to the received waveform and sampled at $t_{\ell k} = kT_p + c_0 T_c + \tau + \ell \frac{\Delta}{\mathbf{c}} \sin \theta_D$. In general, the effect of the interference and noise would be a function of τ_0 and c_0. However, since both interference and noise have been assumed WSS processes, one can assume without any loss of generality that $\tau_0 = 0$ and $c_0 = 0$. By considering a QuadR as shown in Fig. 3.2, and exploiting the
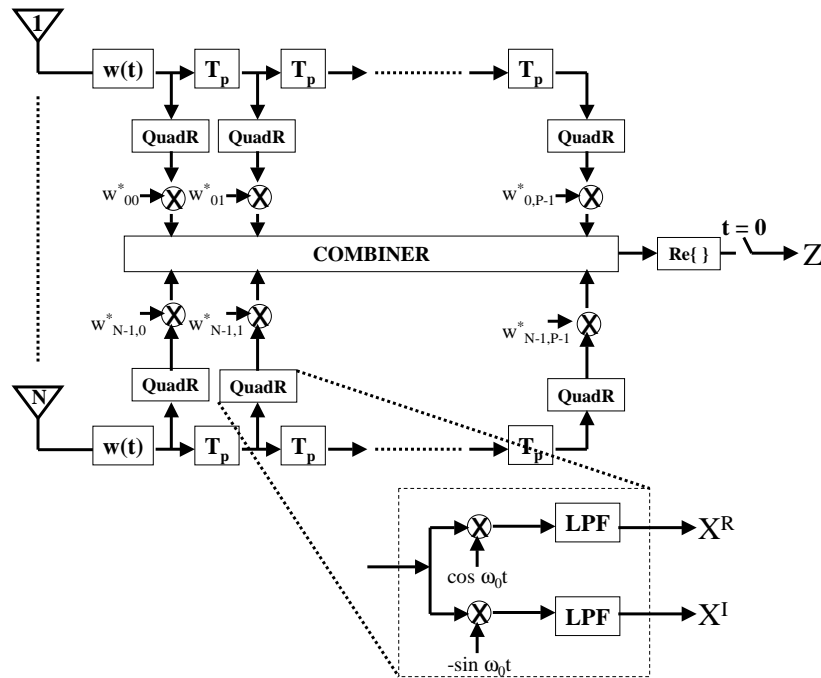
Figure 3.2: Array Receiver Structure.

mathematical relations between the in-phase and quadrature components of a signal and its Hilbert transform [40], the complex-equivalent of the sampled output at the l-th antenna and k-th tap can be written as

$$
\begin{aligned}
\tilde{r}_{\ell k} \;\; := \;\; & \sqrt{E_b} \sum_{h=0}^{P_{tot}-1} \tilde{x}_{\ell h}(0) \, d_0 \, \tilde{s}((k-h)T_p) \\
+ \;\; & \sqrt{E_b} \sum_{i \neq 0} \sum_{h=0}^{P_{tot}-1} \tilde{x}_{\ell h}(i) \, d_i \, \tilde{s}(iT_f - c_i T_c + (k-h)T_p) \\
+ \;\; & \sum_{n=1}^{N_i} \tilde{z}_\ell^{(n)}(kT_p - \ell \frac{\Delta}{\mathbf{c}}(\sin\theta_n - \sin\theta_D)) + \tilde{n}_{\ell k} \qquad (3.9) \\
& \ell = 0,\dots,N_r-1; k = 0,\dots,P-1
\end{aligned}
$$

where $\{\tilde{x}_{\ell h}(i)\}_{\ell=0,\dots,N_r-1}^{h=0,\dots,P_{tot}-1}$ are complex channel taps with i.i.d. real and imaginary parts, $d_i := (-1)^{b_i}$ is the antipodal equivalent of the bit b_i, $\tilde{s}(t) := s(t) + j\hat{s}(t)$, $\tilde{z}_\ell^{(n)}(t) := z_\ell^{(n)}(t) + j\hat{z}_\ell^{(n)}(t)$, the symbol $\hat{}$ stands for the Hilbert transform, and $s(t) = (w*w)(t)$ is the output of the matched-filter (assumed normalized such that $s(0) = 1$); note that the matched-filters for the two modulation formats considered (specifically,

BPSK and BPPM) are given by

$$MF : \begin{cases} h_{BPSK}(t) = w(t) & ; \text{BPSK} \\ h_{BPPM}(t) = \frac{1}{1-\rho}\left[w(t) - w(t - \delta)\right] & ; \text{BPPM} \end{cases} \tag{3.10}$$

where $\rho := \int_{-\infty}^{+\infty} w(t)w(t - \delta)dt$. The term $z_\ell^{(n)}(t)$ is the output of the matched-filter to the n-th interferer, and $\tilde{n}_{\ell k}$ are zero-mean i.i.d. complex Gaussian random variables, with independent components and variance per dimension depending on the modulation format (see [65], [67])

$$\sigma_N^2 := \frac{1}{2}E\left|\tilde{n}_{\ell k}\right|^2 = \begin{cases} N_0 & ; \text{BPSK} \\ 2N_0/(1-\rho) & ; \text{BPPM} \end{cases} \tag{3.11}$$

With the help of [1], it can be shown that for $w(t; T)$ a truncated Gaussian monocycle, $\hat{s}(t)$ also has finite practical duration, i.e., the energy of $\hat{s}(t)$ outside the interval $[-T/2, T/2]$ can be neglected. Therefore, one can assume resolvable paths for $T_p \geq T$. Specifically, we have[3]

$$\tilde{s}(hT_p) = \begin{cases} 1 & ; \text{ for } h = 0 \\ 0 & ; \text{ for } h \neq 0 \end{cases} \tag{3.12}$$

Also, if the frame length is comparable to the delay spread of the channel, and the multipath delay profile decays fast enough, the contribution of inter-symbol-interference (ISI) from frame to frame can be neglected, especially in an interference-limited scenario. Therefore, by defining $\tilde{z}_{\ell k}^{(n)} := \tilde{z}_\ell^{(n)}(kT_p - \ell\frac{\Delta}{c}(\sin\theta_n - \sin\theta_D))$, Eq. (3.9) can be simplified to

$$\tilde{r}_{\ell k} = \sqrt{E_b}d_0\tilde{x}_{\ell k} + \sum_{n=1}^{N_i} \tilde{z}_{\ell k}^{(n)} + \tilde{n}_{\ell k} \qquad \ell = 0, \ldots, N_r - 1; k = 0, \ldots, P - 1 \tag{3.13}$$

---

[3]It is shown in [67] that $s(t)$ is even, which implies that $\hat{s}(t)$ is odd, and $\hat{s}(0) = 0$.

where the dependence of the channel taps on the sampling instant has been dropped for simplicity of notation. We express the above set of equations for $k = 0, 1, \ldots, P-1$, $\ell = 0, 1, \ldots, N_r - 1$ in vector form as

$$\underline{\tilde{r}} = \sqrt{E_b}\, d_0\, \underline{\tilde{x}} + \sum_{n=1}^{N_i} \underline{\tilde{z}}^{(n)} + \underline{\tilde{n}}. \tag{3.14}$$

where $\underline{\tilde{x}} := [\tilde{x}_{0,0}, \tilde{x}_{0,1}, \ldots, \tilde{x}_{0,P-1}, \tilde{x}_{1,0}, \ldots \ldots, \tilde{x}_{N_r-1,P-1}]^T$, and $\underline{\tilde{z}}^{(n)}$ and $\underline{\tilde{n}}$ are defined analogously. In order to exploit the advantage of MMSE beamforming for interference suppression, the second order statistics - specifically, the covariance matrix - of the interference is critical. Since the $\{\underline{\tilde{z}}^{(n)}\}_{n=1}^{N_i}$ are zero-mean independent random vectors, we can write the covariance matrix of the interference as $\Omega := \sum_{n=1}^{N_i} \Omega^{(n)} = \sum_{n=1}^{N_i} E\left[\underline{\tilde{z}}^{(n)} \underline{\tilde{z}}^{(n)H}\right]$, where every element of each covariance matrix $\Omega^{(n)}$ can be readily evaluated in terms of the correlation function (or equivalently the PSD) of the n-th interferer. Specifically,

$$\Omega^{(n)}_{\ell N_r + k, \ell' N_r + k'} := \Omega^{(n)}_{\ell k \ell' k'} \tag{3.15}$$

$$= E\left[\tilde{z}^{(n)}_\ell(kT_p - \ell\frac{\Delta}{\mathbf{c}}(\sin\theta_n - \sin\theta_D))\tilde{z}^{(n)}_{\ell'}(k'T_p - \ell'\frac{\Delta}{\mathbf{c}}(\sin\theta_n - \sin\theta_D))\right]$$

Note that, in general, the auto-correlation function can be factored into the product of a spatial correlation coefficient and the correlation function of a WSS random process [51]. This effect can be intuitively explained as follows: The correlation among antennas is due to some multiplicative spatial coefficients only, independent of time, and statistically independent of the interference random process (see [51], Eq. A-3 for details). For this reason, one can set, in general $\tilde{R}^{(n)}_{\ell\ell'}(\tau) = \sigma^{(n)}_{\ell\ell'} \tilde{R}^{(n)}(\tau) = \sigma^{(n)}_{\ell\ell'}\left[R^{(n)}(\tau) + j\hat{R}^{(n)}(\tau)\right]$, where $R^{(n)}(\tau) := E\left[z^{(n)}_\ell(t)z^{(n)}_\ell(t+\tau)\right]$, for every $\ell = 0, 1, \ldots, N_r - 1$, and $\sigma^{(n)}_{\ell\ell'}$ takes into account the spatial correlation among

different receiving elements. Therefore

$$\Omega^{(n)}_{\ell k \ell' k'} = \sigma^{(n)}_{\ell\ell'} \tilde{R}^{(n)} \left((k - k')T_p - (\ell - \ell')\frac{\Delta}{\mathbf{c}} \left(\sin\theta_n - \sin\theta_D \right) \right). \qquad (3.16)$$

3.2.1 Baseband Correlator Receiver Output

It is readily shown that the sampled output of a baseband CR is just the real part of (3.14), normalized to collect the same desired signal's power of a QuadR. Specifically,

$$\underline{r}^{(CR)} = \sqrt{2E_b}\, d_0 \, \Re e\{\underline{\tilde{x}}\} + \sum_{n=1}^{N_i} \Re e\left\{\underline{\tilde{z}}^{(n)}\right\} + \underline{n} \qquad (3.17)$$

where $\underline{n}$ is a zero-mean real Gaussian random vector with independent components, and variance σ_N^2 per dimension. Furthermore, the interference covariance matrix is simply $\Omega^{(CR)} = \Re e\{\Omega\}$, where the $(\ell N_r + k, \ell' N_r + k')$-th element of Ω is defined in (3.16). Given the above framework, a comparison between different weighting schemes for QuadR and CR is possible, once the system parameters and the interference statistical model have been specified.

3.2.2 MMSE combining for Impulse Radio

The receiver forms a test statistic by weighting each element of $\underline{r}$ by a vector $\underline{w}$, specifically, $\zeta(d_0) = \Re e\left\{\underline{w}^H \underline{\tilde{r}}\right\}$, and compares it with a zero threshold in order to make a decision on the transmitted symbol. Different weighting schemes are possible, and we will focus specifically on MRC and MMSE. The probability of error is given by $P_e = Pr\left[\zeta(d_0) < 0\right]$.

Note that the two aforementioned combining schemes correspond to the weighting vectors [59]

$$\underline{w}_{MMSE} := \left[\Omega + \sigma_N^2 \mathcal{I}\right]^{-1} \underline{\tilde{x}} \qquad ; \qquad \underline{w}_{MRC} := \underline{\tilde{x}} \qquad (3.18)$$

Note also that the above choices for the weights maximize the received Signal-to-

Interference-plus-Noise Ratio (SINR)[4]. Specifically, the SINR's for the above combining schemes are given by [44]

$$SINR_{MMSE} = \underline{\tilde{x}}^H \left[\Omega + \sigma_N^2 \mathcal{I} \right]^{-1} \underline{\tilde{x}} \qquad \text{and} \qquad SINR_{MRC} = \frac{(\underline{\tilde{x}}^H \underline{\tilde{x}})^2}{\underline{\tilde{x}}^H \left[\Omega + \sigma_N^2 \mathcal{I} \right] \underline{\tilde{x}}}. \quad (3.19)$$

3.3   Performance Analysis

A common way of comparing the performance of different combining schemes and different receivers is in terms of BER. Specifically, by considering the received vector

$$\underline{r} = \sqrt{E_b} \, d_0 \underline{x} + \sum_{n=1}^{N_i} \underline{\tilde{z}}^{(n)} + \underline{\tilde{n}} \quad (3.20)$$

the performances of MMSE and MRC combining, in the presence of Gaussian interference, are given by

$$P_e^{(MMSE)} \;=\; E\left[\mathcal{Q}\left(\sqrt{E_b \, \underline{\tilde{x}}^H \left[\Omega + \sigma_N^2 \mathcal{I} \right]^{-1} \underline{\tilde{x}}} \right) \right] \quad (3.21)$$

$$P_e^{(MRC)} \;=\; E\left[\mathcal{Q}\left(\sqrt{\frac{E_b \, (\underline{\tilde{x}}^H \underline{\tilde{x}})^2}{\underline{\tilde{x}}^H \left[\Omega + \sigma_N^2 \mathcal{I} \right] \underline{\tilde{x}}}} \right) \right] \quad (3.22)$$

where $1 - \mathcal{Q}(x)$ is the Gaussian distribution, $\Omega = \sum_{n=1}^{N_i} \Omega^{(n)} = \sum_{n=1}^{N_i} E\left[\underline{\tilde{z}}^{(n)} \underline{\tilde{z}}^{(n)H} \right]$ is the interference covariance matrix, and the dependence on the AoAs $\underline{\theta} = \{\theta_1, \ldots, \theta_{N_i}\}$ (see Eq. (3.16)) has been implicitly assumed, and $\sigma_N^2 \mathcal{I}$ is the noise covariance matrix. Note that for Gaussian[5] channel taps $\underline{\tilde{x}}$ with mean $\tilde{\mu}$ and covariance H, the probability

---

[4]We point out that in order to perform MMSE combining, knowledge of the interference-plus-noise covariance matrix is needed at the receiver. This knowledge can be assumed perfect, or based on some estimate. While in the following analysis we initially assume a perfect (i.e, "genie-aided") estimate, simulations with standard nonparametric estimates will be also presented.

[5]A common model for UWB large-scale fading parameters follows the Nakagami-m statistics. For a reasonable choice of the parameters, a Rician distribution can well approximate a Nakagami

of error in (3.21) when MMSE combining is employed can be obtained analytically, as stated below in Theorem 3.1. Set $\Sigma := E_b \left[\Omega + \sigma_N^2 \mathcal{I} \right]$ and define the following:

1. $\breve{x} := \left[x_R^T \; x_I^T \right]^T$;

2. $\breve{\mu} = E \left[\breve{x} \right]$;

3. $\breve{H} := E \left[\breve{x} \; \breve{x}^T \right]$;

4. $\breve{\Psi} := \begin{bmatrix} \left[\Sigma_R + \Sigma_I \Sigma_R^{-1} \Sigma_I \right]^{-1} & \Sigma_R^{-1} \Sigma_I \left[\Sigma_R + \Sigma_I \Sigma_R^{-1} \Sigma_I \right]^{-1} \\ -\Sigma_R^{-1} \Sigma_I \left[\Sigma_R + \Sigma_I \Sigma_R^{-1} \Sigma_I \right]^{-1} & \left[\Sigma_R + \Sigma_I \Sigma_R^{-1} \Sigma_I \right]^{-1} \end{bmatrix}$;

where $x_R = \Re e\{\tilde{x}\}$, $x_I = \Im\{\tilde{x}\}$, $\Sigma_R = \Re e\{\Sigma\}$, and $\Sigma_I = \Im\{\Sigma\}$. Then

$$\begin{aligned} \breve{\mu} &:= \left[\mu_R^T \; \mu_I^T \right]^T \\ \mu_R &:= E \left[x_R \right] \\ \mu_I &:= E \left[x_I \right] \\ \breve{H} &:= \begin{bmatrix} H/2 & \mathbf{0} \\ \mathbf{0} & H/2 \end{bmatrix} \\ H/2 &:= E \left[\left(x_R - \mu_R \right) \left(x_R - \mu_R \right)^T \right] = E \left[\left(x_I - \mu_I \right) \left(x_I - \mu_I \right)^T \right] \end{aligned}$$

(3.23)

Theorem 3.1 *The probability of error when MMSE combining is employed is given by*

$$P_e = \frac{1}{\pi} \int_0^{\pi/2} \frac{1}{\sqrt{\left| \breve{H} \right| \left| \breve{H}^{-1} + \frac{\breve{\Psi}}{\sin^2 v} \right|}}$$

(3.24)

$$\times \exp \left\{ -\frac{1}{2} \breve{\mu}^T \left[I - \breve{H}^{-T} \left(\breve{H}^{-1} + \frac{\breve{\Psi}}{\sin^2 v} \right)^{-T} \right] \breve{H}^{-1} \breve{\mu} \right\} dv$$

---

distribution [54]. Therefore, the assumption of non-zero-mean complex Gaussian taps is not unreasonable.

Proof: See Appendix B.2.

The result is valid for both MMSE-complex and MMSE-real combining schemes, provided $\breve{H}$, $\breve{\Psi}$ and $\breve{\mu}$ are replaced by H, Σ_R^{-1} and μ, respectively, when real weights are employed.

By specifying the receiver, the interfering process and the channel model, one can readily compare the above systems in different scenarios.

3.3.1 Advantage of the QuadR

Another measure of performance is given by the average signal-to-noise-and-interference ratio (SNIR). In particular, we want to show that, when MMSE combining is employed, the average SNIR for a complex QuadR is higher than it is for a CR. Recall the definition of $\Sigma = E_b \left[\Omega + \sigma_N^2 \mathcal{I} \right]$. Also, recall that when a CR is employed, the received vector is

$$\underline{r}^{(CR)} = \sqrt{2E_b}\, d_0\, \underline{x}_R + \sum_{n=1}^{N_i} \Re e \left\{ \underline{\tilde{z}}^{(n)} \right\} + \underline{n} \qquad (3.25)$$

with $\underline{x}_R$ defined in Theorem 3.1. We have the following:

Theorem 3.2 *Denote the average SNIR's of a CR and a QuadR by $\overline{SNIR}_R$ and $\overline{SNIR}_C$, respectively. Then, $\overline{SNIR}_C \geq \overline{SNIR}_R$.*

Proof: See Appendix B.3.

3.3.2 Covariance Matrix Estimation

In practice, the covariance matrix of the interference and noise is not known *a priori*, and needs to be estimated from data. In order to perform this estimate, we assume a pilot signal with known data is transmitted. In a real system, the channel has also to be estimated from the preamble. Furthermore, an error in the channel estimates would affect both MRC and MMSE combining, resulting in performance degradation of both schemes. In order to simplify the analysis and focus on the interference

cancellation capabilities of the beamformer, we assume that the channel is known at the receiver so that the signal component can be subtracted from the received waveform, leaving just the interference and noise components. Thus, let $\{\underline{\nu}_k\}_{k=1}^K$ be a set of i.i.d. zero-mean complex Gaussian random vectors of dimension $N_r P \times 1$, represent K independent observations of the interference-plus-noise, with covariance matrix $\Sigma := E\left[\underline{\nu}_k \underline{\nu}_k^H\right] = \Omega + \sigma_N^2 \mathcal{I}$. We define

$$\widehat{\Sigma}_K := \frac{1}{K} \sum_{k=1}^K \underline{\nu}_k \underline{\nu}_k^H \tag{3.26}$$

where $\widehat{\Sigma}_K$ has the following properties [7]:

1. *Unbiasedness:* $E\left[\widehat{\Sigma}_K\right] = \Sigma$;

2. *Variance of the Error:* $E\left[\left(\widehat{\Sigma}_K^{(jk)} - \Sigma^{(jk)}\right)\left(\widehat{\Sigma}_K^{(\ell p)} - \Sigma^{(\ell p)}\right)^*\right] = \frac{1}{K}\Sigma^{(j\ell)}\Sigma^{(kp)}$;

3. *Convergence:* $\widehat{\Sigma}_K$ converges in mean-square sense to Σ as $K \to \infty$;

where $A^{(jk)}$ indicates the (j, k)-th element of a matrix A, and the symbol $()^*$ stands for the complex conjugate. Therefore, given an estimator with sample size K, the MMSE weights based on the estimated covariance matrix are given by $\underline{w}_{MMSE} = \widehat{\Sigma}_K^{-1}\underline{x}$.

3.4   Numerical Results

We assume BPSK modulation[6], and we set the desired user's AoA θ_D equal to 0. The system and channel parameters are presented in Table 4.1.

We study the performance of different receivers in terms of BER; furthermore, we look at the behavior of the system in the presence of MAI and NBI. It can be shown

---

[6]The results for BPPM modulation do not qualitatively differ from the presented ones, and are omitted due to space limitations. The use of orthogonal modulation instead of antipodal leads to a degradation in the performance of all combining schemes.

Table 3.1: System and Channel Parameters

	System Parameters	
τ_P	Monocycle parameter	0.0812 nsec
$T = 8\tau_P$	Pulse's Practical duration	0.65 nsec
T_c	Chip Duration	$T_c = T$
T_p	Multipath Resolution	$T_p = T$
T_f	Frame duration	30 nsec
Δ_{rec}	Receiver Size	10 cm
M	Chips per frame	30
P_{tot}	Total Number of paths	50

that the correlation function of a generic UWB user is $R_{MAI}^{(n)}(\tau) = \frac{E_n}{T_f} \, p(\tau)$, where E_n is the n-th user energy-per-bit, and $p(t) = \mathcal{F}^{-1}\{W^4(\omega)\}$, with $W(\omega) = \mathcal{F}\{w(t)\}$. From [1], $p(t) = A^4 \tau_P^{11} \pi \sqrt{2\pi} \, H_8\left(\frac{t}{2\tau_P}\right) \exp\left[-\frac{t^2}{8\tau_P^2}\right]$, where $H_8(x)$ is the 8-th order Hermite polynomial.

By modeling the narrow-band interfering process as a WSS Gaussian process, with center frequency ω_n and base-band equivalent PSD of the form $\mathcal{Q}(\omega) = K_1 sinc^2\left(K_2\omega\right)$, the correlation function after matched-filtering[7] is

$$R_{NBI}^{(n)}(\tau) = \Pi_n |W(\omega_n)|^2 \, \Lambda(\varrho_n\tau) \cos\omega_n\tau \tag{3.27}$$

where Π_n is the n-th interferer power, ω_n and ϱ_n are its center frequency and bandwidth, respectively, and the function $\Lambda(t)$ is defined as

$$\Lambda(t) := \begin{cases} 1 - |t| & ; \text{ for } t \in [-1, 1] \\ 0 & ; \text{ elsewhere} \end{cases} \tag{3.28}$$

Note that the Hilbert transform of (3.27) is readily shown to be $\hat{R}_{NBI}^{(n)}(\tau) = \Pi_n$

---

[7]We are implicitly assuming that the bandwidth of the interference is much smaller than the bandwidth of the matched-filter $MF(\omega)$, so that we can approximate the output PSD as $\mathcal{Q}_{out}(\omega) \approx |MF(\omega_n)|^2 \frac{1}{2} [\mathcal{Q}(\omega - \omega_n) + \mathcal{Q}(\omega + \omega_n)]$

$|W(\omega_n)|^2 \Lambda(\varrho_n\tau) \sin \omega_n\tau$, leading to an expression for the complex covariance matrix by the use of Eq. (3.16).

In this section, we assume two well-known UWB channel models. The first model to be considered is an approximation of the model presented in [10], [11]. In these latter works, the channel is modelled as a conventional tapped delay line, where the multipath coefficients are independent Nakagami variables with random fading parameters. In the numerical results that follow, these parameters are fixed to their mean values, and the Nakagami-m statistics of the channel taps are approximated by a Rician distribution, with the K_r parameter related to the m parameter by [54] $K_r = \frac{\sqrt{m^2-m}}{m-\sqrt{m^2-m}}$, for $m \geq 1$. The second channel model to be considered is the one proposed by the IEEE 802.15 Channel Modeling subcommittee [22]. In this model, the multipaths are assumed to arrive in clusters, and the multipath amplitudes follow a lognormal fading distribution. Due to the complexity of this model, the unconditional probability of error is obtained by averaging, via simulation, the conditional probability of error over different channel realizations. When using the IEEE model, we use a set of input parameters that corresponds to a line of sight (LOS) situation with range equal to $0-4$ m (channel number I in [22]). We also assume spatially correlated receive antennas, where the correlations among array elements follow the model presented in [51], with angular delay spread set to π.

First, we consider the advantages of beamforming for MAI mitigation, where we assume perfect power control among all UWB users. The channel is modeled with complex Gaussian taps and K_r factor derived from [10][8]. Fig. 3.3 shows the BER

---

[8]Results were generated with different values of the parameter K_r, in order to evaluate the sensitivity of the proposed scheme to channel statistics variations. The results show that the relative performance of MMSE-complex as compared to MMSE-real and MRC does not change significantly, and have been omitted due to space limitations.

of the various systems, where 30 UWB users have been considered[9], as a function
of the number of receiving elements N_r, for a fixed receiver size of 10 cm, and for 5
collected paths out of 50 at a SNR of 30dB. The performance obtained through the
analytical expression presented in Theorem 3.1 is compared with simulations, show-
ing an essentially perfect match. As the reader can immediately notice, the use of a
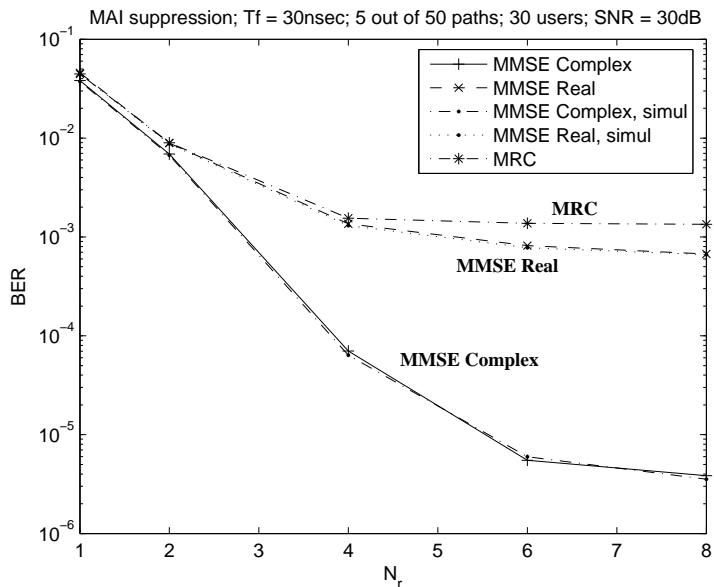
Figure 3.3: MAI Mitigation: BER v_s Number of Receiving Elements.

QuadR (i.e., complex weights), as described in Section 3.2, considerably improves the
performance. On the other hand, MMSE combining with CR (i.e., real weights) and
MRC have practically the same performance. We point out that the saturation effect
in the performance of MMSE combining is a consequence of the noise; by increas-
ing the number of receiving antennas over a fixed length array, the SNR as well as
the interference power per antenna decrease, and the system becomes noise-limited,
rather than interference-limited. This effect implies that no further improvement in
the performance can be achieved by adding more elements above a certain saturation

---

[9]Note that the Gaussian approximation for such a large number of users is fairly accurate, as
shown in [48].

number of antennas. This "saturation threshold" increases with increasing interference power above the noise level; in the limiting case of a purely interference-limited system (where no additive noise is present), there is no saturation effect, and the more receiving elements that are added, the higher the interference cancellation capabilities that can be achieved. In other words, by increasing the number of antennas for a fixed-size receiver, even if diversity improvement saturates due to higher correlation among array elements, the beamformer exploits this correlation to suppress interference and further improve the performance. On the other hand, no protection against interference can be achieved with MRC, since MRC accounts only for the fading. Therefore, the saturation of MRC is primarily due to diversity saturation: after a certain value, because of the spatial correlation, no significant additional spatial diversity is introduced by adding more receiving elements, and no improvement in the performance is noticeable.

Fig. 3.4 shows the performance for the same scenario as Fig. 3.3 for $N_r = 6$ as a function of the SNR. It is seen that the advantage of MMSE combining with complex weights increases by increasing the SNR. Fig. 3.5 shows simulations of the
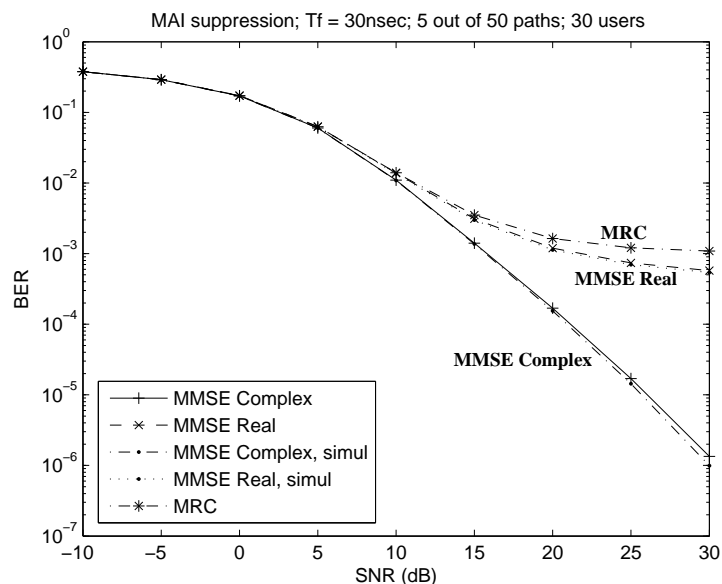
Figure 3.4: MAI Mitigation: BER v_s SNR.

performance under the same system assumptions of Fig. 3.3, but in the presence of the 802.15 channel [22], with log-normal attenuation coefficients.

MAI suppression; Tf = 30nsec; 5 collected paths; 30 users; SNR = 30dB
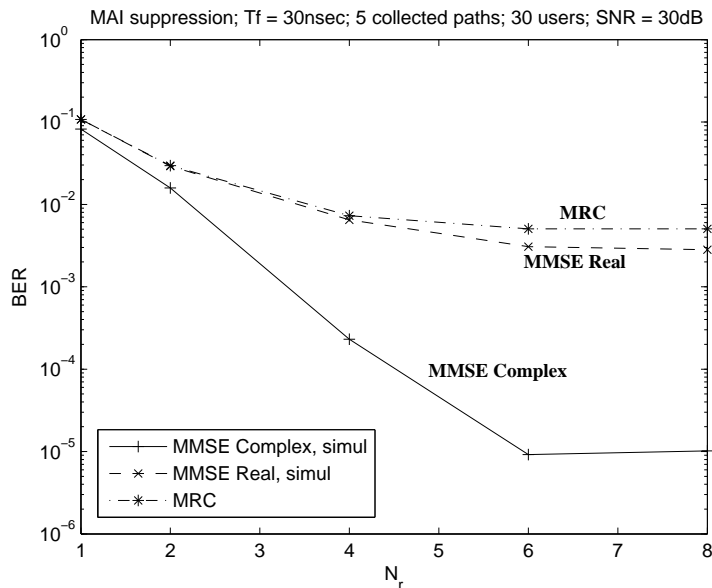
Figure 3.5: MAI Mitigation: BER v_s Number of Receiving Elements. 802.15 Channel.

We plot in Fig. 3.6 the performance of the system when the weights are obtained through an estimate of the interference-plus-noise covariance matrix, as presented in Section 3.3.2, for different values of the estimation sample size. The plot presents the BER for $K = 50$, $K = 100$, and $K = 200$, showing that satisfactory performance can be achieved at a reasonable complexity. As one would expect, the performance of the estimator gets worse as the sample size is shortened, while for $K = 200$, the performance is very close to the ideal case. Note that the convexity of the performance for small values of K is due to the tradeoff between interference mitigation and estimation errors: By increasing the number of receiving elements, while beamforming becomes more effective in reducing the contribution of interference, the power received at each element decreases and estimation errors become dominant.

We next consider a narrow-band interferer with center frequency at either $\omega_i = \omega_0$, or $\omega_i = \frac{3}{2}\omega_0$, or $\omega_i = 2\omega_0$, bandwidth equal to one-thousandth of the UWB bandwidth, and signal-to-interference ratio (SIR) of -20dB. We consider complex Gaussian
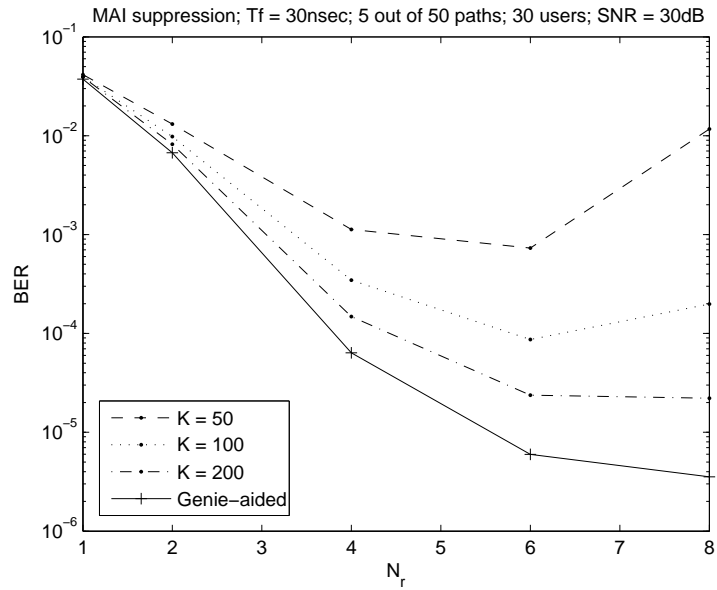
Figure 3.6: MAI Mitigation: BER v_s Number of Receiving Elements. MMSE combining with an estimate of the covariance matrix, for different values of K.

channel taps, a K_r factor derived from [10], and 5 collected paths out of 50. Fig. 3.7
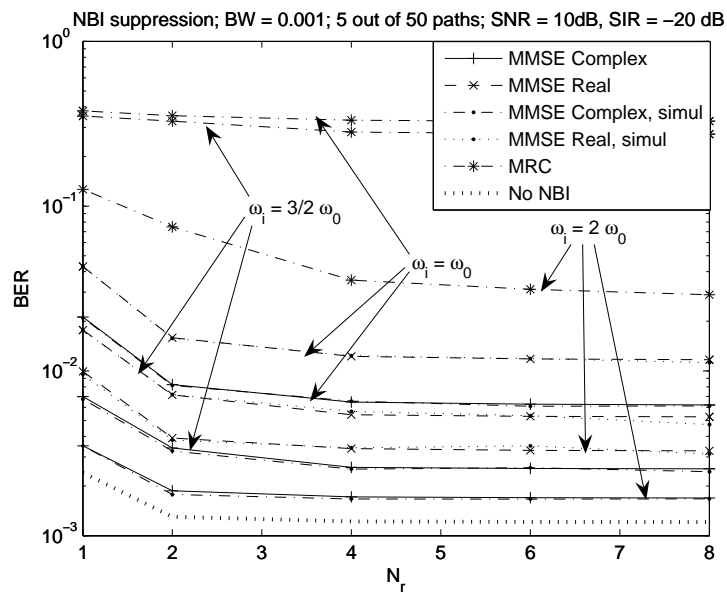
Figure 3.7: NBI Suppression: BER v_s Number of Receiving Elements. 5 Collected Paths.

shows the performance of different combining schemes as a function of the number of receiving elements, N_r, for a fixed size receiver. The performances of different

combining schemes are compared with the ideal case. Note that the same saturation effect discussed previously is also present for MMSE combining and MRC. As the reader can notice, the MMSE combining scheme with complex weights outperforms both other schemes, showing that satisfactory performance can be achieved even in the presence of strong narrow-band jammers. Fig. 3.8 shows the performance as a function of the SNR for 6 receiving elements and $\omega_i = \omega_0$; the interference suppression capabilities of MMSE with QuadR are evident, resulting in a notable improvement in the performance. On the other hand, the system employing MRC is jammed at a SIR of -20dB. Fig. 3.9 presents simulations of the performance under the same system
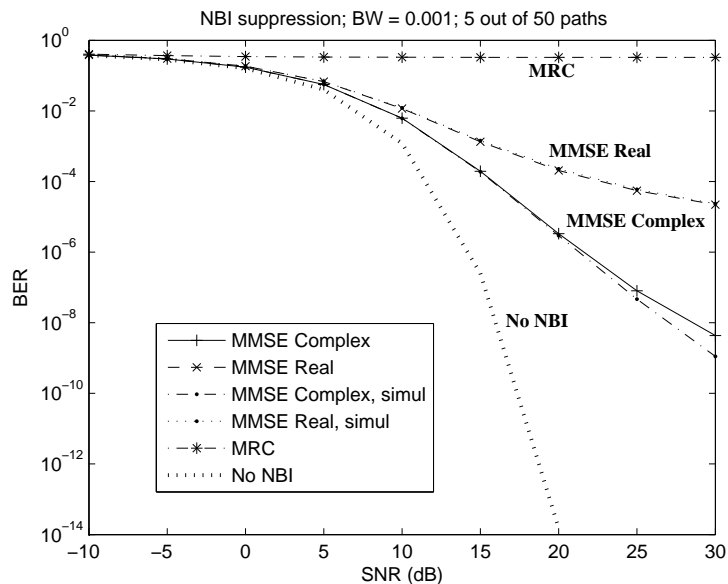
Figure 3.8: NBI Suppression: BER v_s SNR. 5 Collected Paths.

assumptions discussed above, but for the 802.15 channel described in [22]. MMSE combined with QuadR always outperforms both MRC and MMSE with CR, resulting in good interference suppression capabilities.

Finally, Fig. 3.10 shows the performance of different combining schemes as a function of the number of receiving elements in the presence of both MAI and NBI. We assume 10 UWB users, a SNR of 30dB, and a narrow-band jammer with $\omega_i = \omega_0$ and a SIR of -10dB. We consider complex Gaussian channel taps, a K_r factor derived
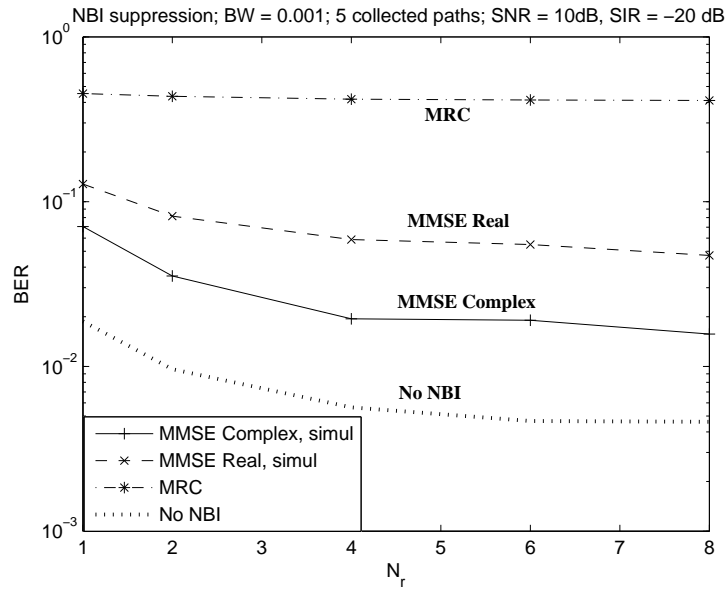
Figure 3.9: NBI Suppression: BER v_s Number of Receiving Elements. 802.15 Cahnnel, 5 Collected Paths.

from [10], and 5 collected paths out of 50.
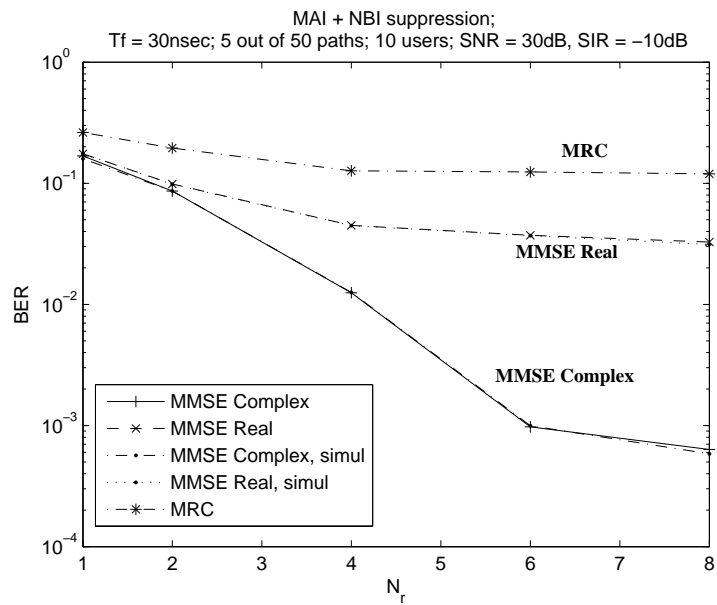
Figure 3.10: MAI and NBI Suppression: BER v_s SNR. 5 Collected Paths.

3.5 Conclusions

We presented a novel approach to MMSE beamforming for IR UWB systems based on a QuadR which exploits the correlation among the in-phase and the quadrature components of the interfering process. The performance of the system in terms of BER has been analyzed and compared to both MRC and MMSE combining with a traditional CR. The results show that the proposed combining scheme always outperforms MRC and a correlator combined with MMSE, the latter giving effectively no advantage over diversity combining when dealing with MAI. Furthermore, spatial diversity is shown to saturate with a small number of receiving antennas, since the small size of typically envisioned UWB devices results in high correlation among elements. On the other hand, beamforming exploits this correlation for interference mitigation, resulting in a large advantage in terms of BER (and/or capacity) in a highly populated UWB scenario, as well as in the presence of NBI from other commercial systems or intentional jammers.

The performance of the system has been also evaluated when a standard nonparametric estimator is adopted to estimate the interference-plus-noise covariance matrix, for different values of a known sample length. Results show that for an estimation sample size of 200 symbols, the quality of the estimates is acceptable, and the beamformer is "steered" correctly. Therefore, the performance of the system approaches the ideal "genie-aided" system. On the other hand, when the estimation time is reduced, the performance deteriorates, especially when a large number of antennas is used.

MMSE beamforming with QuadR has been shown to be a promising technique to mitigate interference from other UWB users and narrow-band jammers, and, consequently, to boost the capacity of IR systems.

The text of Chapter 3 is a reprint of the material as it appears in:

M. Sabattini, E. Masry, and L. B. Milstein, "Beamforming for Interference Mitigation in TH Impulse Radio UWB Systems" - Best Paper Award - 2005 IEEE International Conference on Personal Indoor and Mobile Radio Communications (published)

M. Sabattini, E. Masry, and L. B. Milstein, "Interference Mitigation via Beamforming for Impulse Radio Time Hopping CDMA Systems" - IEEE Transaction on Communications (submitted)

The dissertation author was the primary researcher and author, and the co-authors

listed in these publications directed and supervised the research which forms the basis

for this chapter.

4 Acquisition and Channel Estimation for Overlay UWB Transmission

"Even a broken clock is right twice a day."

Anonymous

$\mathbf{R}$ECENTLY, transmitted reference (TR) systems have been proposed [13], [65], [43], [24] to overcome the complexity of a RAKE receiver with a large number of fingers and channel tap estimates. In TR systems, an unmodulated waveform is transmitted every N_m data-modulated waveforms. The receiver correlates the received signal with this dirty template in order to make a decision on the transmitted symbol. The simplicity of this scheme comes at the price of deteriorated performance, arising from the non-optimality of the receiver in the presence of NBI.

On the other hand, both optimal RAKE and TR systems need to acquire code and/or symbol synchronization. To the best of the authors' knowledge, few chapters deal with acquisition and estimation strategies for UWB systems, and even fewer consider TR systems in the presence of overlayed NBI. In [32], the authors study the performance of maximum likelihood channel estimation for IR UWB transmissions, in the presence of AWGN. In [27], the Cramer-Rao lower bound for UWB IR channel estimation is derived. In [8], the authors present a semi-blind estimation scheme for UWB systems in the presence of white noise. Farhamand *et al.* in [19] analyze the

performance of pulse timing with dirty templates, also in the presence of AWGN. In [61], non-coherent code acquisition techniques for TH IR systems are studied, in the presence of multipaths and AWGN. The authors in [60] present some results on equal-gain combining for acquisition of TH code division multiple access (CDMA) systems in the presence of AWGN. The authors in [9] present a maximum likelihood approach to symbol synchronization for UWB TR systems, also in the presence of AWGN. Some preliminary considerations on NBI effects on TR systems are presented in [39], [41], while in [16], a coarse acquisition strategy for spectral-encoded UWB systems, also in the presence of narrow-band jammer, is presented. The presence of NBI - if not accounted for - can potentially affect dramatically the performance of the system.

This chapter presents a general code acquisition strategy that can be applied to both RAKE (called, from now on, **Receiver A**) and TR (**Receiver B**) schemes. Furthermore, in order to fairly compare both schemes, results for the BER of both receivers will be presented, assuming that code synchronization had been achieved, where **Receiver A** employs the channel estimates in a tapped-delay line correlator optimized for non-white Gaussian noise, while **Receiver B** notches the NBI (through an ideal notch filter) prior to correlating the received signal with a noisy template. The rest of the paper is organized as follows: in Section 4.1, the transmitted and received signal models are presented, while Section 4.2 describes the estimation/acquisition scheme. The probability that the receiver correctly acquires code synchronization is introduced and analyzed in Section 4.3. When **Receiver A** is employed, the receiver jointly estimates the channel attenuation coefficients; the performance of such a scheme in terms of mean-square-error (MSE) is presented in Section 4.4. Numerical results and comments are presented in Section 4.5. Finally, we conclude in Section 4.6.

4.1 Transmitted and Received Signal

Consider an UWB user transmitting a preamble of known data, in order to let the receiver achieve code synchronization and perform channel estimation. For our purpose, we assume the transmitted known preamble is a train of '+1's; also, we assume that the receiver observes such a preamble over an observation window of length at least equal to the preamble duration plus the multipath delay spread. Furthermore, we assume the length of the preamble to be at least one period of the spreading sequence. For analytical simplicity, we model the transmitted signal as follows:

$$s_{tr}(t) = \sqrt{P_W} \sum_{j=-\infty}^{+\infty} c_j x(t - jT) \tag{4.1}$$

where $x(t)$ is a waveform of duration T, and such that $\frac{1}{T} \int_0^T |x(t)|^2 dt = 1$, P_W is the transmitted power, while $\{c_j\}_{j=-\infty}^{+\infty}$ is a periodic pseudo-random sequence of period N_{seq}; that is, $c_{j+N_{seq}} = c_j$, $\forall j$. In order to fairly compare different CDMA schemes, we set $c_j = A\tilde{c}_j$, with A a normalization constant, defined as $A := \frac{1}{\sqrt{\sum_{j=0}^{N_{seq}-1} |\tilde{c}_j|^2}}$, such that $\sum_{j=0}^{N_{seq}-1} |c_j|^2 = 1$ Note that when $\{\tilde{c}_j\}_{j=-\infty}^{+\infty}$ is a sequence of ± 1, Eq. (4.1) represents a direct sequence (DS) CDMA signal. On the other hand, if $\{\tilde{c}_j\}_{j=-\infty}^{+\infty}$ is a sequence of zeros and ones, then Eq. (4.1) can be interpreted as a TH CDMA signal. The third spreading technique is called bi-orthogonal [69] TH (B-TH) CDMA, for which $\{\tilde{c}_j\}_{j=-\infty}^{+\infty}$ is a sequence of $0, \pm 1$. See Fig. 4.1 for details.

We assume the spreading sequence is known at the receiver, whose task is to synchronize to the correct code lag, as well as estimate the channel. We also assume a slowly-varying propagation channel, so that the channel coefficients can be considered constant for the entire estimation process. The signal of Eq. (4.1) goes through a frequency selective channel that can be represented by the impulse response $h_{MP}(t) = \sum_{h=0}^{P-1} \alpha_h^{(0)} \delta(t - hT)$, where the $\left\{\alpha_h^{(0)}\right\}_{h=0}^{P-1}$ are channel attenuation coefficients to be estimated, modelled as jointly distributed random variables, with
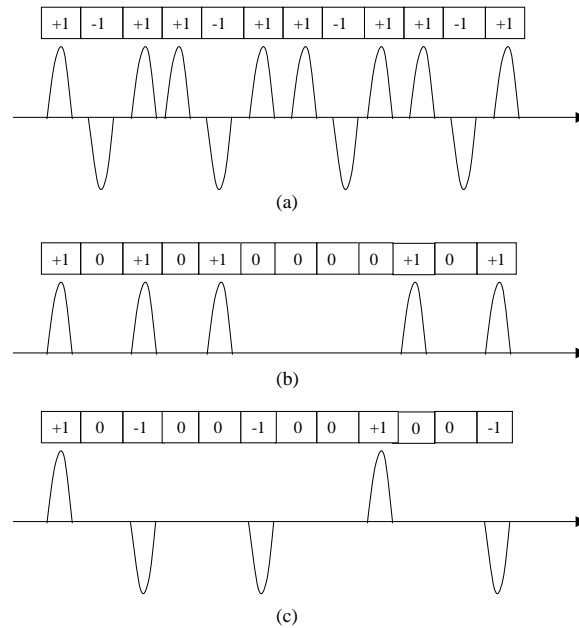
Figure 4.1: Different spreading schemes: (a) DS-CDMA; (b) TH-CDMA; (c) BTH-CDMA.

unknown distribution. Depending upon the modulation scheme adopted (IR versus modulated signals), the channel coefficients can be either real or complex. When we refer to complex channel attenuation coefficients, Eq. (4.1) represents the base-band equivalent of an radio frequency (RF) modulated signal. Also, the superscript '(0)' indicates the true channel coefficients, as opposed to the estimated ones.

The signal is received in colored Gaussian noise:

$$r(t) = \sqrt{P_W} \sum_{j=-\infty}^{+\infty} \sum_{h=0}^{P-1} \alpha_h^{(0)} c_j x(t - (j + h)T - \tau) + w(t) \tag{4.2}$$

where the delay τ is an unknown deterministic delay which depends on the distance between receiver and transmitter, considered *modulo* $N_{seq}T$, taking values in the interval $[0, N_{seq}T]$, and has to be tracked at the receiver, while $w(t)$ is a zero-mean wide-sense-stationary colored Gaussian random process, with auto-covariance function $\phi(u) := E[w(t)w^*(t + u)]$, where the symbol * stands for the complex conjugate. Note that, in general, $w(t)$ represents the sum of thermal noise and NBI.

For simplicity, we assume τ to be an integer multiple of T, i.e., $\tau = n_0 T$ for some integer n_0. Then

$$
\begin{aligned}
r(t) &= \sqrt{P_W} \sum_{j=-\infty}^{+\infty} \sum_{h=0}^{P-1} \alpha_h^{(0)} c_j x(t - (j + h + n_0)T) + w(t) \\
&= \sqrt{P_W} \sum_{i=-\infty}^{+\infty} \sum_{h=0}^{P-1} \alpha_h^{(0)} c_{i-n_0} x(t - (i + h)T) + w(t) \qquad (4.3)
\end{aligned}
$$

where we set $i = j + n_0$. Note that n_0 can take any value into $\{0, 1, \ldots, N_{seq} - 1\}$. By assuming the transmitted power, P_W, known at the receiver[1], we need to estimate the channel $\underline{\alpha}_0 := \left[\alpha_0^{(0)} \ \alpha_1^{(0)} \ \ldots \ \alpha_{P-1}^{(0)} \right]^T$, as well as to synchronize to the code lag n_0, by observing the received waveform $r(t)$ over the window $[0, MT]$, for some integer $M > P$. Furthermore, since $x(t)$ has support over the interval $[0, T]$, the term $x(t-(i+h)T)$ is non-zero when

$$
0 \le t-(i+h)T \le T \Rightarrow (i+h)T \le t \le (i+h+1)T \Rightarrow t \in [(i+h)T, (i+h+1)T] \quad (4.4)
$$

Since $t \in [0, MT]$, the signal component in (4.3) is non-zero only when

$$
[0, MT] \cap [(i+h)T, (i+h+1)T] \neq \emptyset
$$

or, equivalently, when $-h \le i \le M - 1 - h$. Eq. (4.3) can be re-written as

$$
r(t) = \sum_{h=0}^{P-1} \sum_{j=-h}^{M-1-h} \alpha_h^{(0)} c_{j-n_0} x(t - (j + h)T) + w(t), \qquad 0 \le t \le MT \quad (4.5)
$$

---

[1]This assumption is without any loss of generality, since the uncertainty on the signal strength can be, in general, included in the unknown channel coefficients. For this reason, from now on we set $P_W = 1$.

4.2 Data-aided estimation

Let us first define

$$s(t; \underline{\alpha}, n) = \sum_{h=0}^{P-1} \sum_{j=-h}^{M-1-h} \alpha_h c_{j-n} x(t - (j+h)T) \tag{4.6}$$

where P is the number of multipaths. Note that $s(t; \underline{\alpha}, n)$ represents the desired signal, parameterized by $\underline{\alpha}$ and n. If we know the second-order statistics of the noise process $w(t)$, i.e., its auto-covariance function $\phi(u)$, we can use maximum likelihood estimation (MLE)[2] in order to find the optimal estimates $\hat{\underline{\alpha}}$ and $\hat{n}$ for $\underline{\alpha}_0$ and n_0, respectively. Specifically, we maximize the log-likelihood function as in [58]:

$$L_{MLE}(r; \underline{\alpha}, n) = 2 \int_0^{MT} q^*(t; \underline{\alpha}, n) r(t) dt - \int_0^{MT} q^*(t; \underline{\alpha}, n) s(t; \underline{\alpha}, n) dt \tag{4.7}$$

where $q(t; \underline{\alpha}, n)$ is defined as the solution of the integral relation

$$s(t; \underline{\alpha}, n) = \int_0^{MT} q(u; \underline{\alpha}, n) \phi(t - u) du, \qquad 0 \le t \le MT. \tag{4.8}$$

The maximization of $L_{MLE}(r; \underline{\alpha}, n)$ can be carried out in two steps:

$$(a) \qquad \hat{\underline{\alpha}}(n) = \underset{\underline{\alpha}}{argmax}\, L_{MLE}(r; \underline{\alpha}, n) \tag{4.9}$$

$$(b) \qquad \hat{n}_0 = \underset{n}{argmax}\, L_{MLE}(r; \hat{\underline{\alpha}}(n), n) \tag{4.10}$$

Note that $\ell_{MLE}(r; n) := L_{MLE}(r; \hat{\underline{\alpha}}(n), n)$ is a sufficient statistic for the estimation of the code lag [64], and the estimate $\hat{n}_0$ obtained through (4.10) is optimal (in a maximum-likelihood sense). Both estimates $\hat{n}_0$ and $\hat{\underline{\alpha}}(\hat{n}_0)$ are used for **Receiver A**,

---

[2]Conditioning on $\underline{\alpha}_0$, $r(t)$ is a Gaussian random process. All the results presented in this section are implicitly conditioned on the actual channel vector $\underline{\alpha}_0$ to be estimated, assumed constant for the whole observation window.

while only $\hat{n}_0$ is used for **Receiver B** (see [9]).

In general, $\phi(u)$ can be written as $\phi(u) = \frac{N_0}{2}\delta(u) + P_I\psi(u)$, where $N_0/2$ is the two-sided PSD of the white noise, P_I is the power of the narrow-band jammer, and $\psi(u)$ is the interference auto-covariance function, normalized such that $\psi(0) = 1$. Then, Eq. (4.8) becomes

$$s(t;\underline{\alpha},n) = \frac{N_0}{2}q(t;\underline{\alpha},n) + P_I\int_0^{MT} q(u;\underline{\alpha},n)\psi(t-u)du, \qquad 0 \le t \le MT, \quad (4.11)$$

which is known as the Fredholm integral equation of the second kind, and a solution for convolutional kernels exists (see [68], Chapter VIII), provided that $N_0 \ne 0$; in most scenarios, the solution of the above integral equation is extremely difficult, and highly non-linear in the parameters $\underline{\alpha}$ and n, facts that complicate the estimation process. An explicit solution to the above integral equation for rational kernels can be found, for example, in [58]. In order to find an approximate solution for $q(t;\underline{\alpha},n)$, consider the following. Define

$$\tilde{Q}(\omega) := \frac{X(\omega)}{\frac{N_0}{2} + P_I\Psi(\omega)} \qquad (4.12)$$

whose inverse Fourier transform, $\tilde{q}(t)$, solves the convolutional integral

$$x(t) = \int_{-\infty}^{+\infty} \tilde{q}(u)\phi(t-u)du. \qquad (4.13)$$

By plugging (4.13) into (4.6), we obtain

$$\begin{aligned}
s(t;\underline{\alpha},n) &= \sum_{h=0}^{P-1}\sum_{j=-h}^{M-1-h} \alpha_h c_{j-n} x(t-(j+h)T) \qquad (4.14)\\
&= \sum_{h=0}^{P-1}\sum_{j=-h}^{M-1-h} \alpha_h c_{j-n} \int_{-\infty}^{+\infty} \tilde{q}(u)\phi(t-u-(j+h)T)du
\end{aligned}$$

$$= \int_{-\infty}^{+\infty} \sum_{h=0}^{P-1} \sum_{j=-h}^{M-1-h} \alpha_h c_{j-n} \tilde{q}(u - (j+h)T)\phi(t-u)du$$

If $\tilde{q}(t)$ is approximately zero outside the interval $[0, T]$, then

$$s(t; \underline{\alpha}, n) \approx \int_{0}^{MT} \sum_{h=0}^{P-1} \sum_{j=-h}^{M-1-h} \alpha_h c_{j-n} \tilde{q}(u - (j+h)T)\phi(t-u)du \qquad (4.15)$$

and

$$q(t; \underline{\alpha}, n) \approx \sum_{h=0}^{P-1} \sum_{j=-h}^{M-1-h} \alpha_h c_{j-n} \tilde{q}(t - (j+h)T) \qquad (4.16)$$

is an approximate solution to the Fredholm integral equation in (4.8). We point out that when the noise $w(t)$ is white, $\psi(u) = 0$, and (4.7) reduces to the common integral version of the log-likelihood function, namely

$$L_{MLE}^{(AWGN)}(r; \underline{\alpha}, n) = \frac{2}{N_0} \int_0^{MT} s^*(t; \underline{\alpha}, n)r(t)dt - \frac{1}{N_0} \int_0^{MT} |s(t; \underline{\alpha}, n)|^2 dt, \qquad (4.17)$$

and the solution in (4.16) is exact for any window-of-observation.

Note that the exact solution of (4.8) is, from any practical perspective, unfeasible. On the other hand, the approximate solution in (4.16) has two major advantages:

1. The receiver does not need to recalculate the front-end filter for every window-of-observation, since $\tilde{Q}(\omega)$ can be constructed off-line, with the knowledge of the received waveform and the interference PSD;

2. The overall processing in terms of the function $q(t; \underline{\alpha}, n)$ can be regarded as a weighted tapped-delay line, allowing a simple implementation by standard digital signal processing techniques;

A plot of $\tilde{Q}(\omega)$ when $x(t)$ is a Gaussian monocycle [65], [48] and the interference PSD is modelled as a shifted $sinc^2$ function is presented in Fig. 4.2. As the reader can notice, the processing filter $\tilde{Q}(\omega)$ acts as an interference notch-filter, cutting out from
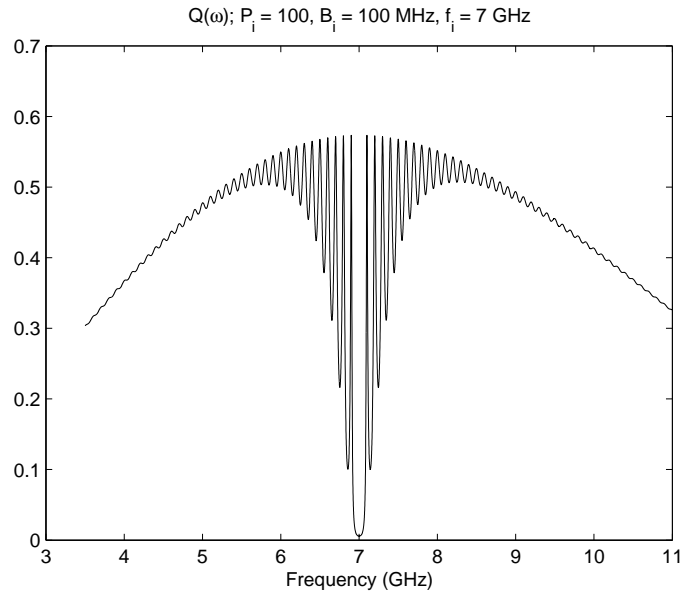
Figure 4.2: Spectrum of $\tilde{q}_T(t)$

the spectrum the frequency band occupied by the NBI.

We also point out that the excision from the spectrum of a narrow band will not drastically affect the energy content of $\tilde{q}(t)$ in time. That is, $\tilde{q}(t)$ has roughly the same duration as does $x(t)$. Fig. 4.3 shows a plot of
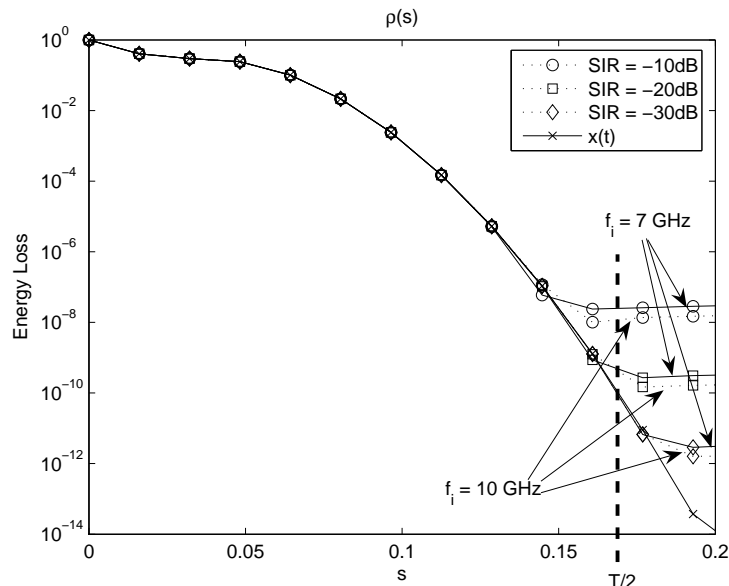
Figure 4.3: Energy Loss for different values of s, compared with the energy content of $x(t)$

$$\rho(s) := 1 - \frac{\int_{T/2-s}^{T/2+s} |\tilde{q}(t)|^2 \, dt}{\int_{-\infty}^{+\infty} |\tilde{q}(t)|^2 \, dt} \qquad (4.18)$$

for different values of the interference power and center frequency, where $x(t)$ is a Gaussian monocycle, normalized to have unit energy:

$$x(t) = A\left(1 - \frac{(t - T/2)^2}{\tau^2}\right) \exp\left[-\frac{(t - T/2)^2}{2\tau^2}\right] \qquad (4.19)$$

where $T = 8\tau$ is its effective duration [65], [48]. We also plot on the same figure the energy content of the monocycle itself; the results show that the energy loss incurred by truncating $\tilde{q}(t)$ is negligible for $s \geq T/2$. Therefore, $\tilde{q}(t)$ can be assumed - for practical purposes - to have finite support over $[0, T]$. We call $\tilde{q}_T(t)$ the truncated version of $\tilde{q}(t)$, defined as

$$\tilde{q}_T(t) := \begin{cases} \tilde{q}(t) & ; \ t \in [0, T] \\ 0 & ; \ \text{elsewhere} \end{cases} \qquad (4.20)$$

and we set

$$q_{app}(t; \underline{\alpha}, n) = \sum_{h=0}^{P-1} \sum_{j=-h}^{M-1-h} \alpha_h c_{j-n} \tilde{q}_T(t - (j+h)T) \qquad (4.21)$$

Let us go back to the log-likelihood function in (4.7). By replacing $r(t)$ and $s(t; \underline{\alpha}, n)$ with their expressions in Eqs. (4.5), (4.6), respectively, and replacing $q(t; \underline{\alpha}, n)$ with the approximate expression in (4.21), an *approximate* log-likelihood function can be written as

$$\begin{aligned} L_{APP}(r; \underline{\alpha}, n) \ = \ & 2 \sum_{h=0}^{P-1} \sum_{j=-h}^{M-1-h} c_{j-n}^* \alpha_h^* \int_0^{MT} \tilde{q}_T^*(t - (j+h)T) r(t) dt \qquad (4.22) \\ & - \sum_{h=0}^{P-1} \sum_{k=0}^{P-1} \sum_{j=-h}^{M-1-h} \sum_{i=-k}^{M-1-k} c_{j-n}^* c_{i-n} \alpha_h^* \alpha_k \\ & \times \int_0^{MT} \tilde{q}_T^*(t - (j+h)T) x(t - (i+k)T) dt \end{aligned}$$

After some manipulations presented in Appendix C.1, one can show that

$$L_{APP}(r; \underline{\alpha}, n) = 2\underline{\alpha}^H \underline{\underline{\mathcal{C}}}(n) \, \underline{y} - \mathcal{E}\underline{\alpha}^H \underline{\underline{\mathcal{C}}}(n) \, \underline{\underline{\mathcal{C}}}(n)^H \underline{\alpha} \tag{4.23}$$

where

$$\underline{\underline{\mathcal{C}}}(n) \; := \; \begin{bmatrix} c_{-n} & c_{-n+1} & \cdots & c_{-n+M-1} \\ c_{-n-1} & c_{-n} & \cdots & c_{-n+M-2} \\ \vdots & \vdots & \ddots & \vdots \\ c_{-n-P+1} & c_{-n-P+2} & \cdots & c_{-n+M-P} \end{bmatrix}^{\star}_{P \times M} \tag{4.24}$$

$$\underline{y} \; := \; [y_0 \, y_1 \, \ldots \, y_{M-1}]^T \tag{4.25}$$

$$y_p \; := \; \int_0^T \tilde{q}_T^*(t) r(t + pT) dt \tag{4.26}$$

$$; \; p = 0, 1, \ldots, M - 1$$

$$\mathcal{E} \; = \; \int_0^T \tilde{q}_T^*(t) x(t) dt \tag{4.27}$$

$\underline{y}$ depends implicitly (through $r(t)$) on the actual parameters $\underline{\alpha}_0$, n_0, and $\mathcal{E}$ can be shown to be a positive quantity[3]. The maximization of (4.23) can be carried out in two steps [49]: first, we find the optimal set of channel estimates for every $n = 0, 1, \ldots, N_{seq} - 1$, and then we maximize over n. The gradient of (4.23) in $\underline{\alpha}$ is [47]

$$\frac{d}{d\underline{\alpha}} L_{APP}(r; \underline{\alpha}, n) = 2\underline{\underline{\mathcal{C}}}(n) \, \underline{y} - 2\mathcal{E}\underline{\underline{\mathcal{C}}}(n) \, \underline{\underline{\mathcal{C}}}(n)^H \underline{\alpha} \tag{4.28}$$

By setting (4.28) to zero, we find the set of channel estimates for a given n. Note that an explicit solution in $\underline{\alpha}$ requires the inverse of $\underline{\underline{\mathcal{C}}}(n) \, \underline{\underline{\mathcal{C}}}(n)^H$ to exist. This is not true in general, especially for small M. Therefore, we resort to a more general least-square

---

[3]By the use of Parseval's theorem, $\mathcal{E}$ can be expressed as the integral of the spectrum of $x(t)$, which is always positive, divided by the PSD of the noise, which is also greater than zero for finite values of N_0 and P_I.

solution as

$$\hat{\underline{\alpha}}(n) = \frac{1}{\mathcal{E}} \left[\underline{\underline{C}}(n) \, \underline{\underline{C}}(n)^H \right]^\dagger \underline{\underline{C}}(n) \, \underline{y} \tag{4.29}$$

where $\underline{\underline{A}}^\dagger = \left(\underline{\underline{A}}^H \underline{\underline{A}} \right)^{-1} \underline{\underline{A}}^H$ is the Moore-Penrose pseudo-inverse of $\underline{\underline{A}}$ [6]. By plugging (4.29) into (4.23), we obtain

$$\ell_{APP}(r; n) := L_{APP}(r; \hat{\underline{\alpha}}(n), n) = \underline{y}^H \underline{\underline{C}}(n)^H \left[\underline{\underline{C}}(n) \, \underline{\underline{C}}(n)^H \right]^\dagger \underline{\underline{C}}(n) \, \underline{y} \tag{4.30}$$

Note that the receiver will synchronize to the code lag $\hat{n}_0$ which maximizes (4.30), specifically,

$$\hat{n}_0 := \underset{n=0,1,\ldots,N_{seq}-1}{argmax} \ell_{APP}(r; n) \tag{4.31}$$

We point out that the code lag estimate $\hat{n}_0$ of (4.31) will be used for both receivers **A** and **B** (see Fig. 4.4).
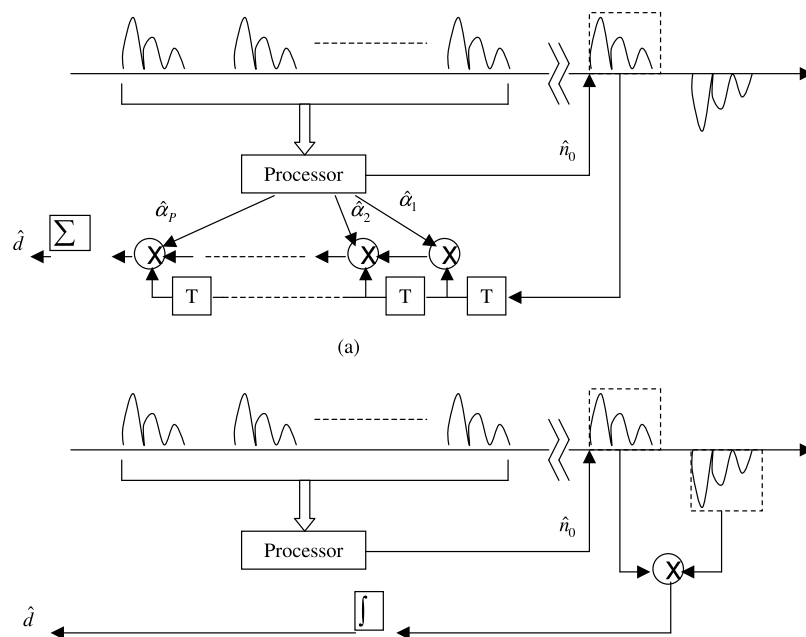
Figure 4.4: Receiving strategies: (a) RAKE receiver; (b) TR receiver.

We define the probability that the receiver synchronizes on lag m as

$$P_L(m) = P_r \left[\hat{n}_0 = m \right] = P_r \left[\underset{n=0,1,\ldots,N_{seq}-1}{max} \ell_{APP}(r; n) = \ell_{APP}(r; m) \right] \tag{4.32}$$

Also, we point out that for a given n_0, the vector $\underline{y}$ is a complex Gaussian random vector, whose statistics are described below.

Recall that $\underline{y}$ as defined in (4.25) is a Gaussian random vector, where the p-th element is given by

$$y_p = \int_0^T \tilde{q}_T^*(t) r(t + pT) \qquad ; \; p = 0, 1, \ldots, M - 1 \tag{4.33}$$

Recalling the expression for $r(t)$, we have

$$
\begin{aligned}
y_p &= \sum_{j=-\infty}^{+\infty} \sum_{h=0}^{P-1} c_{j-n_0} \alpha_h^{(0)} \int_0^T \tilde{q}_T^*(t) x(t - (j + h - p)T) dt \\
&+ \int_0^T \tilde{q}_T^*(t) w(t + pT) dt
\end{aligned}
\tag{4.34}
$$

Since $x(t)$ has support over $[0, T]$,

$$\int_0^T \tilde{q}_T^*(t) x(t - (j + h - p)T) dt = \begin{cases} \int_0^T \tilde{q}_T^*(t) x(t) dt = \mathcal{E} & ; \; j = p - h \\ 0 & ; \; elsewhere \end{cases} \tag{4.35}$$

Therefore

$$y_p = \mathcal{E} \sum_{h=0}^{P-1} \alpha_h^{(0)} c_{p-h-n_0} + \nu_p \tag{4.36}$$

where

$$\nu_p := \int_0^T \tilde{q}_T^*(t) w(t + pT) dt \quad ; \; p = 0, \ldots, M - 1 \tag{4.37}$$

are zero-mean complex Gaussian random variables. Recalling the definition of $\underline{\underline{\mathcal{C}}}(n)$ in (4.24), it is readily shown that

$$\underline{y} = \mathcal{E} \, \underline{\underline{\mathcal{C}}}(n_0)^H \underline{\alpha}_0 + \underline{\nu} \tag{4.38}$$

where $\underline{\nu} = [\nu_0 \; \nu_1 \; \ldots \; \nu_{M-1}]^T$.

Therefore,

$$\underline{\mu}_y := E\left[\underline{y}\right] = \mathcal{E}\underline{\underline{C}}(n_0)^H E\left[\underline{\alpha}_0\right] \tag{4.39}$$

$$\underline{\underline{\Omega}}_y := E\left[\left(\underline{y} - \underline{\mu}_y\right)\left(\underline{y} - \underline{\mu}_y\right)^H\right] = \mathcal{E}^2\underline{\underline{C}}(n_0)^H Cov\left[\underline{\alpha}_0, \underline{\alpha}_0\right]\underline{\underline{C}}(n_0) \tag{4.40}$$

$$+E\left[\underline{\nu}\,\underline{\nu}^H\right]$$

where

$$E\left[\nu_p\nu_{p'}\right] = \int_0^T\int_0^T \tilde{q}_T^*(t_1)\tilde{q}_T(t_2)\phi(t_1 - t_2 - (p - p')T)dt_1dt_2 \tag{4.41}$$

4.3 Probability of correct synchronization

We first define the probability that the receiver synchronizes on lag m, which is the probability that $\ell_{APP}(r;m)$ is larger than $\ell_{APP}(r;n)$, for every $n = 0, 1, \ldots, N_{seq} - 1$, $n \neq m$:

$$P(m) = Pr\left[\max_n \ell_{APP}(r;n) = \ell_{APP}(r;m)\right] \tag{4.42}$$

Note that the probability of correct synchronization is $P_{sync} := P(n_0)$. Eq. (4.42) can be written as

$$P(m) = Pr\left[\ell_{APP}(r;0) < \ell_{APP}(r;m)\,,\; \ell_{APP}(r;1) < \ell_{APP}(r;m)\,,\right. \tag{4.43}$$

$$\left. \ldots\,,\; \ell_{APP}(r;N_{seq} - 1) < \ell_{APP}(r;m)\right]$$

where the m-th term is missing. Equivalently,

$$P(m) = Pr\left[\ell_{APP}(r;0) - \ell_{APP}(r;m) < 0\,,\ldots\,,\; \ell_{APP}(r;N_{seq} - 1) - \ell_{APP}(r;m) < 0\right]$$

$$\tag{4.44}$$

Recalling the expression for $\ell_{APP}(r; n)$ in (4.30), and by defining

$$\underline{\underline{Q}}(n, m) \quad := \quad \underline{\underline{C}}(n)^H \left[\underline{\underline{C}}(n) \, \underline{\underline{C}}(n)^H \right]^\dagger \underline{\underline{C}}(n) \tag{4.45}$$

$$- \, \underline{\underline{C}}(m)^H \left[\underline{\underline{C}}(m) \, \underline{\underline{C}}(m)^H \right]^\dagger \underline{\underline{C}}(m) \quad (n \neq m)$$

we have

$$P(m) = Pr \left[\underline{y}^H \underline{\underline{Q}}(0, m) \underline{y} < 0 \, , \, \ldots \, , \, \underline{y}^H \underline{\underline{Q}}(N_{seq} - 1, m) \underline{y} < 0 \right]. \tag{4.46}$$

Eq. (4.46) can be written as follows:

$$P(m) = 1 - Pr \left[\underline{y}^H \underline{\underline{Q}}(0, m) \underline{y} \geq 0 \text{ or } \underline{y}^H \underline{\underline{Q}}(1, m) \underline{y} \geq 0 \, \ldots \, or \, \underline{y}^H \underline{\underline{Q}}(N_{seq} - 1, m) \underline{y} \geq 0 \right] \tag{4.47}$$

By the union bound,

$$Pr \left[\underline{y}^H \underline{\underline{Q}}(0, m) \underline{y} \geq 0 \text{ or } \underline{y}^H \underline{\underline{Q}}(1, m) \underline{y} \geq 0 \, \ldots \, or \, \underline{y}^H \underline{\underline{Q}}(N_{seq} - 1, m) \underline{y} \geq 0 \right]$$

$$\leq \sum_{n \neq m} Pr \left[\underline{y}^H \underline{\underline{Q}}(n, m) \underline{y} \geq 0 \right] \tag{4.48}$$

At the same time, it is easy to see that

$$P(m) \leq \min_{n \neq m} Pr \left[\underline{y}^H \underline{\underline{Q}}(n, m) \underline{y} < 0 \right] \tag{4.49}$$

Therefore one can bound $P(m)$ by

$$max \left\{ 0 \, , 1 - \sum_{n \neq m} Pr \left[\underline{y}^H \underline{\underline{Q}}(n, m) \underline{y} \geq 0 \right] \right\} \leq P(m) \leq \min_{n \neq m} Pr \left[\underline{y}^H \underline{\underline{Q}}(n, m) \underline{y} < 0 \right] \tag{4.50}$$

Note that the above bounds can be evaluated in a closed form (see Appendix C.2) when $\underline{\alpha}_0$ is Gaussian, i.e., $\underline{y}$ itself is a Gaussian random vector. When $\underline{\alpha}_0$ is not

Gaussian, but has a density $f_{\underline{\alpha}_0}(\underline{u})$, the bounds can be evaluated by first conditioning on $\underline{\alpha}_0$, and then averaging over its pdf, specifically

$$P_L\left(m \mid \underline{\alpha}_0\right) := max\left\{0 \,,\, 1 - \sum_{n \neq m} Pr\left[\underline{y}^H \underline{\underline{Q}}(n,m)\underline{y} \geq 0 \mid \underline{\alpha}_0\right]\right\} \leq \qquad (4.51)$$

$$P\left(m \mid \underline{\alpha}_0\right) \leq \min_{n \neq m} Pr\left[\underline{y}^H \underline{\underline{Q}}(n,m)\underline{y} < 0 \mid \underline{\alpha}_0\right] =: P_U\left(m \mid \underline{\alpha}_0\right)$$

where $P\left(m \mid \underline{\alpha}_0\right)$ is the probability that the receiver synchronizes at lag $\hat{n}_0 = m$, given $\underline{\alpha}_0$. Then

$$\int \cdots \int f_{\underline{\alpha}_0}(\underline{u}) P_L\left(m \mid \underline{u}\right) d\underline{u} \leq P(m) \leq \int \cdots \int f_{\underline{\alpha}_0}(\underline{u}) P_U\left(m \mid \underline{u}\right) d\underline{u} \qquad (4.52)$$

4.4 Mean-square error of the channel estimates

A sensible measure for the performance of a channel estimator is the MSE. We stress that **Receiver B** does not estimate the channel, and thus this section applies only to **Receiver A**.

Recalling Eqs. (4.29) and (4.38), we have

$$\underline{\hat{\alpha}}(n) = \left[\underline{\underline{C}}(n)\underline{\underline{C}}(n)^H\right]^\dagger \underline{\underline{C}}(n)\,\underline{\underline{C}}(n_0)^H \underline{\alpha}_0 + \frac{1}{\mathcal{E}}\left[\underline{\underline{C}}(n)\underline{\underline{C}}(n)^H\right]^\dagger \underline{\underline{C}}(n)\,\underline{\nu} \qquad (4.53)$$

and

$$\underline{\hat{\alpha}}(\hat{n}_0) - \underline{\alpha}_0 = \left\{\left[\underline{\underline{C}}(\hat{n}_0)\underline{\underline{C}}(\hat{n}_0)^H\right]^\dagger \underline{\underline{C}}(\hat{n}_0)\,\underline{\underline{C}}(n_0)^H - \underline{\underline{I}}_{P \times P}\right\}\underline{\alpha}_0 + \frac{1}{\mathcal{E}}\left[\underline{\underline{C}}(\hat{n}_0)\underline{\underline{C}}(\hat{n}_0)^H\right]^\dagger \underline{\underline{C}}(\hat{n}_0)\,\underline{\nu}$$

$$\qquad (4.54)$$

Thus, $||\underline{\hat{\alpha}}(\hat{n}_0) - \underline{\alpha}_0||^2 = ||\underline{\underline{A}}(\hat{n}_0)\underline{\alpha}_0 + \underline{\underline{B}}(\hat{n}_0)\underline{\nu}||^2$, where

$$\underline{\underline{A}}(n) := \left[\underline{\underline{C}}(n)\,\underline{\underline{C}}(n)^H\right]^\dagger \underline{\underline{C}}(n)\,\underline{\underline{C}}(n_0)^H - \underline{\underline{I}}_{P \times P} \qquad (4.55)$$

and

$$\underline{\underline{B}}(n) := \frac{1}{\mathcal{E}} \left[\underline{\underline{C}}(n) \, \underline{\underline{C}}(n)^H \right]^\dagger \underline{\underline{C}}(n) \tag{4.56}$$

Note that $\underline{\underline{A}}(n_0) = \underline{\underline{0}}_{P \times P}$. Clearly, the MSE of an estimator that jointly estimates the channel and the code lag is larger than the MSE of a *"genie-aided"* estimator, which knows the actual code lag *a-priori*. Therefore,

$$E \, ||\underline{\hat{\alpha}}(\hat{n}_0) - \underline{\alpha}_0||^2 \geq E \, ||\underline{\hat{\alpha}}(n_0) - \underline{\alpha}_0||^2 = E \, \left|\left|\underline{\underline{B}}(n_0)\underline{\nu}\right|\right|^2 = tr \left(\underline{\underline{B}}(n_0) E \left[\underline{\nu} \, \underline{\nu}^H \right] \underline{\underline{B}}(n_0)^H \right) \tag{4.57}$$

We stress that the above lower bound represents the lowest achievable MSE: in other words, the right hand side of (4.57) represents the channel estimation error of a receiver which already achieved synchronization. We show in Section 4.5 that the proposed estimation scheme can perform very close to the ideal *"genie-aided"* estimator, even at relatively small SNR values and window-of-observation lengths. On the other hand, $||\underline{\hat{\alpha}}(\hat{n}_0) - \underline{\alpha}_0||^2 \leq 2 \, \left|\left|\underline{\underline{A}}(\hat{n}_0)\underline{\alpha}_0\right|\right|^2 + 2 \, \left|\left|\underline{\underline{B}}(\hat{n}_0)\underline{\nu}\right|\right|^2$. Note that, by the theorem of total probability,

$$\begin{aligned} E \, \left|\left|\underline{\underline{A}}(\hat{n}_0)\underline{\alpha}_0\right|\right|^2 &= \sum_{n \neq n_0} E \left[\left|\left|\underline{\underline{A}}(n)\underline{\alpha}_0\right|\right|^2 \mid \hat{n}_0 = n \right] Pr\left[\hat{n}_0 = n\right] \\ &= E \left\{ \sum_{n \neq n_0} E \left[\left|\left|\underline{\underline{A}}(n)\underline{\alpha}_0\right|\right|^2 \mid \hat{n}_0 = n, \underline{\alpha}_0 \right] Pr\left[\hat{n}_0 = n \mid \underline{\alpha}_0\right] \right\} \end{aligned} \tag{4.58}$$

Since, from Eq. (4.51), $Pr\left[\hat{n}_0 = n \mid \underline{\alpha}_0\right] = P\left(n \mid \underline{\alpha}_0\right) \leq P_U\left(n \mid \underline{\alpha}_0\right)$, we have

$$E \, \left|\left|\underline{\underline{A}}(\hat{n}_0)\underline{\alpha}_0\right|\right|^2 \leq E \left\{ \sum_{n \neq n_0} E \left[\left|\left|\underline{\underline{A}}(n)\underline{\alpha}_0\right|\right|^2 \mid \hat{n}_0 = n, \underline{\alpha}_0 \right] P_U\left(n \mid \underline{\alpha}_0\right) \right\} =: E \left[\mathcal{G}(\underline{\alpha}_0) \right] \tag{4.59}$$

From now on, matrix inequalities are defined, in relation to quadratic forms, as follows:

Definition 4.1 *Given two matrices $\underline{\underline{A}}$ and $\underline{\underline{B}}$, we write $\underline{\underline{A}} \geq \underline{\underline{B}}$ (resp., $\underline{\underline{A}} > \underline{\underline{B}}$), if*

$\underline{\underline{A}} - \underline{\underline{B}}$ is positive semi-definite (resp., positive definite).

Assuming perfectly orthogonal codes, it is shown in Appendix C.3 that $\underline{\underline{B}}(n)^H \underline{\underline{B}}(n) \leq \frac{1}{M^2 \mathcal{E}^2} \tilde{\underline{\underline{C}}}^H \tilde{\underline{\underline{C}}}$, where $\left[\tilde{\underline{\underline{C}}} \right]_{a,b} = c^*_{-a+b}$, for $a = 0, 1, \ldots, N_{seq} - 1$, $b = 0, 1, \ldots, M - 1$. Thus

$$E \left\| \underline{\underline{B}}(\hat{n}_0) \underline{\nu} \right\|^2 = E \left[\underline{\nu}^H \underline{\underline{B}}(\hat{n}_0)^H \underline{\underline{B}}(\hat{n}_0) \underline{\nu} \right] \leq \frac{1}{M^2 \mathcal{E}^2} \, tr \left(\tilde{\underline{\underline{C}}}^H E \left[\underline{\nu} \, \underline{\nu}^H \right] \tilde{\underline{\underline{C}}} \right) \qquad (4.60)$$

Therefore

$$tr \left(\underline{\underline{B}}(n_0) E \left[\underline{\nu} \, \underline{\nu}^H \right] \underline{\underline{B}}(n_0)^H \right) \quad \leq \quad E \left\| \hat{\underline{\alpha}}(\hat{n}_0) - \underline{\alpha}_0 \right\|^2 \qquad (4.61)$$
$$\leq 2E \left[\mathcal{G}(\underline{\alpha}_0) \right] + \frac{2}{M^2 \mathcal{E}^2} \, tr \left(\tilde{\underline{\underline{C}}}^H E \left[\underline{\nu} \, \underline{\nu}^H \right] \tilde{\underline{\underline{C}}} \right)$$

We show in Section 4.5 that the above bounds are always quite tight, regardless of the value of M.

4.5 Numerical Results and Discussion

The parameters used to generate the numerical results are highlighted in Table 4.1. First, the performance of the system in terms of probability of incorrect synchronization (i.e., $1 - P_{sync}$) is shown in Figs. 4.5-4.8. Fig. 4.5 shows the probability of incorrect synchronization as a function of the SNR, for different values of the window-of-observation length. The performance is compared with the upper and lower bounds, and with the performance of the system in the absence of NBI. First, we point out that the bounds are, in general, quite tight, and become extremely precise for SNR values larger than 15/20 dB. We also stress that, while the system not designed for NBI suppression is completely jammed, the proposed scheme can achieve acceptable performance by effectively cancelling out the jammer. Note that by increasing the interference bandwidth (Fig. 4.6) from 10^{-2} to $10^{-1} \times B_W$(signal), the system performs worse, and cannot achieve the performance of the ideal system in

Table 4.1: Parameters used in the numerical results

	System Parameters	
T	Pulse duration	0.25 ns
f_0	Center Frequency	7 GHz
B_W	Bandwidth	3.5 GHz - 10 GHz
Modulation	Baseband	Gauss. Monocycle [65]
M	Window-of-observation	50, 100, 200 (12.8, 25.5, 51 ns)
N_P	Spreading factor	20
SNR_{chip}	SNR per chip	SNR(dB) - $10\log(N_P)$
N_{seq}	Sequence period (in chips)	200
P	Multipath components	20
Channel	Channel model adopted	Cassioli, Win, Molisch [10]
	Interference Parameters	
f_i	Center frequency	5, 7, 10 GHz
B_i	Bandwidth	10^{-2}, $10^{-1} \times B_W$
SIR	SIR	-10, -20 dB

Figure 4.5: Probability of incorrect synchronization as a function of the SNR, for different windows of observation (M=50 $\Rightarrow$ 12.8 ns; M=200 $\Rightarrow$ 51 ns). Interference parameters: $f_i = 7$ GHz, $B_i = 10^{-2} \times B_W$, SIR = -20 dB

the absence of NBI. This is because the advantage in terms of interference suppression comes at the price of larger loss in terms of collected signal power when the jammer becomes wider.
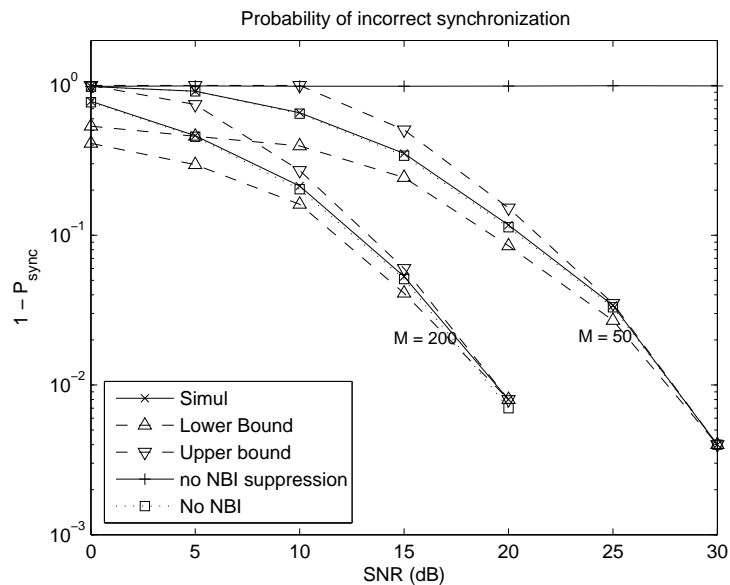
Figure 4.6: Probability of incorrect synchronization as a function of the SNR, for different windows of observation (M=50 $\Rightarrow$ 12.8 ns; M=200 $\Rightarrow$ 51 ns). Interference parameters: $f_i = 7$ GHz, $B_i = 10^{-1} \times B_W$, SIR = -20 dB

Fig. 4.7 shows the performance of the system when the jammer carrier frequency is not centered at the maximum of the desired signal spectrum, and its bandwidth is $10^{-2} \times B_W$(signal). In Fig. 4.8, the effect of the interference center frequency is studied when its bandwidth is increased from 10^{-2} to $10^{-1} \times B_W$(signal). The results are in accordance with intuition, since the system is less "hurt" when the jammer's center frequency is not at the maximum of the desired signal's spectrum; the reason for this effect lies in the lower energy loss by notching areas of the spectrum with lower PSD.

When **Receiver A** is used, the system jointly estimates the code lag and the channel attenuation coefficients. Fig. 4.9 shows the performance of the system in terms of MSE of the channel estimates versus SNR, for different lengths of the window-of-observation, when $B_i = 10^{-2} \times B_W$(signal), and SIR = -20 dB. The analytical upper and lower bounds are compared with simulations. First, we point out that the lower bound represents the estimation error that a *genie-aided* receiver would achieve

Figure 4.7: Probability of incorrect synchronization as a function of the SNR, for different windows of observation and interference center frequencies (M=50 $\Rightarrow$ 12.8 ns; M=200 $\Rightarrow$ 51 ns). Interference parameters: $f_i = 4$ GHz, $B_i = 10^{-2} \times B_W$, SIR = -20 dB
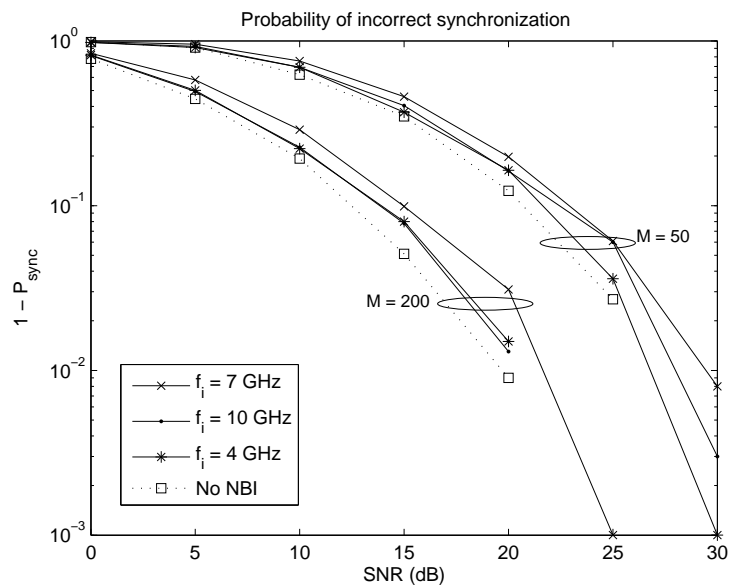
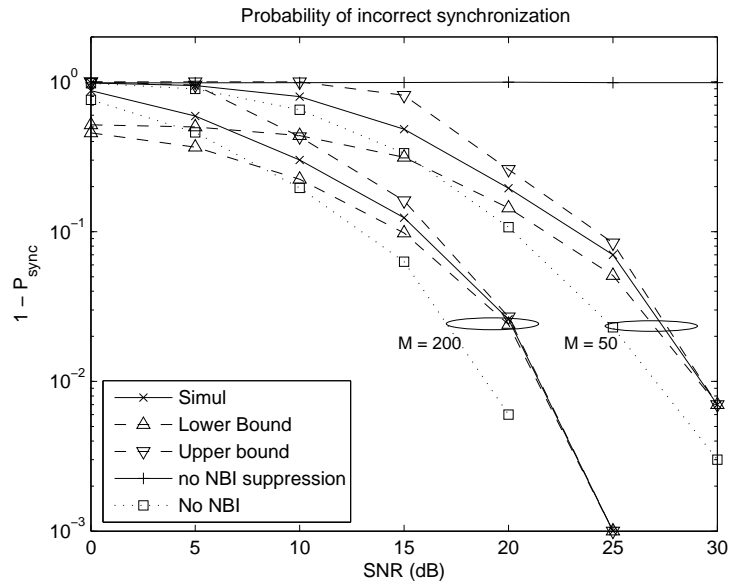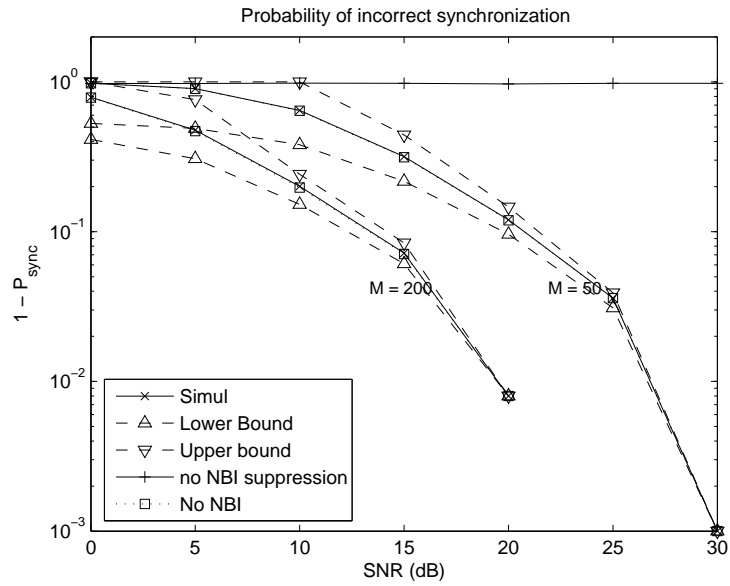

Figure 4.8: Probability of incorrect synchronization as a function of the SNR, for different windows of observation and interference center frequencies (M=50 $\Rightarrow$ 12.8 ns; M=200 $\Rightarrow$ 51 ns). Interference parameters: $f_i = 4$, 7 and 10 GHz, $B_i = 10^{-1} \times B_W$, SIR = -10 dB
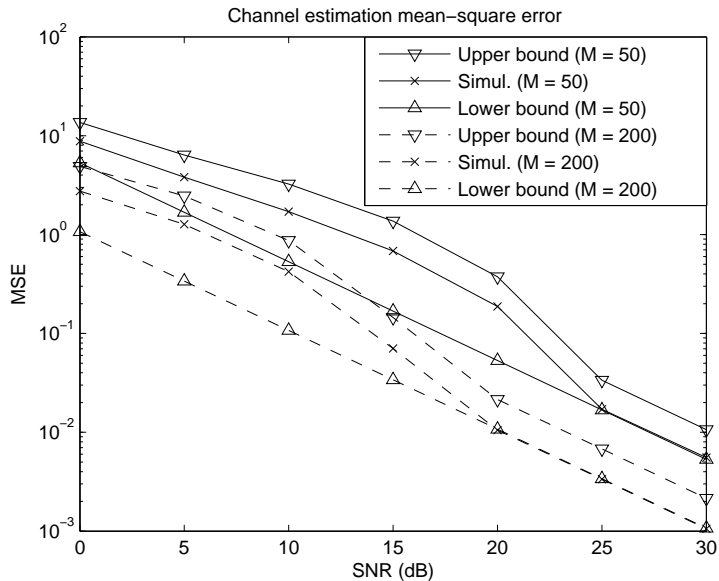
Figure 4.9: Channel estimation error as a function of the SNR, for different windows of observation (M=50 $\Rightarrow$ 12.8 ns; M=100 $\Rightarrow$ 25.6 ns; M=200 $\Rightarrow$ 51 ns). Interference parameters: $f_i = 7$ GHz, $B_i = 10^{-2} \times B_W$, SIR = -20 dB

by knowing the actual code lag n_0 *a-priori*; this is the error achieved by a receiver that estimates the channel taps only. Note that the proposed estimator (jointly estimating the channel **and** the code lag) approaches the minimum error bound at SNR $\approx$ 15/20 dB and relatively small window-of-observation lengths. Note also that the performance of the estimator improves considerably by increasing the length of the window-of-observation. Fig. 4.10 compares the channel estimation error for different window-of-observation lengths, when the interference bandwidth is increased to $B_i = 10^{-1} \times B_W$. As the reader can notice, the performance is affected by both the jammer's bandwidth and the observation window, and larger observation times are needed to compensate for a wider jammer.

Finally, a sensible measure of performance is the BER of the two receivers when code synchronization has been achieved. Fig. 4.11 shows the performance of the two systems - namely, **Receiver A** and **Receiver B** - in terms of simulated BER, for different values of the system and jammer parameters. For this plot, we assume
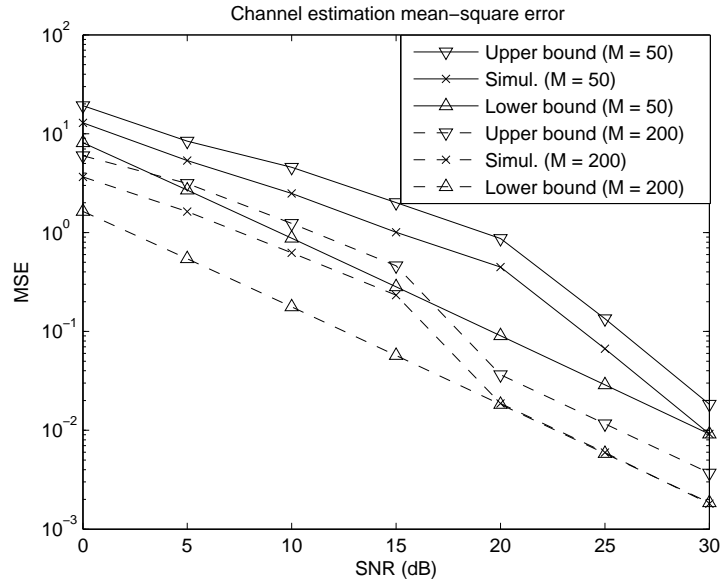
Figure 4.10: Channel estimation error as a function of the SNR, for different windows of observation and interference bandwidths (M=50 $\Rightarrow$ 12.8 ns; M=200 $\Rightarrow$ 51 ns). Interference parameters: $f_i = 7$ GHz, $B_i = 10^{-2}, 10^{-1} \times B_W$, SIR = -20 dB

that the same window of length MT is used by both systems: **Receiver A** uses the received preamble to estimate the channel through (4.29), while **Receiver B** stores the received dirty pulses (after passing them through an ideal notch filter to remove the NBI) and sums them up to construct a correlating template[4]. We point out that **Receiver A** outperforms TR schemes, at the price of an increase in complexity. The reason of this effect lies in the design of **Receiver A**, which estimates the channel taking into account the presence of NBI, and can ultimately cancel the jammer more effectively than a notch-filter. In particular, **Receiver A** can achieve performance comparable to an ideal scenario where NBI is absent, with relatively short windows of observation. On the other hand, a larger observation window is critical in order to improve the performance of **Receiver B**, especially when the jammer's bandwidth increases.

[4]The aim of summing multiple received dirty templates is to reduce the effect of the zero-mean Gaussian noise.
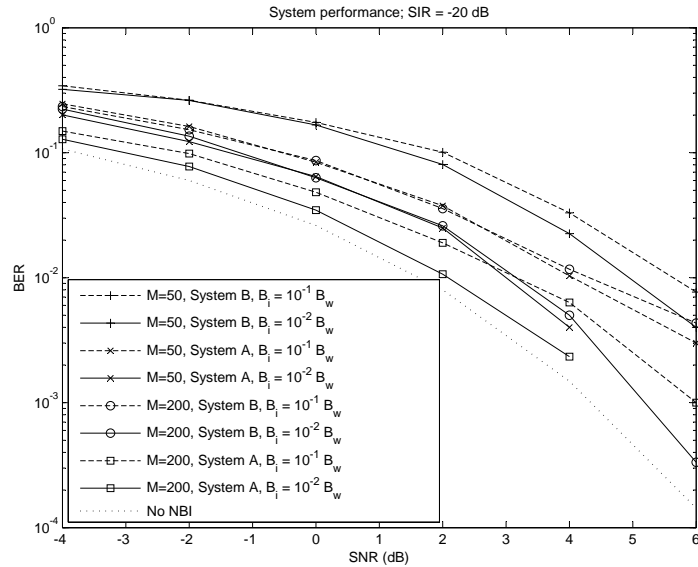
Figure 4.11: Bit error rate as a function of the SNR, for different windows of observation and interference bandwidths (M=50 $\Rightarrow$ 12.8 ns; M=200 $\Rightarrow$ 51 ns). Interference parameters: $f_i = 7$ GHz, $B_i = 10^{-2}, 10^{-1} \times B_W$, SIR = -20 dB

4.6 Conclusions

This chapter presents a general code acquisition strategy that can be applied to both RAKE and TR schemes. We show how the same proposed scheme can be employed by the receiver in order to jointly estimate the channel and acquire synchronization. The estimation and acquisition in the presence of AWGN and a narrow-band jammer are based on an approximate solution to the maximum-likelihood equation.

Several performance measures and means of comparison are presented. Results show that, while the same strategy can be employed by both TR and RAKE systems to acquire synchronization, RAKE reception with channel estimation outperforms TR systems in the presence of NBI, at the price of increased complexity.

The text of Chapter 4, is a reprint of the material as it appears in:

M. Sabattini, E. Masry, and L. B. Milstein, "Joint Code Acquisition and Channel Estimation for UWB Transmission" - Invited chapter - 2006 IEEE Sarnoff Symposium

M. Sabattini, E. Masry, and L. B. Milstein, "Joint Acquisition/Channel Estimation for UWB Communications in the Presence of Narrow-band Interference" - Invited Paper - 2006 IEEE Military Communications Conference (submitted)

M. Sabattini, E. Masry, and L. B. Milstein, "Acquisition and Channel Estimation for Overlay UWB Transmission" - IEEE Transaction on Communications (submitted)

The dissertation author was the primary researcher and author, and the co-authors listed in these publications directed and supervised the research which forms the basis for this chapter.

5 Conclusions

"Thence issuing we again beheld the stars."

Dante Alighieri

$\mathbf{O}$NE of the main issues for UWB communications is the need to operate in the presence of multiple interference sources: the indoor transmission environments (such as office spaces or apartment buildings) as well as the large bandwidth impose stringent conditions for coexistence capabilities with MAI and NBI.

In order to accurately model the interference from other UWB devices, the Gaussian approximation fails in predicting the performance of the system. For this reason, Chapter 2 was devoted to a new approach, based on a characteristic function argument, that enabled us to predict the performance very accurately. Since the exact characteristic function (and, consequently, the pdf) for the MAI is not known, and the Gaussian approximation has been shown to be very poor, a new non-Gaussian approach was proposed.

Theorem 2.1 presented the exact characteristic function for multi-user interference, which depended on the desired user's spreading sequence. In order to obtain a generic result, the dependance on the spreading sequence had to be eliminated. In Theorem 2.2, an approximate version of the MAI characteristic function was presented, where the dependance on the spreading sequence was avoided; furthermore, it was shown that the fractional error between the approximate and the exact characteristic functions decreased as the processing gain M increased, specifically, at rate $O(M^{-2})$.

The expression for the characteristic function presented in Theorem 2.2 led to the principal result of this chapter, presented in Theorem 2.3: An approximate, but explicit expression for the probability of error of the system for an arbitrary pulse shape was derived, which did not involve the pdf of the MAI. The result stated in Theorem 2.3 involved multiple finite-limit integrals, where the dimension was of the order of the number of users. For a typical UWB scenario, wherein the number of users is small, this expression could be readily evaluated by numerical techniques. Note that it was the region of small number of users where the Gaussian approximation performed the worst. Note also that in the case of a rectangular-shaped pulse, the multiple integration was carried out explicitly, leading to a closed-form expression for the probability of error given in (2.16). Finally, it was verified via comparison with simulation that our analytical results for the probability of error were very accurate, and represented a novel analytical tool to study the performance of UWB transmissions in the presence of MAI.

In order to reduce the effects of both MAI and NBI, Chapter 3 presented an MMSE beamforming approach to reject interference. The use of multiple antennas - providing marginal improvements from a spatial diversity perspective, given the large frequency diversity normally available in typical UWB environments - was very effective from a beamforming perspective to boost the capacity of the system. The results showed that the proposed combining scheme always outperformed both MRC and a correlator combined with MMSE, the latter giving effectively no advantage over diversity combining when dealing with MAI. Furthermore, spatial diversity was shown to saturate with a small number of receiving antennas, since the small size of typically envisioned UWB devices results in high correlation among elements. On the other hand, beamforming exploits this correlation for interference mitigation, resulting in a large advantage in terms of BER (and/or capacity) in a highly populated UWB scenario, as well as in the presence of NBI from other commercial systems or

intentional jammers.

The performance of the system has been also evaluated when a standard nonparametric estimator is adopted to estimate the interference-plus-noise covariance matrix, for different values of a known sample length. Results show that for an estimation sample size of 200 symbols, the quality of the estimates is acceptable, and the beamformer is "steered" correctly. Therefore, the performance of the system approaches the ideal "genie-aided" system. On the other hand, when the estimation time is reduced, the performance deteriorates, especially when a large number of antennas is used.

MMSE beamforming with QuadR has been shown to be a promising technique to mitigate interference from both other UWB users and narrow-band jammers, and, consequently, to boost the capacity of IR systems.

The presence of narrow-band jammers can hurt many receiving operations, such as channel estimation and spreading code acquisition. Chapter 4 presents a joint acquisition/estimation technique based on an approximation of the maximum likelihood scheme.

We have shown how the same proposed scheme can be employed by the receiver in order to jointly estimate the channel and acquire synchronization. The estimation and acquisition in the presence of AWGN and a narrow-band jammer were based on an approximate solution of the maximum-likelihood equation.

Several performance measures and means of comparison have been presented. Results showed that, while the same strategy can be employed by both TR and RAKE systems to acquire synchronization, RAKE reception with channel estimation outperforms TR systems in the presence of NBI, at the price of increased complexity.

A Derivations for Chapter 2

A.1 Justification of the approximation $c^{(k)}_{j-\eta_k} T_c + \delta d^{(k)}_i$

$$\approx c^{(k)}_{j-\eta_k} T_c$$

To justify the approximation, we show that

$$\left| \frac{E\left[\left(\delta d^{(k)}_i \right)^2 \right]}{E\left[\left(c^{(k)}_{j-\eta_k} T_c \right)^2 \right]} \right| \ll 1.$$

Recall that $\left\{ c^{(k)}_j \right\}^{+\infty}_{j=-\infty}$ is an M-ary equiprobable random sequence, while $\left\{ d^{(k)}_i \right\}_{i=-1,0}$ is a binary equiprobable random sequence, independent from $c^{(k)}_j$. The numerator is clearly equal to $\frac{1}{2}\delta^2$, while

$$E\left[\left(c^{(k)}_{j-\eta_k} T_c \right)^2 \right] = \frac{(M-1)(2M-1)T^2_c}{6}.$$

Since $T_c > \delta$, for M large, the above ratio is indeed much smaller than one.

A.2 "Continuity" of the Probability of Error

Denoting the approximate single-interferer characteristic function by $\hat{\varphi}_{m_1}(\omega; M)$ and the exact characteristic function by $\varphi_{m_1}(\omega)$, we have already shown that

$$\hat{\varphi}_{m_1}(\omega; M) \overset{M \to \infty}{\longrightarrow} \varphi_{m_1}(\omega)$$

It follows that

$$\hat{\varphi}_{m_I}(\omega; M)\varphi_n(\omega) = [\hat{\varphi}_{m_1}(\omega; M)]^{N_u-1}\varphi_n(\omega) \overset{M \to \infty}{\longrightarrow} [\varphi_{m_1}(\omega)]^{N_u-1}\varphi_n(\omega) = \varphi_{m_I}(\omega)\varphi_n(\omega)$$

where $\varphi_n(\omega)$ is the noise characteristic function. We have

$$\beta = E_b + m_I + n$$

where n is due to the AWGN, E_b is the signal component due to the desired user, and m_I is the MAI with characteristic function $\varphi_{m_I}(\omega)$.

The approximate expression for the probability of error, as a function of M, is

$$\hat{P}_e(M) = \int_{\infty}^{-E_b} \frac{1}{2\pi} \int_{-\infty}^{+\infty} \hat{\varphi}_{m_I}(\omega; M)\varphi_n(\omega)e^{-j\omega x} d\omega dx$$

We want to show that the approximate expression for the probability of error converges for M large to the exact probability of the system. To show that, we take the limit as M goes to infinity of the above expression, and we swap the limit inside the integral using dominated convergence. Since $|\hat{\varphi}_{m_I}(\omega; M)\varphi_n(\omega)e^{-j\omega x}| \leq |\varphi_n(\omega)| \in L_1(d\omega)$, we have:

$$\lim_{M \to \infty} \hat{P}_e(M) = \lim_{M \to \infty} \int_{\infty}^{-E_b} \frac{1}{2\pi} \int_{-\infty}^{+\infty} \hat{\varphi}_{m_I}(\omega; M)\varphi_n(\omega)e^{-j\omega x} d\omega dx$$

$$= \int_\infty^{-E_b} \frac{1}{2\pi} \int_{-\infty}^{+\infty} \lim_{M\to\infty} \hat{\varphi}_{m_I}(\omega; M)\varphi_n(\omega)e^{-j\omega x} d\omega dx$$

$$= \int_\infty^{-E_b} \frac{1}{2\pi} \int_{-\infty}^{+\infty} \varphi_{m_I}(\omega)\varphi_n(\omega)e^{-j\omega x} d\omega dx = P_e \qquad \text{(A.1)}$$

A.3   Probability of Error for rectangular pulses

Assume $T = \delta$, with $T_c = 2T + \delta = 3T$, and

$$x(t) = \begin{cases} \sqrt{\frac{e_b}{T}} & ; \text{ for } t \in [0, T] \\ \\ 0 & ; \text{ elsewhere} \end{cases}$$

It can be readily shown that

$$p(t) = \begin{cases} \left(\frac{t}{T} + 1\right) e_b & ; \text{ for } -T \le t < 0 \\ \\ \left(1 - \frac{2t}{T}\right) e_b & ; \text{ for } 0 \le t < T \\ \\ \left(\frac{t}{T} - 2\right) e_b & ; \text{ for } T \le t \le 2T. \end{cases}$$

The expression for the probability of error (Equation (2.15)) becomes

$$
\begin{aligned}
\hat{P}_e = {} & \left(1 - \frac{N_s}{M}\right)^{N_u - 1} \Phi\left(-\frac{N_s e_b}{\sqrt{N_s e_b \eta_0}}\right) \\
& + \sum_{k=1}^{N_u-1} \binom{N_u - 1}{k} \left(1 - \frac{N_s}{M}\right)^{N_u - k - 1} \left(\frac{N_s}{M}\frac{1}{T_c}\right)^k \\
& \times \underbrace{\int_{-T}^{2T} \int_{-T}^{2T} \cdots \int_{-T}^{2T}}_{k\ times} \Phi\left(-\frac{N_s e_b + \sum_{l=1}^k p(t_l)}{\sqrt{N_s e_b \eta_0}}\right) dt_1 dt_2 \ldots dt_k \qquad \text{(A.2)}
\end{aligned}
$$

With the goal of simplifying the above expression as much as possible, we write the j-th integral (with $j = 1, 2, \ldots, k$) as follows:

$$\int_{-T}^{2T} \Phi\left(-\sqrt{\frac{N_s e_b}{\eta_0}} - \frac{p(t_j)}{\sqrt{N_s e_b \eta_0}} - \frac{\sum_{l\neq j} p(t_l)}{\sqrt{N_s e_b \eta_0}}\right) dt_j$$

$$= \int_{-T}^{0} \Phi\left(-\sqrt{\frac{N_s e_b}{\eta_0}} - \frac{(\frac{t_j}{T}+1)e_b}{\sqrt{N_s e_b \eta_0}} - \frac{\sum_{l \neq j} p(t_l)}{\sqrt{N_s e_b \eta_0}}\right) dt_j \qquad (A.3)$$

$$+ \int_{0}^{T} \Phi\left(-\sqrt{\frac{N_s e_b}{\eta_0}} - \frac{(1-\frac{2t_j}{T})e_b}{\sqrt{N_s e_b \eta_0}} - \frac{\sum_{l \neq j} p(t_l)}{\sqrt{N_s e_b \eta_0}}\right) dt_j \qquad (A.4)$$

$$+ \int_{T}^{2T} \Phi\left(-\sqrt{\frac{N_s e_b}{\eta_0}} - \frac{(\frac{t_j}{T}-2)e_b}{\sqrt{N_s e_b \eta_0}} - \frac{\sum_{l \neq j} p(t_l)}{\sqrt{N_s e_b \eta_0}}\right) dt_j \qquad (A.5)$$

$$= \frac{3T}{2e_b} \int_{-e_b}^{e_b} \Phi\left(-\sqrt{\frac{N_s e_b}{\eta_0}} - \frac{s_j}{\sqrt{N_s e_b \eta_0}} - \frac{\sum_{l \neq j} p(t_l)}{\sqrt{N_s e_b \eta_0}}\right) ds_j \qquad (A.6)$$

where the last step is obtained with the change of variables $s_j = (\frac{t_j}{T}+1)e_b$, $s_j = (1-\frac{2t_j}{T})e_b$ and $s_j = (\frac{t_j}{T}-2)e_b$ in (A.3), (A.4) and (A.5), respectively.

Plugging (A.6) into (A.2) and repeating the same argument for every integral, the approximate probability of error expression is readily found to be

$$\hat{P}_e = \left(1 - \frac{N_s}{M}\right)^{N_u-1} \Phi\left(-\sqrt{\frac{N_s e_b}{\eta_0}}\right)$$

$$+ \sum_{k=0}^{N_u-1} \binom{N_u-1}{k} \left(1 - \frac{N_s}{M}\right)^{N_u-1-k} \left(\frac{N_s}{M}\right)^k \left(\frac{1}{2e_b}\right)^k$$

$$\times \underbrace{\int_{-e_b}^{e_b} \ldots \int_{-e_b}^{e_b}}_{k \text{ times}} \Phi\left(-\sqrt{\frac{N_s e_b}{\eta_0}} - \frac{\sum_{l=1}^{k} s_l}{\sqrt{N_s e_b \eta_0}}\right) ds_1 \ldots ds_k$$

where $\Phi(x)$ is the Gaussian distribution.

Note that, by setting

$$y_l := \frac{1}{k}\sqrt{\frac{N_s e_b}{\eta_0}} + \frac{s_l}{\sqrt{N_s e_b \eta_0}} \implies ds_l = \sqrt{N_s e_b \eta_0}\, dy_l$$

we have

$$\underbrace{\int_{-e_b}^{e_b} \ldots \int_{-e_b}^{e_b}}_{k \text{ times}} \Phi\left(-\sqrt{\frac{N_s e_b}{\eta_0}} - \frac{\sum_{l=1}^{k} s_l}{\sqrt{N_s e_b \eta_0}}\right) ds_1 \ldots ds_k$$

$$= (N_s e_b \eta_0)^{\frac{k}{2}} \underbrace{\int_{\frac{1}{k}\sqrt{\frac{N_s e_b}{\eta_0}} - \sqrt{\frac{e_b}{N_s \eta_0}}}^{\frac{1}{k}\sqrt{\frac{N_s e_b}{\eta_0}} + \sqrt{\frac{e_b}{N_s \eta_0}}} \ldots \int_{\frac{1}{k}\sqrt{\frac{N_s e_b}{\eta_0}} - \sqrt{\frac{e_b}{N_s \eta_0}}}^{\frac{1}{k}\sqrt{\frac{N_s e_b}{\eta_0}} + \sqrt{\frac{e_b}{N_s \eta_0}}}}_{k \text{ times}} \Phi\left(-\sum_{l=1}^{k} y_l\right) dy_1 \ldots dy_k$$

In order to further simplify the above expression and arrive at a final expression for the probability of error, we will make use of the following Lemma, which is proven at the end of this appendix:

Lemma A.1 *One can prove by induction the following relationship:*

$$\underbrace{\int_a^b \ldots \int_a^b}_{k \text{ times}} g\left(\sum_{i=1}^{k} x_i\right) dx_1 \ldots dx_k = \sum_{m=0}^{k} \binom{k}{m} (-1)^m G_k\left[(k-m)b + ma\right]$$

where $G_k(x)$ is the k-th indefinite integral of $g(x)$, defined as

$$G_k(x) := \underbrace{\int^x du_1 \int^{u_1} du_2 \ldots \int^{u_{k-1}}}_{k \text{ times}} g(y) dy$$

Therefore

$$\underbrace{\int_{-e_b}^{e_b} \ldots \int_{-e_b}^{e_b}}_{k \text{ times}} \Phi\left(-\sqrt{\frac{N_s e_b}{\eta_0}} - \frac{\sum_{l=1}^{k} s_l}{\sqrt{N_s e_b \eta_0}}\right) ds_1 \ldots ds_k$$

$$= \frac{1}{2}(-1)^k (2N_s e_b \eta_0)^{\frac{k}{2}} \sum_{m=0}^{k} \binom{k}{m} (-1)^m$$

$$\times F_k\left[(k-m)\left(\frac{1}{k}\sqrt{\frac{N_s e_b}{2\eta_0}} + \sqrt{\frac{e_b}{2N_s \eta_0}}\right) + m\left(\frac{1}{k}\sqrt{\frac{N_s e_b}{2\eta_0}} - \sqrt{\frac{e_b}{2N_s \eta_0}}\right)\right]$$

$$= \frac{1}{2}(-1)^k (2N_s e_b \eta_0)^{\frac{k}{2}} \sum_{m=0}^{k} \binom{k}{m} (-1)^m F_k \left[\sqrt{\frac{e_b}{2N_s \eta_0}} (N_s + k - 2m) \right]$$

where $\frac{(-1)^k}{\sqrt{2}} F_k(x)$ is the k-th integral of $\Phi(x)$ (see [1]), and $F_k(x)$ is defined as

$$F_k(x) := 2^{-k} e^{-x^2} \left[\frac{{}_1F_1\left(\frac{1+k}{2}; \frac{1}{2}; x^2\right)}{\Gamma\left(1 + \frac{k}{2}\right)} - 2x \frac{{}_1F_1\left(1 + \frac{k}{2}; \frac{3}{2}; x^2\right)}{\Gamma\left(\frac{1+k}{2}\right)} \right]$$

where ${}_1F_1(a; b; x)$ is the confluent hypergeometric function of the first kind and $\Gamma(x)$ is the gamma function. Note that this result is derived from Lemma A.1 for $g(x) = \Phi(x)$ and $G_k(x) = \frac{(-1)^k}{\sqrt{2}} F_k(x)$.

Therefore, the final expression for the probability of error is given by

$$\hat{P}_e = \left(1 - \frac{N_s}{M}\right)^{N_u - 1} \Phi\left(-\sqrt{\frac{N_s e_b}{\eta_0}}\right)$$

$$+ \frac{1}{2} \sum_{k=1}^{N_u - 1} \binom{N_u - 1}{k} \left(1 - \frac{N_s}{M}\right)^{N_u - 1 - k} \left(\frac{N_s}{M}\right)^k \left(-\sqrt{\frac{N_s \eta_0}{2e_b}}\right)^k$$

$$\times \sum_{m=0}^{k} \binom{k}{m} (-1)^m F_k \left[\sqrt{\frac{e_b}{2N_s \eta_0}} (N_s + k - 2m) \right].$$

Proof of Lemma A.1:

We prove it by induction on k. For $k = 1$, the result is obvious. Assume the statement true for $k = h$. We want to show that it is true also for $k = h + 1$.

$$\int_a^b \underbrace{\int_a^b \ldots \int_a^b}_{h \text{ times}} g\left(y + \sum_{i=1}^{h} x_i\right) dx_1 \ldots dx_h dy$$

$$= \int_a^b \underbrace{\int_a^b \ldots \int_a^b}_{h \text{ times}} g\left(\sum_{i=1}^h \underbrace{\left(x_i + \frac{y}{h}\right)}_{z_i}\right) dx_1 \ldots dx_h dy$$

$$= \int_a^b \underbrace{\int_{a+\frac{y}{h}}^{b+\frac{y}{h}} \ldots \int_{a+\frac{y}{h}}^{b+\frac{y}{h}}}_{h \text{ times}} g\left(\sum_{i=1}^h z_i\right) dz_1 \ldots dz_h dy$$

$$= \int_a^b \sum_{l=0}^h \binom{h}{l} (-1)^l G_h \left[(h-l)\left(b + \frac{y}{h}\right) + l\left(a + \frac{y}{h}\right)\right] dy$$

$$= \sum_{l=0}^h \binom{h}{l} (-1)^l \int_a^b G_h \left[\underbrace{(h-l)b + la + y}_{z} - \frac{l}{h}y + \frac{l}{h}y\right] dy$$

$$= \sum_{l=0}^h \binom{h}{l} (-1)^l \int_{(h-l)b+(l+1)a}^{(h-l+1)b+la} G_h(z) dz$$

$$= \sum_{l=0}^h \binom{h}{l} (-1)^l \left\{G_{h+1}\left[(h-l+1)b + la\right] - G_{h+1}\left[(h-l)b + (l+1)a\right]\right\}$$

$$= \sum_{l=0}^h \binom{h}{l} (-1)^l G_{h+1}\left[(h-l+1)b + la\right]$$

$$+ \sum_{l=1}^{h+1} \binom{h}{l-1} (-1)^l G_{h+1}\left[(h+1-l)b + la\right]$$

$$= G_{h+1}\left[(h+1)b\right] + \sum_{l=1}^h \left[\binom{h}{l} + \binom{h}{l-1}\right] (-1)^l G_{h+1}\left[(h+1-l)b + la\right]$$

$$+ (-1)^{h+1} G_{h+1}\left[(h+1)a\right]$$

It is easy to show that $\binom{h}{l} + \binom{h}{l-1} = \binom{h+1}{l}$. Therefore, the above expression becomes

$$\sum_{l=0}^{h+1} \binom{h+1}{l} (-1)^l G_{h+1} \left[(h+1-l)b + la\right] \quad \square$$

A.4 Upper bound on the variance of the MAI

Let us recall the expression for the exact single-interferer characteristic function (2.10):

$$\varphi_{m_1}(\omega) = \frac{1}{T_f} \frac{1}{M^{N_s}} \sum_{k=0}^{M-1} \int_{-T}^{T+\delta} M^{z(k)} \left(2e^{j\omega p(s)} + M - 2\right)^{z(k)} \left(e^{j\omega p(s)} + M - 1\right)^{N_s - 2z(k)} ds$$

Define

$$
\begin{aligned}
\Xi_0 &:= \{k \in \{0, 1, \ldots, M-1\} : z(k) = 0\} \\
\Xi_1 &:= \left\{k \in \{0, 1, \ldots, M-1\} : z(k) = \frac{N_s}{2}\right\} \\
\Xi_2 &:= \left\{k \in \{0, 1, \ldots, M-1\} : z(k) \neq 0 \ \& \ z(k) \neq \frac{N_s}{2}\right\}
\end{aligned}
$$

Then, we rewrite the above expression of $\varphi_{m_1}(\omega)$ as follows:

$$
\begin{aligned}
\varphi_{m_1}(\omega) = \ & \frac{1}{T_f} \frac{1}{M^{N_s}} \sum_{k \in \Xi_0} \int_{-T}^{T+\delta} \left(e^{j\omega p(s)} + M - 1\right)^{N_s} ds \\
+ \ & \frac{1}{T_f} \frac{1}{M^{N_s}} \sum_{k \in \Xi_1} \int_{-T}^{T+\delta} M^{\frac{N_s}{2}} \left(2e^{j\omega p(s)} + M - 2\right)^{\frac{N_s}{2}} ds \\
+ \ & \frac{1}{T_f} \frac{1}{M^{N_s}} \sum_{k \in \Xi_2} \int_{-T}^{T+\delta} M^{z(k)} \left(2e^{j\omega p(s)} + M - 2\right)^{z(k)} \\
& \times \left(e^{j\omega p(s)} + M - 1\right)^{N_s - 2z(k)} ds
\end{aligned}
$$

Indicating with $|\mathcal{A}|$ the number of elements in a set $\mathcal{A}$, since m_1 is zero mean

$$Var(m_1) = -\left.\frac{\partial^2 \varphi_{m_1}}{\partial \omega^2}\right|_{\omega=0} = |\Xi_0| \frac{N_s}{M^2 T_c} \left(1 + \frac{N_s - 1}{M}\right) \int_{-T}^{T+\delta} p^2(s) ds$$

$$+ \quad |\Xi_1| \frac{N_s}{M^2 T_c} \left(1 + \frac{N_s - 2}{M}\right) \int_{-T}^{T+\delta} p^2(s) ds$$

$$+ \quad \frac{N_s}{M^2 T_c} \sum_{k \in \Xi_2} \left(1 + \frac{N_s - 1 - \frac{2z(k)}{N_s}}{M}\right) \int_{-T}^{T+\delta} p^2(s) ds$$

$$\leq \quad (|\Xi_0| + |\Xi_1| + |\Xi_2|) \frac{N_s}{M^2 T_c} \left(1 + \frac{N_s - 1}{M}\right) \int_{-T}^{T+\delta} p^2(s) ds$$

$$= \quad \frac{N_s}{M T_c} \left(1 + \frac{N_s - 1}{M}\right) \int_{-T}^{T+\delta} p^2(s)$$

since $|\Xi_0| + |\Xi_1| + |\Xi_2| = M$. Because users are independent of each other, the MAI variance is bounded as follows:

$$Var(m_I) \leq \frac{N_s (N_u - 1)}{M T_c} \left(1 + \frac{N_s - 1}{M}\right) \int_{-T}^{T+\delta} p^2(s) =: \sigma_{max}^2 \qquad (A.7)$$

B Derivations for Chapter 3

B.1 Proof of Proposition 3.1

The Fourier transforms of $\varphi(t)$ and $w(t; T)$, respectively, are

$$\Phi(u) = Ku^2 e^{-\frac{u^2 \tau_P^2}{2}} \quad ; \quad K = A\tau_P^2 \sqrt{2\pi\tau_P^2} \quad \text{and} \quad W(u) = \Phi(u) * \frac{\sin uT/2}{u/2} \quad \text{(B.1)}$$

By Parseval's relationship,

$$\lambda_n(T) := \frac{\int_{-\infty}^{+\infty} [\Phi^n(u) - W^n(u)]^2 \, du}{\int_{-\infty}^{+\infty} \Phi^{2n}(u) du} \quad \text{(B.2)}$$

and by [1]

$$\int_{-\infty}^{+\infty} \Phi^{2n}(u) du = K^{2n} \int_{-\infty}^{+\infty} u^{4n} e^{-nu^2 \tau_P^2} du = K^{2n} \Gamma\left(2n + \frac{1}{2}\right) (n\tau_P^2)^{-(2n+\frac{1}{2})} \quad \text{(B.3)}$$

Noting thet $a^n - b^n = (a - b) [a^{n-1} + a^{n-2}b + a^{n-3}b^2 + \ldots + a\, b^{n-2} + b^{n-1}]$, the numerator in (B.2) can be bounded as follows:

$$\int_{-\infty}^{+\infty} [\Phi^n(u) - W^n(u)]^2 \, du \quad \text{(B.4)}$$

$$\leq \sup_u \left|\Phi^{n-1}(u) + \Phi^{n-2}(u)W(u) + \ldots + W^{n-1}(u)\right| \int_{-\infty}^{+\infty} [\Phi(u) - W(u)]^2 \, du$$

Note that $\Phi(u) \geq 0$ for every u. Also, $\sup_u \Phi^m(u) = (\sup_u \Phi(u))^m = K^m \left(\frac{2}{\tau_P}\right)^m e^{-m}$ and comparison of $W(u)$ and $\Phi(u)$ shows that $\sup_u |W(u)| \leq \sup_u \Phi(u)$. Thus,

$sup_u |W^m(u)| \leq sup_u \; \Phi^m(u)$. Then

$$\left| \Phi^{n-1}(u) + \Phi^{n-2}(u)W(u) + \ldots + W^{n-1}(u) \right| \tag{B.5}$$

$$\leq \quad n \, \underset{u}{sup} \, \Phi^{n-1}(u) = n K^{n-1} \left(\frac{2}{\tau_P^2} \right)^{n-1} e^{-(n-1)}$$

Now

$$\int_{-\infty}^{+\infty} [\Phi(u) - W(u)]^2 \, du = 2\pi \int_{-\infty}^{+\infty} [\varphi(t) - w(t;T)]^2 \, dt = 2\pi \int_{|t|>T/2} \varphi^2(t) dt$$

$$= \quad 2\pi A^2 \int_{|t|>T/2} \left(1 - \frac{t^2}{\tau_P^2} \right)^2 e^{-t^2/\tau_P^2} dt = 4\pi A^2 \tau_P \int_{T/2\tau_P}^{+\infty} (1 - v^2)^2 e^{-v^2} dv \tag{B.6}$$

Now, note that

$$\int_{T/2\tau_P}^{+\infty} (1 - v^2)^2 e^{-v^2} dv = \frac{1}{2} \int_{(T/2\tau_P)^2}^{+\infty} \frac{1}{\sqrt{r}} (1 - 2r^2 + r^4) e^{-r^2} dr \tag{B.7}$$

Since the incomplete Gamma function is defined as $\Gamma(a;x) = \int_x^{+\infty} u^{a-1} e^{-u} du$, we have

$$\int_{T/2\tau_P}^{+\infty} (1 - v^2)^2 e^{-v^2} dv = \frac{1}{2} \Gamma \left(\frac{1}{2}; \left(\frac{T}{2\tau_P} \right)^2 \right) - \Gamma \left(\frac{3}{2}; \left(\frac{T}{2\tau_P} \right)^2 \right)$$

$$+ \frac{1}{2} \Gamma \left(\frac{5}{2}; \left(\frac{T}{2\tau_P} \right)^2 \right) =: \mathcal{P} \left(\frac{T}{\tau_P} \right) \tag{B.8}$$

It follows from (B.4)-(B.6) that

$$\int_{-\infty}^{+\infty} [\Phi^n(u) - W^n(u)]^2 \, du \leq n K^{n-1} \left(\frac{2}{\tau_P^2} \right)^{n-1} e^{-(n-1)} 4\pi A^2 \tau_P \mathcal{P} \left(\frac{T}{\tau_P} \right) \tag{B.9}$$

and this completes the proof. $\square$

B.2 Proof of Theorem 3.1

We want to analytically compute $P_e = E\left[Q\left(\sqrt{\tilde{x}^H \Sigma^{-1} \tilde{x}}\right)\right]$ for $\tilde{x}$ a non-zero-mean complex Gaussian random vector of dimension N, with

$$H := E\left[(\tilde{x} - E[\tilde{x}])(\tilde{x} - E[\tilde{x}])^H\right]$$

and Σ a complex positive-definite covariance matrix of dimension $N \times N$.

First, we write Σ in terms of real and imaginary parts as $\Sigma = \Sigma_R + j\Sigma_I$, and we define $\Sigma^{-1} = \Psi_R + j\Psi_I$, where Ψ_R, Ψ_I are two real positive-definite matrices of dimension $N \times N$. It is readily shown that

$$\tilde{x}^H \Sigma^{-1} \tilde{x} = \begin{bmatrix} \underline{x}_R^T & \underline{x}_I^T \end{bmatrix} \begin{bmatrix} \Psi_R & \Psi_I \\ -\Psi_I & \Psi_R \end{bmatrix} \begin{bmatrix} \underline{x}_R \\ \underline{x}_I \end{bmatrix}, \tag{B.10}$$

where $\underline{x}_R = \Re e\{\tilde{x}\}$ and $\underline{x}_I = \Im\{\tilde{x}\}$ are independent components. Also

$$E[\underline{x}_R] = \underline{\mu}_R \quad , \quad E[\underline{x}_I] = \underline{\mu}_I \tag{B.11}$$

$$E\left[\left(\underline{x}_R - \underline{\mu}_R\right)\left(\underline{x}_R - \underline{\mu}_R\right)^T\right] = E\left[\left(\underline{x}_I - \underline{\mu}_I\right)\left(\underline{x}_I - \underline{\mu}_I\right)^T\right] = H/2 \tag{B.12}$$

$$E\left[\left(\underline{x}_R - \underline{\mu}_R\right)\left(\underline{x}_I - \underline{\mu}_I\right)^T\right] = E\left[\left(\underline{x}_I - \underline{\mu}_I\right)\left(\underline{x}_R - \underline{\mu}_R\right)^T\right] = \mathbf{0} \tag{B.13}$$

Since $\Sigma_I^T = -\Sigma_I$, we have the following:

$$[\Sigma_R + j\Sigma_I][\Psi_R + j\Psi_I] = \mathcal{I}_{N \times N} \quad \Rightarrow \quad \begin{cases} \Sigma_R \Psi_R - \Sigma_I \Psi_I = \mathcal{I}_{N \times N} \\ \Sigma_I \Psi_R + \Sigma_R \Psi_I = \mathcal{O}_{N \times N} \end{cases} \tag{B.14}$$

$$\Rightarrow \quad \begin{cases} \Psi_R = \left[\Sigma_R + \Sigma_I \Sigma_R^{-1} \Sigma_I\right]^{-1} \\ \Psi_I = -\Sigma_R^{-1} \Sigma_I \left[\Sigma_R + \Sigma_I \Sigma_R^{-1} \Sigma_I\right]^{-1} \end{cases}$$

where $\mathcal{I}_{N\times N}$ and $\mathcal{O}_{N\times N}$ are $N \times N$ identity and zero matrices, respectively. Let

$$\breve{\underline{x}} := \left[\underline{x}_R^T \; \underline{x}_I^T\right]^T$$

$$\breve{\underline{\mu}} := E\left[\breve{\underline{x}}\right]$$

$$\breve{H} := E\left[\left(\breve{\underline{x}} - \breve{\underline{\mu}}\right)\left(\breve{\underline{x}} - \breve{\underline{\mu}}\right)^T\right]$$

$$\breve{\Psi} := \begin{bmatrix} \Psi_R & -\Psi_I \\ \Psi_I & \Psi_R \end{bmatrix}$$

Note that from the definitions of $\underline{x}_R$, $\underline{x}_I$, and from (B.11)-(B.13), it is immediate that

$$\breve{\underline{\mu}} = \left[\underline{\mu}^T \underline{\mu}^T\right]^T \tag{B.15}$$

$$\breve{H} = \begin{bmatrix} H/2 & \mathbf{0} \\ \mathbf{0} & H/2 \end{bmatrix} \tag{B.16}$$

The probability of error can be written as $P_e = E\left[\mathcal{Q}\left(\sqrt{\breve{\underline{x}}^T \breve{\Psi} \breve{\underline{x}}}\right)\right]$. We use Nuttal's formula for the $\mathcal{Q}$ function:

$$\mathcal{Q}(x) = \frac{1}{\pi}\int_0^{\pi/2} \exp\left[-\frac{x^2}{2\sin^2 v}\right] dv \tag{B.17}$$

The joint pdf of $\breve{\underline{x}}$ is given by

$$f_{\breve{\underline{x}}}(\underline{u}) = \frac{1}{(2\pi)^N \left|\breve{H}\right|^{1/2}} \exp\left[-\frac{1}{2}(\underline{u} - \breve{\underline{\mu}})^T \breve{H}^{-1}(\underline{u} - \breve{\underline{\mu}})\right] \tag{B.18}$$

where $|A|$ denotes the determinant of a matrix A. The unconditional probability of error is

$$P_e = \frac{1}{(2\pi)^N \left|\breve{H}\right|^{1/2}} \underbrace{\int_{-\infty}^{+\infty} \cdots \int_{-\infty}^{+\infty}}_{2N \text{ times}} \frac{1}{\pi}\int_0^{\pi/2} \exp\left[-\frac{1}{2}\underline{u}^T \frac{\breve{\Psi}}{\sin^2 v}\underline{u}\right] \tag{B.19}$$

$$\times \exp\left[-\frac{1}{2}(\underline{u} - \underline{\breve{\mu}})^T \breve{H}^{-1}(\underline{u} - \underline{\breve{\mu}})\right] dv d\underline{u}$$

We set

$$\left(\underline{u} - \underline{\breve{\mu}}\right)^T \breve{H}^{-1} \left(\underline{u} - \underline{\breve{\mu}}\right) + \underline{u}^T B(v)\underline{u} = (\underline{u} - \underline{m}(v))^T C(v)^{-1} (\underline{u} - \underline{m}(v)) + k(v) \quad \text{(B.20)}$$

where $B(v) = \frac{\breve{\Psi}}{\sin^2 v}$, and we find $C(v)$, $\underline{m}(v)$ and $k(v)$. After some algebra, we obtain

$$
\begin{aligned}
C(v) &= (\breve{H}^{-1} + B(v))^{-1} \\
\underline{m}(v) &= (\breve{H}^{-1} + B(v))^{-1} \breve{H}^{-1} \underline{\breve{\mu}} \\
k(v) &= \underline{\mu}^T \left[I - \breve{H}^{-T}(\breve{H}^{-1} + B(v))^{-T} \right] \breve{H}^{-1} \underline{\breve{\mu}}
\end{aligned}
\quad \text{(B.21)}
$$

Therefore, we can write

$$
\begin{aligned}
P_e &= \frac{1}{(2\pi)^N \left|\breve{H}\right|^{1/2}} \underbrace{\int_{-\infty}^{+\infty} \cdots \int_{-\infty}^{+\infty}}_{2N \text{ times}} \frac{1}{\pi} \int_0^{\pi/2} \exp\left[-\frac{1}{2}k(v)\right] \\
&\quad \times \exp\left\{-\frac{1}{2}\left[\underline{u} - \underline{m}(v)\right]^T C(v)^{-1} \left[\underline{u} - \underline{m}(v)\right]\right\} dv d\underline{u} \quad \text{(B.22)}
\end{aligned}
$$

By swapping the order of integration, we have

$$
\begin{aligned}
P_e &= \frac{1}{\pi} \int_0^{\pi/2} \exp\left[-\frac{1}{2}k(v)\right] \quad \text{(B.23)} \\
&\quad \times \frac{1}{(2\pi)^N \left|\breve{H}\right|^{1/2}} \underbrace{\int_{-\infty}^{+\infty} \cdots \int_{-\infty}^{+\infty}}_{2N \text{ times}} \exp\left\{-\frac{1}{2}\left[\underline{u} - \underline{m}(v)\right]^T C(v)^{-1} \left[\underline{u} - \underline{m}(v)\right]\right\} d\underline{u}\, dv
\end{aligned}
$$

Since the above $2N$-folded integral can be written as the integral of a Gaussian

function, after further algebraic calculations, we obtain

$$
P_e = \frac{1}{\pi} \int_0^{\pi/2} \frac{1}{\sqrt{\left|\breve{H}\right|\left|\breve{H}^{-1} + \frac{\breve{\Psi}}{\sin^2 v}\right|}} \tag{B.24}
$$

$$
\times \exp\left\{-\frac{1}{2}\underline{\breve{\mu}}^T\left[I - \breve{H}^{-T}\left(\breve{H}^{-1} + \frac{\breve{\Psi}}{\sin^2 v}\right)^{-T}\right]\breve{H}^{-1}\underline{\breve{\mu}}\right\}dv \quad \square
$$

B.3 Proof of Theorem 3.2

From (3.19), the SNIR's when a CR and a QuadR are employed are $\text{SNIR}_R = 2\underline{x}_R^T\Sigma_R^{-1}\underline{x}_R$ and $\text{SNIR}_C = \underline{\tilde{x}}^H\Sigma^{-1}\underline{\tilde{x}}$, where $\Sigma_R = \Re e\{\Sigma\}$. From (B.12) and (B.13) in Appendix B.2,

$$
E\left[(\underline{x}_R - \underline{\mu})(\underline{x}_R - \underline{\mu})^T\right] = E\left[(\underline{x}_I - \underline{\mu})(\underline{x}_I - \underline{\mu})^T\right] = H/2 \tag{B.25}
$$

$$
E\left[(\underline{x}_R - \underline{\mu})(\underline{x}_I - \underline{\mu})^T\right] = E\left[(\underline{x}_I - \underline{\mu})(\underline{x}_R - \underline{\mu})^T\right] = \mathbf{0} \tag{B.26}
$$

Also, from (B.10) in Appendix B.2,

$$
\underline{\tilde{x}}^H\Sigma^{-1}\underline{\tilde{x}} = \underline{x}_R^T\Psi_R\underline{x}_R + \underline{x}_I^T\Psi_R\underline{x}_I - \underline{x}_I^T\Psi_I\underline{x}_R + \underline{x}_R^T\Psi_I\underline{x}_I \tag{B.27}
$$

where $\Psi_R = \left[\Sigma_R - \Sigma_I^T\Sigma_R^{-1}\Sigma_I\right]^{-1}$ and $\Psi_I = -\Sigma_R^{-1}\Sigma_I\left[\Sigma_R - \Sigma_I^T\Sigma_R^{-1}\Sigma_I\right]^{-1}$. By using the relation $\underline{v}^T A\underline{v} = tr\left[A\underline{v}^T\underline{v}\right]$, the average SNIR's are

$$
\overline{\text{SNIR}}_R = 2tr\left[\Sigma_R^{-1}E\left(\underline{x}_R\underline{x}_R^T\right)\right] \quad ; \quad \overline{\text{SNIR}}_C = tr\left[\Psi_R E\left(\underline{x}_R\underline{x}_R^T\right)\right] + tr\left[\Psi_R E\left(\underline{x}_I\underline{x}_I^T\right)\right] \tag{B.28}
$$

Without loss of generality, we can assume that $\underline{\mu}_R = \underline{\mu}_I$. Thus, from (B.25), we have $E\left(\underline{x}_R\underline{x}_R^T\right) = E\left(\underline{x}_I\underline{x}_I^T\right) = H/2 + \underline{\mu}\underline{\mu}^T$. Thus,

$$
\overline{\text{SNIR}}_R = tr\left[\Sigma_R^{-1}H\right] + 2\underline{\mu}^T\Sigma_R^{-1}\underline{\mu} \quad ; \quad \overline{\text{SNIR}}_C = tr\left[\Psi_R H\right] + 2\underline{\mu}^T\Psi_R\underline{\mu} \tag{B.29}
$$

The proof that $\overline{\text{SNIR}}_C \geq \overline{\text{SNIR}}_R$ will be carried out in two steps. We first show that $\Psi_R \geq \Sigma_R^{-1}$, in the sense that, for every $\underline{v}$, $\underline{v}^T \Psi_R \underline{v} \geq \underline{v}^T \Sigma_R^{-1} \underline{v}$. We write $\Psi_R = \left(\mathcal{I} - \Sigma_R^{-1} \Sigma_I^T \Sigma_R^{-1} \Sigma_I \right)^{-1} \Sigma_R^{-1}$, where Σ_R^{-1} is positive definite because it is the inverse of a positive definite matrix. Therefore, we need to show that, for every $\underline{v}$, $\underline{v}^T \left[\left(\mathcal{I} - \Sigma_R^{-1} \Sigma_I^T \Sigma_R^{-1} \Sigma_I \right)^{-1} - \mathcal{I} \right] \underline{v} > 0$. By an eigendecomposition, we write $\Sigma_R^{-1} \Sigma_I^T \Sigma_R^{-1} \Sigma_I = V^T \Lambda V$, where Λ is a diagonal matrix with elements λ_i. Also, since $\Sigma_R^{-1} \Sigma_I^T \Sigma_R^{-1} \Sigma_I$ is positive definite, $\lambda_i > 0$. Thus

$$\underline{v}^T \left[\left(\mathcal{I} - \Sigma_R^{-1} \Sigma_I^T \Sigma_R^{-1} \Sigma_I \right)^{-1} - \mathcal{I} \right] \underline{v} = \underline{v}^T \left[\left(\mathcal{I} - V^T \Lambda V \right)^{-1} - \mathcal{I} \right] \underline{v} \quad \text{(B.30)}$$
$$= \underline{v}^T V^T \left[\left(\mathcal{I} - \Lambda \right)^{-1} - \mathcal{I} \right] V \underline{v} = \underline{v}^T V^T \Delta V \underline{v}$$

where $\Delta := \left(\mathcal{I} - \Lambda \right)^{-1} - \mathcal{I}$, and its i-th element is $\Delta_i = \frac{1}{1-\lambda_i} - 1 > 0$. Therefore, by calling $\underline{u} = V \underline{v}$, we have $\underline{v}^T V^T \Delta V \underline{v} = \sum_i \Delta_i u_i^2 > 0$.

We now use the following result from [15]: If A_1, A_2, B_1, B_2 are positive definite matrices, with $0 < A_1 \leq B_1$ and $0 < A_2 \leq B_2$, then we have $0 < tr\left[A_1 A_2 \right] \leq tr\left[B_1 B_2 \right]$. By setting $A_1 = \Sigma_R^{-1}$, $B_1 = \left(\Sigma_R - \Sigma_I^T \Sigma_R^{-1} \Sigma_I \right)^{-1}$, and $A_2 = B_2 = H$, we have $tr\left[\Psi_R H \right] \geq tr\left[\Sigma_R^{-1} H \right]$, and $\overline{\text{SNIR}}_C \geq \overline{\text{SNIR}}_R$. $\square$

C   Derivations for Chapter 4

C.1   From Eq. (4.22) to Eq. (4.23)

Let us start from Eq. (4.22), and break the interval of integration $[0, MT]$ into M intervals of length T:

$$L_{APP}(r; \underline{\alpha}, n) = 2 \sum_{j=-\infty}^{+\infty} \sum_{h=0}^{P-1} c_{j-n}^* \alpha_h^* \sum_{p=0}^{M-1} \int_{pT}^{(p+1)T} \tilde{q}_T^*(t - (j+h)T)r(t)dt \qquad (C.1)$$

$$- \sum_{j=-\infty}^{+\infty} \sum_{i=-\infty}^{+\infty} \sum_{h=0}^{P-1} \sum_{k=0}^{P-1} c_{j-n}^* c_{i-n} \alpha_h^* \alpha_k \sum_{p=0}^{M-1} \int_{pT}^{(p+1)T} \tilde{q}_T^*(t - (j+h)T)x(t - (i+k)T)dt$$

Since $x(t)$ and $\tilde{q}_T(t)$ have support in $[0, T]$, we have

$$\int_{pT}^{(p+1)T} \tilde{q}_T^*(t - (j+h)T)r(t)dt \qquad (C.2)$$

$$= \begin{cases} \int_{pT}^{(p+1)T} \tilde{q}_T^*(t - pT)r(t)dt & ; j+h = p \Rightarrow j = p - h \\ 0 & ; j+h \neq p \end{cases}$$

and

$$\int_{pT}^{(p+1)T} \tilde{q}_T^*(t - (j+h)T)x(t - (i+k)T)dt \qquad (C.3)$$

$$= \begin{cases} \int_{pT}^{(p+1)T} \tilde{q}_T^*(t - pT)x(t - pT)dt & ; j+h = i+k = p \\ 0 & ; \text{elsewhere} \end{cases}$$

Thus

$$
\begin{aligned}
L_{APP}(r;\underline{\alpha},n) &= 2\sum_{h=0}^{P-1}\sum_{p=0}^{M-1} c^*_{p-h-n}\alpha^*_h \int_{pT}^{(p+1)T} \tilde{q}^*_T(t-pT)r(t)dt \\
&\quad - \sum_{h=0}^{P-1}\sum_{k=0}^{P-1}\sum_{p=0}^{M-1} c^*_{p-h-n}c_{p-k-n}\alpha^*_h\alpha_k \int_{pT}^{(p+1)T} \tilde{q}^*_T(t-pT)x(t-pT)dt \\
&= \sum_{h=0}^{P-1}\sum_{p=0}^{M-1} \alpha^*_h\left[c^*_{p-h-n}\right]\left[2\int_0^T \tilde{q}^*_T(t)r(t+pT)dt\right] \\
&\quad - \mathcal{E}\sum_{h=0}^{P-1}\sum_{k=0}^{P-1}\alpha^*_h\alpha_k\left[\sum_{p=0}^{M-1} c^*_{p-h-n}c_{p-k-n}\right] \\
&= 2\underline{\alpha}^H\underline{\underline{C}}(n)\,\underline{y} - \mathcal{E}\underline{\alpha}^H\underline{\underline{C}}(n)\,\underline{\underline{C}}(n)^H\underline{\alpha}
\end{aligned}
$$
(C.4)

C.2 $\quad Pr\left[\underline{y}^H\underline{\underline{A}}\,\underline{y} < 0\right]$

From [57], the moment generating function of $\underline{y}^H\underline{\underline{A}}\,\underline{y}$, for $\underline{\underline{A}}$ Hermitian, and $\underline{y}$ a complex Gaussian random vector with mean $\underline{\mu} := E\left[\underline{y}\right]$ and covariance $\underline{\underline{\Sigma}} := E\left[(\underline{y}-\underline{\mu})(\underline{y}-\underline{\mu})^H\right]$, is

$$
\phi(s) := E\left[\exp\left(sx\right)\right] = \frac{1}{\left|\underline{\underline{\mathcal{I}}} - s\underline{\underline{\Sigma}}\,\underline{\underline{A}}\right|}\exp\left\{-\underline{\mu}^H\underline{\underline{\Sigma}}^{-1}\left[\underline{\underline{\mathcal{I}}} - \left(\underline{\underline{\mathcal{I}}} - s\underline{\underline{\Sigma}}\,\underline{\underline{A}}\right)^{-1}\right]\underline{\mu}\right\}
$$
(C.5)

Alternatively,

$$
\phi(s) = \frac{\exp\left[\sum_{n=1}^N \frac{s\lambda_n|b_n|^2}{1-s\lambda_n}\right]}{\prod_{n=1}^N (1-s\lambda_n)^{v_n}}
$$
(C.6)

where v_n is the multiplicity of λ_n, the n-th eigenvalue of $\underline{\underline{\Sigma}}^{1/2}\underline{\underline{A}}\,\underline{\underline{\Sigma}}^{1/2}$, N is the total number of distinct eigenvalues, and $|b_n|^2 := \sum_{k\in\mathcal{K}_n}|d_k|^2$, where $\mathcal{K}_n$ denotes the set of indices associated with the n-th distinct eigenvalue. For instance, if λ_1 and λ_2 have multiplicities 3 and 2, respectively, then $\mathcal{K}_1 = \{1,2,3\}$ and $\mathcal{K}_2 = \{4,5\}$. The terms d_n are the elements of the vector $\underline{d}$, defined by the relation $\underline{d} := \underline{\underline{U}}_2^H\underline{\underline{M}}\underline{\underline{U}}_1^H\underline{\mu}$, where $\underline{\underline{U}}_1$ is

the normalized modal matrix[1] of $\underline{\underline{\Sigma}}^{-1}$, $\underline{\underline{M}}^2 := \underline{\underline{U}}_1^H \underline{\underline{\Sigma}}^{-1} \underline{\underline{U}}_1$, while $\underline{\underline{U}}_2$ is the normalized modal matrix of $\underline{\underline{M}}^{-1} \underline{\underline{U}}_1^H \underline{\underline{A}} \, \underline{\underline{U}}_1 \underline{\underline{M}}^{-1}$. Note that the moment generating function is analytic in the whole s plane except at a few isolated poles $s = \{1/\lambda_k\}_{k=1}^N$.

Lemma C.1 *The moment generating function in (C.6) converges to zero as $|s| \to \infty$.* *Specifically*

$$\lim_{|s| \to \infty} |\phi(s)| = 0 \tag{C.7}$$

Proof: Let $s = Re^{i\theta}$; then

$$
\begin{aligned}
|\phi(s)| &= \prod_{k=1}^N \frac{\left| \exp\left[\frac{s b_k^2 \lambda_k}{1 - s\lambda_k} \right] \right|}{|1 - s\lambda_k|^{v_k}} \\
&= \prod_{k=1}^N \frac{\left| \exp\left[\frac{Re^{i\theta} b_k^2 \lambda_k}{1 - Re^{i\theta}\lambda_k} \right] \right|}{|1 - Re^{i\theta}\lambda_k|^{v_k}} \\
&= \prod_{k=1}^N \frac{\left| \exp\left[\frac{Re^{i\theta} b_k^2 \lambda_k \left(1 - Re^{-i\theta}\lambda_k^*\right)}{\left(1 - Re^{i\theta}\lambda_k\right)\left(1 - Re^{-i\theta}\lambda_k^*\right)} \right] \right|}{\left(1 + R^2 |\lambda_k|^2 - 2R \, \Re e \left\{ e^{i\theta}\lambda_k \right\}\right)^{v_k/2}} \\
&= \prod_{k=1}^N \frac{\exp\left[\frac{R b_k^2 \, \Re e\left\{ e^{i\theta}\lambda_k \right\} - R^2 b_k^2 |\lambda_k|^2}{1 + R^2 |\lambda_k|^2 - 2R \, \Re e\left\{ e^{i\theta}\lambda_k \right\}} \right]}{\left(1 + R^2 |\lambda_k|^2 - 2R \, \Re e \left\{ e^{i\theta}\lambda_k \right\}\right)^{v_k/2}}
\end{aligned}
\tag{C.8}
$$

Clearly, for $v_k \neq 0$,

$$\prod_{k=1}^N \frac{\exp\left[\frac{R b_k^2 \, \Re e\left\{ e^{i\theta}\lambda_k \right\} - 2R^2 b_k^2 \, |\lambda_k|^2}{1 + R^2 |\lambda_k|^2 - 2R \, \Re e\left\{ e^{i\theta}\lambda_k \right\}} \right]}{\left(1 + R^2 |\lambda_k|^2 - 2R \, \Re e \left\{ e^{i\theta}\lambda_k \right\}\right)^{v_k/2}} \xrightarrow[R \to +\infty]{} 0 \quad \forall \theta \quad \square \tag{C.9}$$

C.2.1 Closed form expression for $Pr\left[\underline{y}^H \underline{\underline{A}} \, \underline{y} < 0 \right]$

We derive a closed form expression for $Pr\left[\underline{y}^H \underline{\underline{A}} \, \underline{y} < 0 \right]$ by using the residue inversion formula for the moment generating function.

---

[1]The normalized modal matrix $\underline{\underline{V}}$ of a matrix $\underline{\underline{\Lambda}}$ is defined by the diagonalization $\underline{\underline{\Lambda}} = \underline{\underline{V}}^H \underline{\underline{\Delta}} \, \underline{\underline{V}}$, where $\underline{\underline{V}}^H \underline{\underline{V}} = \underline{\underline{V}} \, \underline{\underline{V}}^H = \underline{\underline{I}}$

Assume the eigenvalues are ordered such that

$$\Re e\left\{\frac{1}{\lambda_1}\right\} \le \Re e\left\{\frac{1}{\lambda_2}\right\} \le \ldots \le \Re e\left\{\frac{1}{\lambda_{N_1}}\right\} < 0 < \Re e\left\{\frac{1}{\lambda_{N_1+1}}\right\} \le \ldots \le \Re e\left\{\frac{1}{\lambda_N}\right\}$$

(C.10)

and such that there are N_1 (in general, complex) poles in the left half-plane. By using Jordan's lemma and the residue theorem, the pdf of the random variable $\underline{y}^H \underline{\underline{A}}\, \underline{y}$ can be written as

$$f(u) = \sum_{k=1}^{N_1} f_k(u) \quad , u \le 0$$

(C.11)

where $f_k(u)$ is the residue of $\phi(s)e^{-su}$ at pole $1/\lambda_k$, for $k = 1, \ldots, N_1$. Clearly,

$$P_r\left[\underline{y}^H \underline{\underline{A}}\, \underline{y} < 0\right] = \int_{-\infty}^{0} f(u)du = \sum_{k=1}^{N_1} \int_{-\infty}^{0} f_k(u)du$$

(C.12)

We will now derive a closed-form expression for $f(u)$. For the general case where the b_k's are non-zero for $k = 1, \ldots, N_1$, the N_1 poles in the left half-plane are essential poles. Since $f_k(u)$ is the residue of $\phi(s)e^{-su}$ at the pole $1/\lambda_k$, we have

$$f_k(u) = \operatorname*{Res}_{s=1/\lambda_k} \phi(s)e^{-su} = \frac{1}{2\pi i}\int_{\Gamma_k} \phi(s)e^{-su}ds$$

(C.13)

where Γ_k is a closed contour enclosing only the pole $s = 1/\lambda_k$. First, we decompose $\phi(s)e^{-su} = A_k(s)B_k(s, u)$ for $k = 1, \ldots, N_1$, where

$$A_k(s) := \prod_{m=1, m\neq k}^{N} \left[(1 - s\lambda_m)^{-v_m} \exp\left(\frac{s\, b_m^2\, \lambda_m}{1 - s\lambda_m}\right)\right]$$

(C.14)

and

$$\begin{aligned} B_k(s, u) &:= (1 - s\lambda_k)^{-v_k} \exp\left(-su + \frac{s\, b_k^2\, \lambda_k}{1 - s\lambda_k}\right) \\ &= \exp(-su - b_k^2)(1 - s\lambda_k)^{-v_k} \exp\left(\frac{b_k^2}{1 - s\lambda_k}\right). \end{aligned}$$

(C.15)

With the above definitions, the expression in (C.12) becomes

$$P_r\left[\underline{y}^H\underline{\underline{A}}\,\underline{y}<0\right]=\sum_{k=1}^{N_1}\int_{-\infty}^{0}\frac{1}{2\pi i}\int_{\Gamma_k}A_k(s)B_k(s,u)dsdu \qquad (C.16)$$

By expanding $B_k(s,u)$ in a power series, we have

$$B_k(s,u)=\exp(-su-b_k^2)\sum_{n=0}^{\infty}\frac{b_k^{2n}}{n!}(1-s\lambda_k)^{-n-v_k}=:\sum_{n=0}^{\infty}B_{k,n}(s,u) \qquad (C.17)$$

Therefore

$$P_r\left[\underline{y}^H\underline{\underline{A}}\,\underline{y}<0\right]=\sum_{k=1}^{N_1}\int_{-\infty}^{0}\frac{1}{2\pi i}\int_{\Gamma_k}\sum_{n=0}^{\infty}A_k(s)B_{k,n}(s,u)dsdu \qquad (C.18)$$

Note that we would like to swap the infinite sum with the double integral, so that the integration in s would become the residue of $A_k(s)B_{k,n}(s,u)$ at $1/\lambda_k$. First, let

$$\Gamma_k:=\left\{s:s=1/\lambda_k+r_ke^{i\theta_k},\theta\in[0,2\pi)\right\} \qquad (C.19)$$

be the circle of radius r_k centered in $s=1/\lambda_k$, where $r_k>0$ has to be chosen such that no pole other than $1/\lambda_k$ is contained in Γ_k (i.e., $1/\lambda_h\neq\Gamma_k$, for $h\neq k$), and Γ_k is fully contained in the left half s-plane. Therefore, we need

$$r_k<min\left\{\left|\Re e\left\{\frac{1}{\lambda_k}\right\}\right|,\underset{h\neq k}{min}\left\|\frac{1}{\lambda_k}-\frac{1}{\lambda_h}\right\|\right\} \qquad (C.20)$$

Clearly, $r_k<\left|\Re\left\{\frac{1}{\lambda_k}\right\}\right|=-\Re e\left\{\frac{1}{\lambda_k}\right\}$, since $1/\lambda_k$ is in the left-half plane. Let us write the integral over Γ_k in polar coordinates as

$$\frac{1}{2\pi i}\int_{\Gamma_k}\sum_{n=0}^{\infty}A_k(s)B_{k,n}(s,u)ds$$

$$=\frac{1}{2\pi}\int_{0}^{2\pi}r_ke^{i\theta}\sum_{n=0}^{\infty}A_k(1/\lambda_k+r_ke^{i\theta})B_{k,n}(1/\lambda_k+r_ke^{i\theta},u)d\theta \qquad (C.21)$$

In order to swap the infinite sum with the double integral in (C.18), we use dominated convergence, where we need to show that

$$\left| A_k(1/\lambda_k + r_k e^{i\theta}) \right| \left| B_{k,n}(1/\lambda_k + r_k e^{i\theta}, u) \right| \leq g_{k,n}(\theta, u) \tag{C.22}$$

such that

$$\sum_{n=0}^{\infty} \int_{-\infty}^{0} \frac{1}{2\pi} \int_{0}^{2\pi} g_{k,n}(\theta, u) d\theta du < +\infty \tag{C.23}$$

First, we notice that $A_k(s)$ is analytic over Γ_k, thus $\left| A_k(1/\lambda_k + r_k e^{i\theta}) \right|$ is a continuous function for $\theta \in [0, 2\pi)$. Therefore, we need to bound $\left| B_{k,n}(1/\lambda_k + r_k e^{i\theta}, u) \right|$ only.

Recalling the expression for $B_{k,n}(s, u)$, we have

$$
\begin{aligned}
B_{k,n}(1/\lambda_k + r_k e^{i\theta}, u) &= \exp(-b_k^2) \exp\left[-u \left(\frac{1}{\lambda_k} + r_k e^{i\theta} \right) \right] \frac{b_k^{2n}}{n!} \left(-r_k \lambda_k e^{i\theta} \right)^{-n-v_k} \\
&= \exp(-b_k^2) \exp\left[-u \frac{\Re e\{\lambda_k\} - i \Im m\{\lambda_k\}}{||\lambda_k||^2} \right] \\
&\times \exp\left[-u r_k (\cos\theta + i\sin\theta) \right] \frac{b_k^{2n}}{n!} \left(-r_k \lambda_k e^{i\theta} \right)^{-n-v_k}
\end{aligned} \tag{C.24}
$$

Therefore,

$$
\begin{aligned}
\left| B_{k,n}(1/\lambda_k + r_k e^{i\theta}, u) \right| &= \exp(-b_k^2) \exp\left[-u \frac{\Re e\{\lambda_k\}}{||\lambda_k||^2} \right] \\
&\times \exp\left[-u r_k \cos\theta \right] \frac{b_k^{2n}}{n!} r_k^{-n-v_k} |\lambda_k|^{-n-v_k}
\end{aligned} \tag{C.25}
$$

Note that, by definition, $r_k < -\Re e\left\{ \frac{1}{\lambda_k} \right\} = -\frac{\Re e\{\lambda_k\}}{||\lambda_k||^2}$. Thus,

$$\exp\left[-u \left(\frac{\Re e\{\lambda_k\}}{||\lambda_k||^2} + r_k \cos\theta \right) \right] \leq \exp\left[-u \left(\frac{\Re e\{\lambda_k\}}{||\lambda_k||^2} + r_k \right) \right] \tag{C.26}$$

with $\frac{\Re e\{\lambda_k\}}{||\lambda_k||^2} + r_k < 0$. Therefore,

$$g_{k,n}(\theta, u) = \left| A_k(1/\lambda_k + r_k e^{i\theta}) \right| \exp(-b_k^2) \frac{b_k^{2n}}{n!} r_k^{-n-v_k} \left| \lambda_k \right|^{-n-v_k} \exp\left[-u \left(\frac{\Re e\{\lambda_k\}}{||\lambda_k||^2} + r_k \right) \right]$$
(C.27)

and

$$\int_{-\infty}^0 \frac{1}{2\pi} \int_0^{2\pi} g_{k,n}(\theta, u) d\theta du = \exp(-b_k^2) \frac{b_k^{2n}}{n!} r_k^{-n-v_k} \left| \lambda_k \right|^{-n-v_k} \alpha_k \beta_k$$
(C.28)

where

$$\alpha_k := \int_{-\infty}^0 \exp\left[-u \left(\frac{\Re e\{\lambda_k\}}{||\lambda_k||^2} + r_k \right) \right] du < +\infty$$
(C.29)

$$\beta_k := \frac{1}{2\pi} \int_0^{2\pi} \left| A_k(1/\lambda_k + r_k e^{i\theta}) \right| d\theta < +\infty$$
(C.30)

Thus

$$\sum_{n=0}^{\infty} \int_{-\infty}^0 \frac{1}{2\pi} \int_0^{2\pi} g_{k,n}(\theta, u) d\theta du = \alpha_k \beta_k \exp(-b_k^2) \sum_{n=0}^{\infty} \frac{b_k^{2n}}{n!} r_k^{-n-v_k} \left| \lambda_k \right|^{-n-v_k} \quad \text{(C.31)}$$

$$= \frac{\alpha_k \beta_k}{r_k^{v_k} \left| \lambda_k \right|^{v_k}} \exp\left[-b_k^2 \left(1 - \frac{1}{r_k \left| \lambda_k \right|} \right) \right] < +\infty$$

Let us now go back to Eq. (C.18). Since the swap between the infinite sum and the double integral is justified, we have

$$P_r \left[\underline{y}^H \underline{\underline{A}} \, \underline{y} < 0 \right] = \sum_{k=1}^{N_1} \sum_{n=0}^{\infty} \int_{-\infty}^0 \frac{1}{2\pi i} \int_{\Gamma_k} A_k(s) B_{k,n}(s, u) ds du$$
(C.32)

Note that

$$\frac{1}{2\pi i} \int_{\Gamma_k} A_k(s) B_{k,n}(s, u) ds = \operatorname*{Res}_{s=1/\lambda_k} A_k(s) B_{k,n}(s, u)$$
(C.33)

Recalling the expression for $B_{k,n}(s,u)$, namely

$$B_{k,n}(s,u) = \exp(-su - b_k^2)\frac{b_k^{2n}}{n!}(1 - s\lambda_k)^{-n-v_k} \tag{C.34}$$

we have

$$
\begin{aligned}
\underset{s=1/\lambda_k}{Res}\, A_k(s)B_{k,n}(s,u) &= \lim_{s\to 1/\lambda_k} \frac{1}{(v_k + n - 1)!} \\
&\quad \times \frac{\partial^{v_k+n-1}}{\partial s^{v_k+n-1}}\left[A_k(s)B_{k,n}(s,u)\,(1 - 1/\lambda_k)^{v_k+n}\right] \\
&= \frac{(-\lambda_k)^{-v_k-n}\exp(-b_k^2)b_k^{2n}}{(v_k + n - 1)!\,n!} \\
&\quad \times \lim_{s\to 1/\lambda_k} \frac{\partial^{v_k+n-1}}{\partial s^{v_k+n-1}}\left[A_k(s)\exp(-su)\right] \\
&= \frac{(-\lambda_k)^{-v_k-n}\exp(-b_k^2)b_k^{2n}}{(v_k + n - 1)!\,n!} \\
&\quad \times \sum_{r=0}^{v_k+n-1}\binom{v_k + n - 1}{r}(-u)^{v_k+n-1-r} \\
&\quad \times \lim_{s\to 1/\lambda_k} A_k^{(r)}(s)\exp(-su)
\end{aligned}
\tag{C.35}
$$

where $A_k^{(r)}(s)$ is the r-th complex derivative[2] of $A_k(s)$ with respect to s.

---

[2] Given a complex-valued function

$$z(s) = z(x + iy) = u(x + iy) + iv(x + iy) \tag{C.36}$$

with $u(s)$, $v(s)$ real-valued functions, the Cauchy-Riemann differential equations [30]

$$\frac{\partial u}{\partial x} = \frac{\partial v}{\partial y} \tag{C.37}$$

$$\frac{\partial u}{\partial y} = -\frac{\partial v}{\partial x} \tag{C.38}$$

are necessary and sufficient conditions for the existence of the derivative of z in s, defined as

$$\frac{dz}{ds} := \lim_{|\Delta s|\to 0} \frac{z(s + \Delta s) - z(s)}{\Delta s} \tag{C.39}$$

Lemma C.2 *The derivatives of $A_k(s)$, $A_k^{(r)}(s)$, for $r \geq 1$, are defined iteratively as*

$$A_k^{(r)}(s) = \sum_{n=0}^{r-1} \binom{r-1}{n} A_k^{(n)}(s) g_k^{(r-1-n)}(s) \tag{C.42}$$

with

$$g_k^{(r)}(s) = \sum_{m=1,m\neq k}^{N} \left[r!\, v_m \left(\frac{\lambda_m}{1-s\lambda_m} \right)^{r+1} + (r+1)!\, b_m^2 \left(\frac{\lambda_m}{1-s\lambda_m} \right)^{r+1} \frac{1}{1-s\lambda_m} \right] \tag{C.43}$$

Proof: We have

$$A_k^{(1)}(s) = A_k(s) g_k(s) \tag{C.44}$$

where $g_k(s) = \frac{d}{ds} \ln A_k(s)$, defined in the whole s plane except at $s = \{1/\lambda_h\}_{h=1}^{N}$, $h \neq k$, and its r-th derivative is shown in [34] to have the form as in (C.43). From (C.44), the result is immediate by the Leibnitz differentiation rule [30]   □.

Since $A_k(s)$ is analytic in s inside the contour Γ_k, it is therein continuous and differentiable. Therefore, the limit in (C.35) for $s \to 1/\lambda_k$ exists and is finite, and

$$\operatorname*{Res}_{s=1/\lambda_k} A_k(s) B_{k,n}(s,u) = \frac{(-\lambda_k)^{-v_k-n} \exp(-b_k^2) b_k^{2n}}{(v_k+n-1)!n!} \tag{C.45}$$

$$\times \sum_{r=0}^{v_k+n-1} \binom{v_k+n-1}{r} (-u)^{v_k+n-1-r} A_k^{(r)}(1/\lambda_k) \exp(-u/\lambda_k)$$

where $\Delta s = \Delta x + i\Delta y$. In particular, the derivative can be defined in either of the following ways:

$$\frac{dz}{ds} = \frac{\partial u}{\partial x} + i \frac{\partial v}{\partial x} \tag{C.40}$$

$$\frac{dz}{ds} = \frac{\partial v}{\partial y} - i \frac{\partial u}{\partial y} \tag{C.41}$$

Since

$$\int_{-\infty}^{0} (-u)^{v_k+n-1-r} \exp\left(-u/\lambda_k\right) du = (-\lambda_k)^{v_k+n-r} \Gamma(v_k + n - r) \qquad \text{(C.46)}$$

we obtain

$$
\begin{aligned}
P_r \left[\underline{y}^H \underline{\underline{A}} \, \underline{y} < 0 \right] &= \sum_{k=1}^{N_1} \sum_{n=0}^{\infty} \frac{\exp(-b_k^2)b_k^{2n}}{(v_k + n - 1)!n!} \\
&\quad \times \sum_{r=0}^{v_k+n-1} \binom{v_k + n - 1}{r} A_k^{(r)}(1/\lambda_k) \frac{\Gamma(v_k + n - r)}{(-\lambda_k)^r} \\
&= \sum_{k=1}^{N_1} \exp(-b_k^2) \sum_{n=0}^{\infty} \frac{b_k^{2n}}{n!} \sum_{r=0}^{v_k+n-1} \frac{1}{r!} \frac{A_k^{(r)}(1/\lambda_k)}{(-\lambda_k)^r} \qquad \text{(C.47)}
\end{aligned}
$$

C.2.2 Complex conjugate pairs of eigenvalues

Let $\underline{\underline{A}}$ be a Hermitian symmetric matrix. We now want to show that for complex conjugate pairs, the pdf of $\underline{y}^H \underline{\underline{A}} \, \underline{y}$ is, in fact, real. Note that this condition on the eigenvalues is necessary and sufficient for the matrix $\underline{\underline{A}}$ to be Hermitian. Let N and N_1 be even quantities, while, for k odd

$$\lambda_k = \lambda_{k+1}^* \qquad \text{(C.48)}$$

$$v_k = v_{k+1} \qquad \text{(C.49)}$$

$$b_k = b_{k+1} \qquad \text{(C.50)}$$

By recalling Eq. (C.53), the pdf of $\underline{y}^H \underline{\underline{A}} \, \underline{y}$, $f(u)$, is

$$f(u) = \sum_{n=0}^{\infty} \sum_{k=1}^{N_1} \underset{s=1/\lambda_k}{Res} \, A_k(s) B_{k,n}(s, u) \qquad \text{(C.51)}$$

By the symmetry of the eigenvalues, we write

$$f(u) = \sum_{n=0}^{\infty} \sum_{k=1,k\ odd}^{N_1} \left[\operatorname*{Res}_{s=1/\lambda_k} A_k(s)B_{k,n}(s,u) + \operatorname*{Res}_{s=1/\lambda_k^*} A_{k+1}(s)B_{k+1,n}(s,u) \right] \qquad (C.52)$$

Thus

$$f(u) = \sum_{n=0}^{\infty} \sum_{k=1,k\ odd}^{N_1} \frac{\exp(-b_k^2)b_k^{2n}}{(v_k+n-1)!n!} \sum_{r=0}^{v_k+n-1} \binom{v_k+n-1}{r} (-u)^{v_k+n-1-r} \qquad (C.53)$$
$$\times \left[(-\lambda_k)^{-v_k-n} A_k^{(r)}(1/\lambda_k) \exp(-u/\lambda_k) + (-\lambda_k^*)^{-v_k-n} A_k^{(r)}(1/\lambda_k^*) \exp(-u/\lambda_k^*) \right]$$

For k odd, we write $A_k(s)$ isolating the $(k+1)$-th term as follows:

$$A_k(s) = (1 - s\lambda_k^*)^{-v_k} \exp\left(\frac{b_k^2 s\lambda_k^*}{1 - s\lambda_k^*} \right) C_k(s) \qquad (C.54)$$

with

$$C_k(s) = \prod_{m=1,m\neq k,m\ odd}^{N} \left\{ \left[(1 - s\lambda_m)^{-v_m} \exp\left(\frac{b_m^2 s\lambda_m}{1 - s\lambda_m} \right) \right] \qquad (C.55)$$
$$\times \left[(1 - s\lambda_m^*)^{-v_m} \exp\left(\frac{b_m^2 s\lambda_m^*}{1 - s\lambda_m^*} \right) \right] \right\}$$

Clearly, $C_k(s^*) = C_k(s)^*$. Now, also for k odd, we write $A_{k+1}(s)$ isolating the k-th term as

$$A_{k+1}(s) = (1 - s\lambda_k)^{-v_k} \exp\left(\frac{b_k^2 s\lambda_k}{1 - s\lambda_k} \right) C_k(s) \qquad (C.56)$$

It is readily shown that

$$A_{k+1}(s^*) = (1 - s^*\lambda_k)^{-v_k} \exp\left(\frac{b_k^2 s^*\lambda_k}{1 - s^*\lambda_k} \right) C_k(s^*)$$
$$= \left[(1 - s\lambda_k^*)^{-v_k} \exp\left(\frac{b_k^2 s\lambda_k^*}{1 - s\lambda_k^*} \right) \right]^* C_k(s)^* = A_k(s)^* \qquad (C.57)$$

We will now show that the above symmetry property is valid for every complex derivative of $A_{k+1}(s)$.

Lemma C.3 *For every integer $r \geq 0$, and for every $k = 1, 3, \ldots, N_1$, k odd, the following symmetry property holds:*

$$A_{k+1}^{(r)}(s^*) = A_k^{(r)}(s)^* \tag{C.58}$$

Proof: From Lemma C.2, we know that

$$A_k^{(r)}(s) = \sum_{n=0}^{r-1} \binom{r-1}{n} A_k^{(n)}(s) g_k^{(r-1-n)}(s) \tag{C.59}$$

and

$$g_k^{(r)}(s) = \sum_{m=1, m \neq k}^{N} \left[r! \, v_m \left(\frac{\lambda_m}{1 - s\lambda_m} \right)^{r+1} + (r+1)! \, b_m^2 \left(\frac{\lambda_m}{1 - s\lambda_m} \right)^{r+1} \frac{1}{1 - s\lambda_m} \right] \tag{C.60}$$

If we can show that $g_{k+1}^{(r)}(s^*) = g_k^{(r)}(s)^*$ for k odd, and for all $r \geq 0$, we prove the lemma. For k odd, write $g_k^{(r)}(s)$ and $g_{k+1}^{(r)}(s)$ isolating the $(k+1)$-th and k-th eigenvalue, respectively, as

$$g_k^{(r)}(s) = \left[r! \, v_k \left(\frac{\lambda_k^*}{1 - s\lambda_k^*} \right)^{r+1} + (r+1)! \, b_k^2 \left(\frac{\lambda_k^*}{1 - s\lambda_k^*} \right)^{r+1} \frac{1}{1 - s\lambda_k^*} \right] \tag{C.61}$$
$$+ D_{k,r}(s)$$

$$g_{k+1}^{(r)}(s) = \left[r! \, v_k \left(\frac{\lambda_k}{1 - s\lambda_k} \right)^{r+1} + (r+1)! \, b_k^2 \left(\frac{\lambda_k}{1 - s\lambda_k} \right)^{r+1} \frac{1}{1 - s\lambda_k} \right] \tag{C.62}$$
$$+ D_{k,r}(s)$$

with

$$D_{k,r}(s) = \sum_{m=1, m \neq k, m \neq k+1}^{N} \left[r! \, v_m \left(\frac{\lambda_m}{1 - s\lambda_m} \right)^{r+1} \right.$$

$$
+ (r+1)!\, b_m^2 \left(\frac{\lambda_m}{1 - s\lambda_m} \right)^{r+1} \frac{1}{1 - s\lambda_m} \Bigg]
$$

$$
= \sum_{m=1, m \neq k, m \text{ odd}}^{N} \Bigg\{ r!\, v_m \left[\left(\frac{\lambda_m}{1 - s\lambda_m} \right)^{r+1} + \left(\frac{\lambda_m^*}{1 - s\lambda_m^*} \right)^{r+1} \right] \tag{C.63}
$$

$$
+ \quad (r+1)!\, b_m^2 \left[\left(\frac{\lambda_m}{1 - s\lambda_m} \right)^{r+1} \frac{1}{1 - s\lambda_m} + \left(\frac{\lambda_m^*}{1 - s\lambda_m^*} \right)^{r+1} \frac{1}{1 - s\lambda_m^*} \right] \Bigg\}
$$

Since $D_{k,r}(s^*) = D_{k,r}(s)^*$,

$$
g_{k+1}^{(r)}(s^*) = \left[r!\, v_k \left(\frac{\lambda_k}{1 - s^*\lambda_k} \right)^{r+1} + (r+1)!\, b_k^2 \left(\frac{\lambda_k}{1 - s^*\lambda_k} \right)^{r+1} \frac{1}{1 - s^*\lambda_k} \right] \tag{C.64}
$$

$$
+ D_{k,r}(s^*)
$$

$$
= \left[r!\, v_k \left(\frac{\lambda_k^*}{1 - s\lambda_k^*} \right)^{r+1} + (r+1)!\, b_k^2 \left(\frac{\lambda_k^*}{1 - s\lambda_k^*} \right)^{r+1} \frac{1}{1 - s\lambda_k^*} \right]^*
$$

$$
+ D_{k,r}(s)^* = g_k^{(r)}(s)^* \quad \square
$$

By using Lemma C.3, Eq. (C.53) can be written as

$$
f(u) = \sum_{n=0}^{\infty} \sum_{k=1, k \text{ odd}}^{N_1} \frac{\exp(-b_k^2)\, b_k^{2n}}{(v_k + n - 1)!\, n!} \sum_{r=0}^{v_k+n-1} \binom{v_k + n - 1}{r} (-u)^{v_k+n-1-r}
$$

$$
\times \quad \Big\{ (-\lambda_k)^{-v_k-n} A_k^{(r)}(1/\lambda_k) \exp(-u/\lambda_k)
$$

$$
+ \left[(-\lambda_k)^{-v_k-n} A_k^{(r)}(1/\lambda_k) \exp(-u/\lambda_k) \right]^* \Big\}
$$

$$
= \sum_{n=0}^{\infty} \sum_{k=1, k \text{ odd}}^{N_1} \frac{\exp(-b_k^2)\, b_k^{2n}}{(v_k + n - 1)!\, n!} \sum_{r=0}^{v_k+n-1} \binom{v_k + n - 1}{r} (-u)^{v_k+n-1-r}
$$

$$
\times \quad \Re e \left\{ (-\lambda_k)^{-v_k-n} A_k^{(r)}(1/\lambda_k) \exp(-u/\lambda_k) \right\} \tag{C.65}
$$

C.3   Proof of Eq. (4.60)

Recall the definition of $\underline{\mathcal{C}}(n)$, where the (h, p)-th element is defined as

$$\left[\underline{\mathcal{C}}(n)\right]_{h,p} = c^*_{-n-h+p} \quad ; h = 0, 1, \ldots, P - 1, \ p = 0, 1, \ldots, M - 1 \tag{C.66}$$

and c_j is periodic with period N_{seq}, such that $c_{j+N_{seq}} = c_j, \ \forall j$. Then,

$$\left[\underline{\mathcal{C}}(n)^H \underline{\mathcal{C}}(n)\right]_{p_1,p_2} = \sum_{h=0}^{P-1} c^*_{-n-h+p_1} c_{-n-h+p_2} \quad ; p_1, p_2 = 0, 1, \ldots, M - 1 \tag{C.67}$$

which can be written as

$$\left[\underline{\mathcal{C}}(n)^H \underline{\mathcal{C}}(n)\right]_{p_1,p_2} = \sum_{k=n}^{P-1+n} c^*_{-k+p_1} c_{-k+p_2}. \tag{C.68}$$

For $0 \le n < N_{seq} - P + 1$, we have $P - 1 + n < N_{seq}$, and

$$\sum_{k=n}^{P-1+n} c^*_{-k+p_1} c_{-k+p_2} = \sum_{k=0}^{N_{seq}-1} c^*_{-k+p_1} c_{-k+p_2} \delta_k(n) \tag{C.69}$$

where

$$\delta_k(n) = \begin{cases} 1 & n \le k \le P - 1 + n \\ 0 & \text{elsewhere} \end{cases} \tag{C.70}$$

For $N_{seq} - P + 1 \le n \le N_{seq} - 1$

$$\begin{aligned}
\sum_{k=n}^{P-1+n} c^*_{-k+p_1} c_{-k+p_2} &= \sum_{k=n}^{N_{seq}-1} c^*_{-k+p_1} c_{-k+p_2} + \sum_{k=N_{seq}}^{P-1+n} c^*_{-k+p_1} c_{-k+p_2} \\
&= \sum_{k=n}^{N_{seq}-1} c^*_{-k+p_1} c_{-k+p_2} + \sum_{h=0}^{P-1+n-N_{seq}} c^*_{N_{seq}-h+p_1} c_{N_{seq}-h+p_2} \\
&= \sum_{k=n}^{N_{seq}-1} c^*_{-k+p_1} c_{-k+p_2} + \sum_{h=0}^{P-1+n-N_{seq}} c^*_{-h+p_1} c_{-h+p_2}
\end{aligned}$$

$$= \sum_{k=0}^{N_{seq}-1} c^*_{-k+p_1} c_{-k+p_2} \delta_k(n) \tag{C.71}$$

where

$$\delta_k(n) = \begin{cases} 1 & 0 \leq k \leq P - 1 + n - N_{seq} \textbf{ or } n \leq k \leq N_{seq} - 1 \\ 0 & \text{elsewhere} \end{cases} \tag{C.72}$$

Define the $N_{seq} \times M$ matrix $\underline{\tilde{\mathcal{C}}}$, whose (a, b)-th element is $[\underline{\tilde{\mathcal{C}}}]_{a,b} = c_{-a-b}$. Also, define $\underline{\underline{\Delta}}(n) := \text{diag}\,[\delta_0(n)\; \delta_1(n)\; \ldots\; \delta_{M-1}(n)]$. Clearly,

$$\underline{\mathcal{C}}(n)^H \underline{\mathcal{C}}(n) = \underline{\tilde{\mathcal{C}}}^H \underline{\underline{\Delta}}(n) \underline{\tilde{\mathcal{C}}}. \tag{C.73}$$

Since $\underline{\underline{\Delta}}(n) \leq \underline{\underline{\mathbf{I}}}_{N_{seq} \times N_{seq}}$, where matrix inequalities are defined according to Definition 4.1,

$$\underline{\mathcal{C}}(n)^H \underline{\mathcal{C}}(n) = \underline{\tilde{\mathcal{C}}}^H \underline{\underline{\Delta}}(n) \underline{\tilde{\mathcal{C}}} \leq \underline{\tilde{\mathcal{C}}}^H \underline{\tilde{\mathcal{C}}}. \tag{C.74}$$

For perfectly orthogonal codes, $\underline{\underline{B}}(n) = \frac{1}{M\mathcal{E}} \underline{\mathcal{C}}(n)$; thus

$$\underline{\underline{B}}(n)^H \underline{\underline{B}}(n) = \left(\frac{1}{M\mathcal{E}}\right)^2 \underline{\mathcal{C}}(n)^H \underline{\mathcal{C}}(n) = \left(\frac{1}{M\mathcal{E}}\right)^2 \underline{\tilde{\mathcal{C}}}^H \underline{\underline{\Delta}}(n) \underline{\tilde{\mathcal{C}}} \leq \frac{1}{M^2\mathcal{E}^2} \underline{\tilde{\mathcal{C}}}^H \underline{\tilde{\mathcal{C}}} \tag{C.75}$$

Bibliography

[1] M. Abramowitz, and I. A. Stegun, *Handbook of Mathematical Functions with formulas, graphs, and mathematical tables*, New York: Dover Publications, 1972.

[2] H.R. Ahmadi and M. Nasiri-Kenari, "Performance analysis of time-hopping ultra-wideband systems in multipath fading channels (uncoded and coded schemes)", *The 13th IEEE Int. Symp. on Personal, Indoor and Mobile Radio Communications, 2002*, pp. 1694-1698.

[3] B. Allen, T. Brown, K. Schwieger, E. Zimmermann, W. Malik, D. Edwards, L. Ouvry, and I. Oppermann, "Ultra Wideband: Applications, Technology and Future perspectives," in *Proc. Int. Workshop on Convergent Tech. (IWTC '05)*, Jun. 2005, pp. 1-6.

[4] H. Bateman, *"Tables of Integral Transforms"*, New York: McGraw-Hill, 1954.

[5] N. Boubaker, and K. B. Letaief, "A Low complexity MMSE-RAKE Receiver in a Realistic UWB Channel and in the presence of NBI," in *Proc. IEEE Wireless Commun. and Network. Conf. (WCNC '03)*, vol. 1, New Orleans, LA, Mar. 2003, pp. 233-237.

[6] S. Boyd, L. El Ghaoui, E. Feron, and V. Baakrishnan, *Linear Matrix Inequalities in System and Control Theory*, Philadelphia: SIAM, 1994.

[7] D.R. Brillinger, *Time Series Data Analysis and Theory*, New York: Holt, Rinehart and Winston, 1975.

[8] J. Cai, X. Shen, J. W. Mark, H. Liu, and T. D. Todd, "Semiblind channel estimation for pulse-based ultra-wideband wireless communication systems," *Vehicular Tech., IEEE Trans. on*, vol. 55, Jan. 2006, pp. 95-103.

[9] C. Carbonelli, S. Franz, U. Mengali, and U. Mitra, "Semi-Blind ML Synchronization for UWB Transmitted Reference Systems," in *Proc. of the Asilomar Conference on Signals, Systems and Computers*, Nov. 2004, pp. 1491-1495.

[10] D. Cassioli, M. Z. Win, and A. F. Molish, "The ultra-wide bandwidth indoor channel: from statistical model to simulations," *IEEE J. Select. Areas Commun.*, vol. 20, Issue: 6, pp. 1247-1257, Aug. 2002.

[11] D. Cassioli, M. Z. Win, F. Vatalaro, and A. F. Molish, "Performance of Low-Complexity Rake Reception in a Realistic UWB Channel," in *Proc. IEEE Int. Conf. on Commun. (ICC '02)*, vol. 2, New York City, NY, Apr. 2002, pp. 763-767.

[12] Y-L. Chao, and R. A. Scholtz, "Ultra-Wideband Transmitted Reference Systems," *Vehicular Tech., IEEE Trans. on*, vol. 54, Sept. 2005, pp. 1556-1569.

[13] J. D. Choi, and W. E. Stark, "Performance of Ultra-Wideband Communications with Suboptimal Receivers in Multipath Channels," *Comm., IEEE J. on Selected Areas in*, vol. 20, Dec. 2002, pp. 1754-1766.

[14] R. J-M. Cramer, M. Z. Win, and R. A. Scholtz, "Impulse Radio Multipath Characteristics and Diversity Reception," in *Proc. IEEE Int. Conf. Commun. (ICC '98)*, vol. 3, Atlanta, GA, Jun. 1998, pp. 1650-1654.

[15] F. M. Dannan, "Matrix and Operator Inequalities," *J. of Inequalities in Pure and Applied Math.*, vol. 2, issue 3, 2001.

[16] C. R. C. M. da Silva, and L. B. Milstein, "Coarse Acvquisition Performance of Spectral-Encoded UWB Communication Systems in the Presence of Narrow-Band Interference," submitted to the *IEEE Trans. On Communications*.

[17] D. M. Dlugos, and R. A. Scholtz, "Acquisition of Spread Spectrum Signals by an Adaptive Array," *Acoustics, Speech, and Signal Processing, IEEE Trans. on*, vol. 37, Aug. 1989, pp. 1253-1270.

[18] G. Durisi and G. Romano, "On the validity of gaussian approximation to characterize the multiuser capacity of UWB TH PPM", *IEEE Conf. on Ultra Wideband Systems and Technologies, Digest of Papers*, pp. 157-162, 2002.

[19] S. Farahmand, X. Luo, G. B. Giannakis, "Demodulation and Tracking with Dirty Templates for UWB Impulse Radio: Algorithms and Performance," *Vehicular Tech., IEEE Trans. on*, vol. 54, Sept. 2005, pp. 1595-1608.

[20] FCC, "Revision of Part 15 the Commission's rules regarding ultra-wideband transmission systems," ET Docket 98-153, 2002.

[21] A. Finger, and S. Zeisberg, "Ultra Wideband Technique," *IEEE feature UWB*, Dresden 2003, pp. 1-2.

[22] J. Foerster, and Q. Li, "UWB Channel Modeling Contribution from Intel," *IEEE P802.15-02/279-SG3a*.

[23] A.R. Forouzan, M. Nasiri-Kenari and J.A. Salehi, "Performance analysis of ultrawideband time-hopping code division multiple access systems: uncoded and coded schemes", *ICC 2001*, pp. 3017-3021, Jun. 2001.

[24] R. T. Hector, and H. W. Tomlinson, "An Overview of Delay-Hopped, Transmitted-Reference RF Communications," *Technique Information Series: General Electric Company Research and Development Center*, Jan. 2002.

[25] C.W. Helstrom, *Statistical Theory of Signal Detection*, New York: Pergamon Press, 1960.

[26] http://grouper.ieee.org/groups/802/15/pub/2003/Mar03/.

[27] L. Huang, and C. C. Ko, "Performance of Maximum-Likelihood Channel Estimator for UWB Communications," *IEEE Comm. Letters*, vol. 8, June 2004, pp. 356-358.

[28] G. M. Hussain, "Principles of Space-Time Array Processing for Ultrawide-Band Impulse Radar and Radio Communications," *IEEE Trans. Vehicular Tech.*, vol. 51, Issue:3, pp. 393-403, May 2002.

[29] S. M. Kay, *Foundamentals of Statistical Signal Processing: Estimation Theory*, Englewood Cliffs: Prentice-Hall, 1993.

[30] S. Lang, *Complex analysis*, New York: Springer-Verlag, 1985

[31] M. Loeve, *Probability Theory I & II*, New York: Springer Verlag, 1978.

[32] V. Lottici, A. D'Andrea, and U. Mengali, "Channel Estimation for Ultra-Wideband Communications," *Comm., IEEE J. on select. areas in*, vol. 20, Dec. 2002, pp. 52-55.

[33] E. Lukacs, *"Characteristic Functions"*, London: Griffin, 1970.

[34] Y. Ma, T.J. Lim, "Bit Error Probability for MDPSK and NCFSK over Arbitrary Rician Fading Channels," *Comm., IEEE J. on select. areas in*, vol. 18, Nov. 2000, pp. 2179-2189.

[35] A. M. Mathai, and S. B. Provost, *Quadratic Forms in Random Variables: Theory and Applications.* New York: Marcel Dekker, 1992.

[36] J. Oh, S. Yang, and Y. Shin, "A Rapid Acquisition Scheme for UWB Signals in Indoor Wireless Channels," in *Proc. IEEE Wireless Commun. Network. Conf. (WCNC '04)*, vol. 2, Atlanta, GA, Mar. 2004 ,pp. 1143-1147.

[37] A. Papoulis, *"Probability, Random Variables, and Stochastic Processes"*, New York: McGraw-Hill, 1984.

[38] L. D. Paulson, "Will Ultrawideband Technology Connect in the Marketplace?," *IEEE Computer*, vol. 36, pp. 15-17, Dec. 2003.

[39] M. Pausini, and G. J. M. Janssen, "On the Narrowband Interference in Transmitted Reference UWB Receivers," *UWB, 2005 IEEE Int. Conf. on*, Sep. 2005, pp. 571-575.

[40] J. G. Proakis, *Digital Communications*, 4th ed., New York: McGraw-Hill, 2001.

[41] T. Q. S. Quek, M. Z. Win, and D. Dardari, "UWB Transmitted Reference Signaling Schemes - Part II: Narrowband interference Analysis," *UWB, 2005 IEEE Int. Conf. on*, Sep. 2005, pp. 593-598.

[42] L. Quinghua, and L. A. Rusch, "Multiuser receivers for DS-CDMA UWB," in *Proc. IEEE Conf. Ultra-Wideband Systems Tech. (UWBST '02)*, Baltimore, MD, May 2002, pp. 163-168.

[43] A. Rabbachin, and I. Oppermann, "Comparison of UWB transmitted reference schemes," *Comm., IEE Proceedings*, vol. 153, Feb. 2006, pp. 136-142.

[44] B. D. Rao, M. Wengler, and B. Judson, "Performance analysis and comparison of MRC and optimal combining in antenna array systems," *IEEE Int. Conf. Acoustics, Speech, Signal Processing (ICASSP '01)*, vol. 5, Salt Lake City, UT, May 2001 , pp. 2949-2952.

[45] H. F. Rashvand, B. Allen, and M. Ghavami, "Editorial: Ultra wideband systems technologies and applications," in *Proc. IEEE Int. Conf. Commun. (ICC '06)*, vol. 153, pp. 81-82, Feb. 2006.

[46] R. R. Rick, and L. B. Milstein, "Optimal Decision Strategies for Acquisition of Spread-Spectrum Signals in Frequency-Selective Fading Channels," *Comm., IEEE Trans. on*, vol. 46, May 1998, pp. 686-694.

[47] G. S. Rogers, *Matrix Derivatives*, Series edited by: D. B. Owen, Dept. of Statistics, Southern Methodist University, Dallas, 1980. *Acoustics, Speech, and Signal Processing, IEEE Transactions on*, vol. 37, Aug. 1989, pp. 1253-1270.

[48] M. Sabattini, E. Masry, and L. B. Milstein, "A Non-Gaussian Approach to the Performance Analysis of UWB TH-BPPM Systems," in *Proc. IEEE Conf. Ultra-Wideband Systems Tech. (UWBST '03)*, Reston, VA, Nov. 2003, pp. 52-55.

[49] M. Sabattini, E. Masry, and L. B. Milstein, "Joint Code Acquisition and Channel Estimation for UWB Transmission," *2006 IEEE Sarnoff Symposium*, Mar. 2006.

[50] A. Saleh, and R. Valenzuela, "A Statistical Model for Indoor Multipath Propagation," Communications, *IEEE J. Select. Areas Commun.*, vol. 5, Issue: 2, pp. 128-137, Feb. 1987.

[51] J. Salz, and J. H. Winters, "Effect of Fading Correlation on Adaptive arrays in Digital Mobile Radio," *IEEE Trans. Vehicular Tech.*, vol. 43, Issue: 4, pp. 1049-1057, Nov. 1994.

[52] M. K. Simon, *Probability Distributions Involving Gaussian Random Variables: A Hendbook for Engineers and Scientists*, 1st ed., Norwell: Kluwer Acad. Press, 2002.

[53] K. Siwiak, P. Withington, and S. Phelan, "Ultra-Wide Band Radio: The Emergence of an Important New Technology," in *Proc. IEEE Vehicular Tech. Conf. (VTC)*, vol. 2, pp. 1169-1172, May 2001.

[54] G. L. Stueber, *Principles of Mobile Communication*, 2nd ed., Boston: Kluwer Academic Press, 2000.

[55] S. Tan, B. Kannan, and A. Nallanathan, "Performance of Ultra-Wideband Time-Hopping Spread Spectrum Impulse Radio Systems with Antenna Array," in *Proc. IEEE Int. Conf. Commun. Systems (ICCS '02)*, vol. 1, Amsterdam, the Netherlands, Nov. 2002, pp. 399-403.

[56] G. L. Turin, "Communication through noisy, random-multipath channels," MIT Lincoln Lab., Tech. Rep. 116, May 1956.

[57] G. L. Turin, "The characteristic function of Hermitian quadratic forms in complex normal variables," *Biometrika*, pp. 199-201, June 1960.

[58] H.L. Van Trees, *Detection, Estimation, and Modulation Theory*, vol. II, New York: Wiley & Sons, 1971.

[59] B. D. Van Veen, and K. M. Buckley, "Beamforming: a Versatile Approach to Spatial Filtering," *IEEE Acoustics, Speech, Signal Processing Magaz.*, vol. 5 , Issue: 2, pp. 4-24, Apr. 1988.

[60] S. Vijayakumaran, and T. F. Wong, "On Equal-Gain Combining for Acquisition of Time-Hopping Ultra-Wideband Signals," *Comm., IEEE Trans. on*, vol. 54, Mar. 2006, pp. 479-490.

[61] M. Villanti, M. Sabattini, G. M. Maggio, and L. B. Milstein, "Non-coherent code acquisition for UWB systems in dense multipath fading channels," *Vehicular Technology Conference, VTC 2005-Spring*, 30 May-1 June 2005.

[62] J. Walko, "Agree to Disagree," *IEE Review*, vol. 50, May 2004 pp. 28-29.

[63] C. Wildey, "UWB: The Start of a Dark Age?" *IEE Comm. Engineer*, vol. 2, Apr. 2004, pp. 7-7.

[64] M.Z. Win and R.A. Scholtz, "Impulse radio: how it works", *IEEE Comm. Letters*, vol. 2, pp. 36-38, Feb 1998.

[65] M.Z. Win and R.A. Scholtz, "Ultra-wide bandwidth time-hopping spread-spectrum impulse radio for wireless multiple-access communications", *IEEE Trans. Communications*, vol. 48, pp. 679 -689, Apr 2000.

[66] D. Wu, P. Spasojevic, and I. Seskar, "Multipath Beamforming for UWB: channel Unknown at the receiver," *Asilomar Conf. Signals, Systems Computers*, vol. 1, Pacific Grove, CA, Nov. 2002 , pp. 599-603.

[67] F. Zabini, *Beamforming Techniques in Multiple Antennas Ultra Wide Band Systems in the presence of Interference*, Master Thesis, University of Bologna, Mar. 2004.

[68] P. P. Zabreyko *et al.*, *Integral Equations - a reference text*, translatad and edited by T. O. Shaposhnikova, R. S. Anderssen, and S. G. Mikhlin, 1st ed., Leyden: Noordhoff International Publishing, 1975.

[69] H. Zhang, and T. A. Gulliver, "Biorthogonal pulse position modulation for time-hopping multiple access UWB communications," *Comm., IEEE Trans. on*, vol. 4, May 2005, pp. 1154-1162.